10-10-2019

Turn-On Near-Infrared Fluorescent Sensors for Selective Monitoring of Kinase Activity

Gerard Thomas Ducharme
Louisiana State University and Agricultural and Mechanical College

TURN-ON NEAR-INFRARED FLUORESCENT SENSORS FOR SELECTIVE MONITORING OF KINASE ACTIVITY

A Dissertation

Submitted to the Graduate Faculty of the
Louisiana State University and
Agricultural and Mechanical College
in partial fulfillment of the
requirements for the degree of
Doctor of Philosophy

in

The Department of Chemistry

by
Gerard Thomas Ducharme
B.S., University of Louisiana at Lafayette, 2013
December 2019

To my wife, Amanda.

All of those weekends in the lab were for something.

53-116-92

Acknowledgments

My tenure at Louisiana State University has been filled with numerous people to whom I will be eternally grateful. First, I would like to thank my advisor, Dr. Evgueni E. Nesterov, without whom I am uncertain if I would have had the motivation or energy to complete my research. I would like to recognize the willingness and effort put forth by Dr. Carol M. Taylor, who was willing to host me in her lab during my last year of study when Dr. Nesterov made the move to Northern Illinois University. The work and effort of Dr. Irina V. Nesterova is also greatly appreciated, from her advice on creating and troubleshooting HPLC gradients, providing chemicals, and her collaborative work in testing of our probe. I would like to thank my committee members, Drs. Antonieta Guerrero-Plata and Justin R. Ragains, for their encouragement and willingness to be a part of my graduate study. Thank you to Drs. Linda Allen, Fedra Leonik, and Tamara Nauman; without their guidance and encouragement my self-confidence in my ability to effectively communicate my knowledge of chemistry would not be what it is. Thank you to my former and current group members, my friends Drs. Adan Bruner and Caite Breshnahan, for their friendship and mentorship. I would also like to thank fellow Taylorite, Joshua Lutz for his advice, help, and being a fellow commiserate while writing.

Special thanks to my wife, Amanda Ducharme, who provided encouragement and a shoulder to cry on when reactions failed and shared in my joy when they worked. I would also like to thank my mother and father whose support and care were always appreciated and felt, even when we are apart.

Table of Contents

List of Abbreviations and Symbols

δ	chemical shift
Φ_f	quantum fluorescent yield
ATP	adenosine triphosphate
Boc	*tert*-butyloxycarbonyl
BSA	bovine serum albumin
^{n}BuOH	*n*-butanol
DBU	1,8 diazabicyclo[5.4.0]undec-7-ene
DBN	1,5-diazabicyclo[4.3.0]non-5-ene
DCC	dicyclohexylcarbodiimide
DCM	dichloromethane
DIC	diisopropylcarbodiimide
DIPEA	diisopropylethylamine (Hünigs Base)
DMAP	*N,N*-dimethyl-4-aminopyridine
DMF	dimethylformamide
EDC	*N*-(3-dimethylaminopropyl)-*N*'-ethycarbodiimide hydrochloride
EGF	epidermal growth factor
EGFR	epidermal growth factor receptor

ELISA	enzyme-linked immunosorbent assay
ESI	electrospray ionization
Fmoc	fluorenylmethyoxycarbonyl
HBTU	hexafluorophosphate benzotriazole tetramethyl uronium
HOAt	1-hydroxy-7-azabenzotriazole
HOBt	hydroxybenzotriazole
HEPES	2-[4-(2-hydroxyethyl)piperazin-1-yl]ethanesulfonic acid
HPLC	high performance liquid chromatography
HRMS	high resolution mass spectrometry
IC_{50}	inhibitory concentration
IR	infrared
MPc	metallophthalocyanine
MALDI	matrix assisted laser desorption ionization
Mtt	4-methyltrityl
NIR	near-infrared
NMP	*N*-methylpyrrolidone
PBS	phosphate buffered saline
Pc(s)	phthalocyanine(s)

PET	positron emission tomography
PEG	polyethylene glycol
S/B	signal-to-background
SPS	solid phase synthesis
T790M	threonine replaced by methionine
TEG	triethyleneglycol monomethyl ether
TFA	trifluoroacetic acid
THF	tetrahydrofuran
TIPS	triisopropylsilane
TKI	tyrosine kinase inhibitor
UV	ultraviolet
ZnPc	zinc phthalocyanine

Abstract

Reliable and selective detection of specific biopolymers is critical in a broad range of biomedical and technological areas, including availability of simple and efficient point-of-care-compatible systems for the detection of prognostic, pharmacodynamic and predictive biomarkers. Monitoring epidermal growth factor receptor (EGFR) tyrosine kinase is of major significance due to its link to many epithelial cancers. This task is complicated by the high rate of mutation occurring in patients treated with kinase inhibitors. This dissertation describes a conceptually novel design and synthesis of turn-on near-infrared fluorescent sensors for selective and sensitive detection of EGFR. The fluorescent signal generation mechanism is based on the aggregation/de-aggregation of phthalocyanine chromophores controlled by selective binding of small-molecule "anchor" groups to a specific binding site of a target biopolymer. Due to universality of the signal generation mechanism, and the response selectivity independently coming from a proper choice of a small-molecule "anchor" group, this approach can offer broad capabilities in designing turn-on fluorescent sensors for EGFR kinase as well as for various other protein targets, and facilitate use of this system in point-of-care centers in order to decrease monetary and time cost of treatment for the patients.

Chapter 1. Overview of Phthalocyanines and the Biological Importance of EGFR

1.1. Biological Need for Near-Infrared Fluorophores

Modern medicine has a need for improved monitoring of biological processes, particularly with regard to cancer. Many processes, or biological targets, can be monitored throughout the treatment process using fluorophores that are viable under physiological conditions.[1] This approach reduces the number of incisions on the patient. Moreover, this tactic gives the medical professional the potential to monitor treatment in real time or use the dye as a marker for cancerous tissue during surgery. The use of fluorescent dyes has seen wide application in cancer diagnosis and treatment. They allow for simplified monitoring of cancerous tumor size changes and accumulation of drugs in the patient without multiple biopsies being taken.

Many of these dyes, though, have a maximum absorbance frequency in either the ultra-violet [(UV) 10 – 400 nm] or visible [400 – 650 nm] region of the electromagnetic spectrum. Ultra-violet radiation can harm healthy cells as well as is readily scattered upon entering tissue hindering deep tissue penetration of the patient's body (i.e., for internal organ monitoring).[2] Visible light radiation does not harm cells, but the most energetic light is scattered as it passes through tissue and can cause autofluorescence in cells; which effectively masks any emission from a fluorescent probe. Infrared light [(IR) 650 nm – 1mm]; however, can pass through cell tissue, does not harm cells, does not induce cell autofluorescence, and can be monitored using existing technology.[3]

Fluorescent dyes can be tuned for both absorbance and emission in a variety of ways. Commonly, extended π-conjugation, in concert with enforced planarity, are used to shift maxima toward longer wavelengths (bathochromic shift). Specific wavelength windows can thereby be accessed by including electron-rich or electron-poor substrates to fine tune the photophysical properties of the dye.

The focus of this research has been on the development of a near-infrared [(NIR) 650 – 1100 nm] fluorescent markers for cancers associated with the overexpression of epidermal growth factor receptor (EGFR), a tyrosine kinase that is commonly overexpressed in epithelial cell carcinomas.

1.2. Phthalocyanines: Historical and Modern Perspective

Phthalocyanines (Pcs) are tetrapyrrolic compounds that range in color from blue to green. They are structurally related to the naturally occurring porphyrin macrocycle (Figure 1.1), the best known example being the heme group in hemoglobin. While porphyrins have methylene carbons linking the pyrrole units, Pcs have nitrogen atoms instead. Additionally, Pcs incorporate isoindole groups instead of pyrroles, affording extension of the π-electron system, thereby improving the stability and photoluminescence properties.

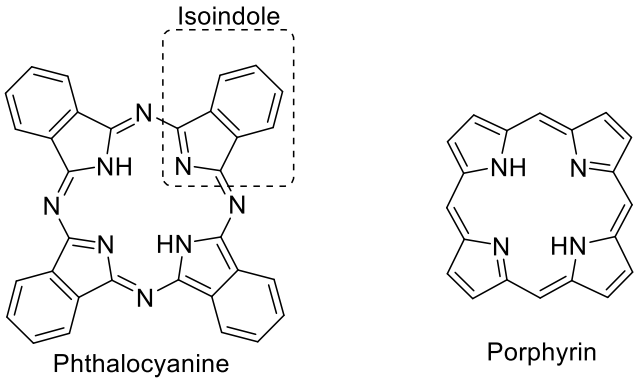

Figure 1.1. Phthalocyanine and Porphyrin Structures

Phthalocyanine was first reported as an impurity in 1907 by Braun and Tcherniac[4] in their synthesis of *o*-cyanobenzamide from phthalimide and acetic anhydride (Scheme 1.1).

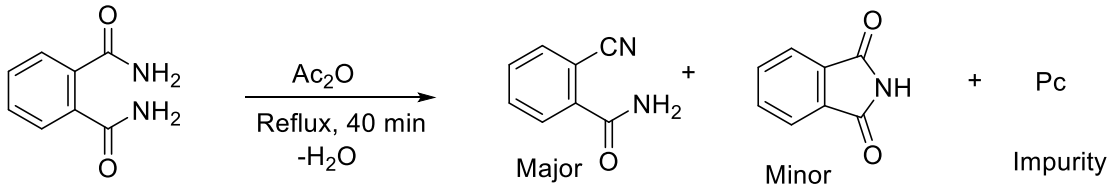

Scheme 1.1. Braun and Tcherniac Synthesis of o-cyanobenzamide.[4]

Isolation of Pc was not reported until 1927, by von der Weid and de Diesbach, from reactions of *o*-dibromobenzene and copper cyanide in pyridine.[5] For most of their early use, Pcs were seen as simple dyes for blue and green color. More recently, advances in synthesis and isolation have opened the door for more complex structures and applications.[6] Absorption spectra of Pcs normally feature maxima in the visible region (Figure 1.2), but their long wavelength band (Q-band) can extend into the NIR region; making them useful in many applications from dye-sensitized solar cells to singlet oxygen generators. Generally, Pcs are dyes with large molar extinction

coefficients (typically in the order of 10^5 cm^{-1} M^{-1}) that are stable and robust, both chemically and photochemically.

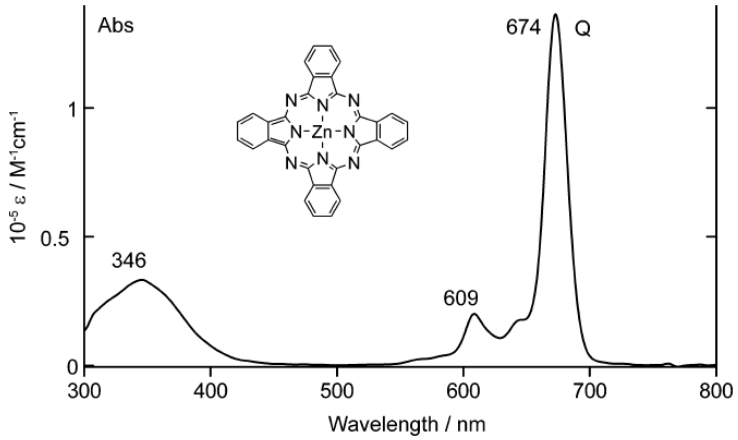

Figure 1.2. Typical Pc Absorption Spectrum (ZnPc in Pyridine).[6] Reprinted with Permission from *Source:* UV-Visible Absorption Spectroscopic Properties of Phthalocyanines and Related Macrocycles. Kadish, K. M.; Smith, K. M.; Guilard, R., Eds, Copyright ® 2010 World Scientific: Singapore.

Absorption and emission maxima can be tuned by changing the substituents on the macrocycle and/or the coordinating metal center. For example, Güzel and coworkers showed that exchanging Zn metal with Ga or Si could lead to some small changes in the absorbance behavior of the resulting Pc compounds (Figure 1.3).[7] Phthalocyanines also display relatively high fluorescence quantum yields (Φ_f) for NIR emitting organic compounds. Quantum yields are expressed as a ratio between the number of emitted and absorbed photons of an emissive substance.

$$\Phi_f = \frac{\#\ photons\ emitted}{\#\ photons\ absorbed}$$

For example, unsubstituted Zinc Pc (ZnPc, Figure 1.2) shows a quantum yield around 0.17 in most organic solvents.[8,9] The inherent insolubility of Pc in most common

solvents is due to the high propensity to form aggregates.[9] This aggregation greatly hinders their efficiency in many applications due to insolubility and self-quenching.

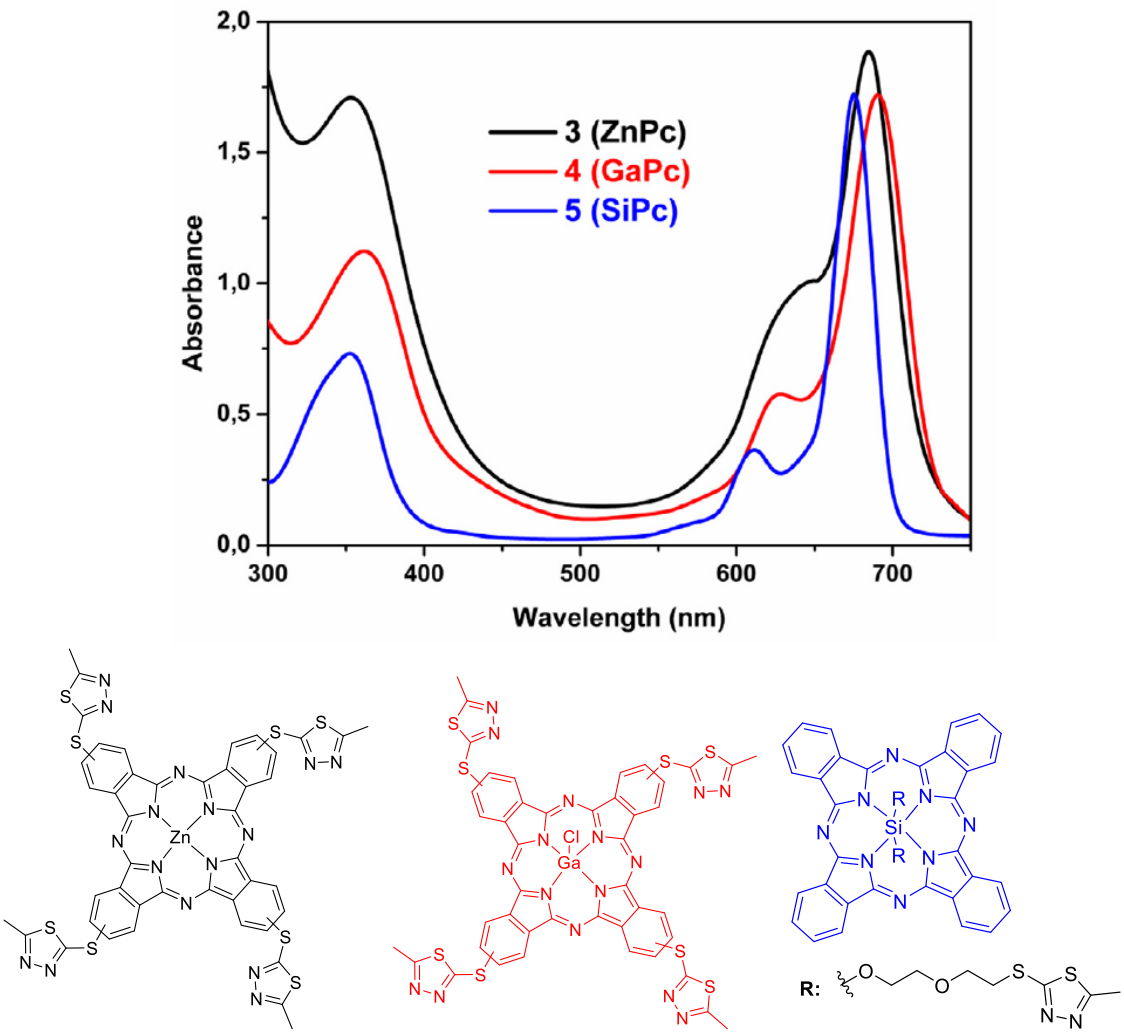

Figure 1.3. Absorption Comparison of Pc with Different Metal Centers[7]. Reprinted with Permission from Ref. 7. Copyright ® 2017 Elsevier.

A solution to the solubility issue is the incorporation of solubilizing groups on the isoindole benzene rings (Figure 1.1; *vide supra*) which can be designed for organic or aqueous environments. These solubilizing groups also help break up aggregates by creating steric or electronic repulsion between Pc rings, depending on the group's structure. Functional groups of all kinds have been used to effectively solubilize Pcs and

include alkyl chains, ethers, quaternary amines, and sulfates.[10] These modifications have increased the usefulness of Pcs and expanded their applications beyond their use as simple clothing dyes. Solvent greatly affects the properties of the Pc, depending on the ability of the solvent to break up the aggregation. As an example, Göksel *et al*. found that their tetra-ethylamino ether substituted Pc compound exhibited some small variation of the absorption spectra dependent upon the solvent used (Figure 1.4).[9,11] They did not separate out constitutional isomers of their Pc, as this process is often time-consuming and does not have much effect on absorbance properties of the Pc.[12]

Functionalization of the Pc is typically effected through two avenues: direct addition to the fully formed macrocycle, or attachment of the solubilizing group on a precursor (Figure 1.5) prior to cyclization. Most additions occur on the isoindole benzene ring and can be attached at either the peripheral (Figure 1.6) or non-peripheral sites (Figure 1.7). The simplest method for substituent group attachment is to functionalize the chosen precursor before the cyclotetramerization reaction, which allows the newly formed Pc molecule to have the desired solubility properties at the outset. A separate approach has been to functionalize the metal center with solubilizing ligands,[7] which offers more variability in tuning the absorbance of the Pc. Common precursors (Figure 1.5) to Pc are phthalic anhydride, phthalic acid, phthalimide, phthalonitrile, diiminoisoindoline, *o*-cyanobenzamide, and *o*-dibromobenzene.

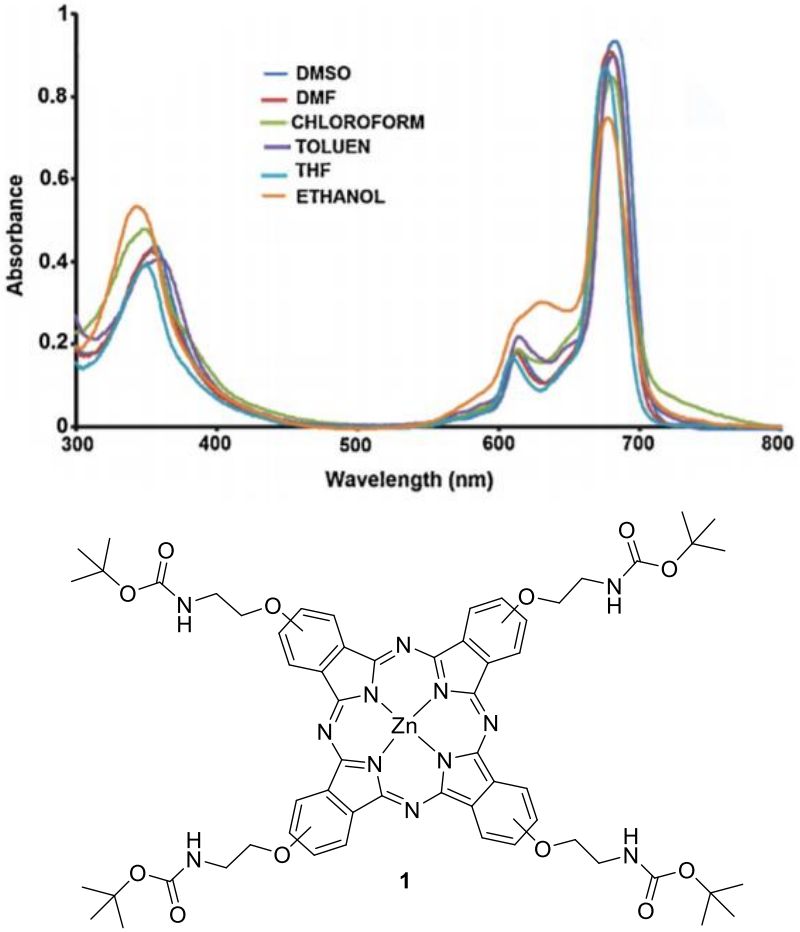

Figure 1.4. Effect of Solvent on Absorption Spectra. Pc **1**, 1.00 x 10^{-5} M.[11] Reprinted with Permission from Ref. 11. Copyright ® 2013 Elsevier.

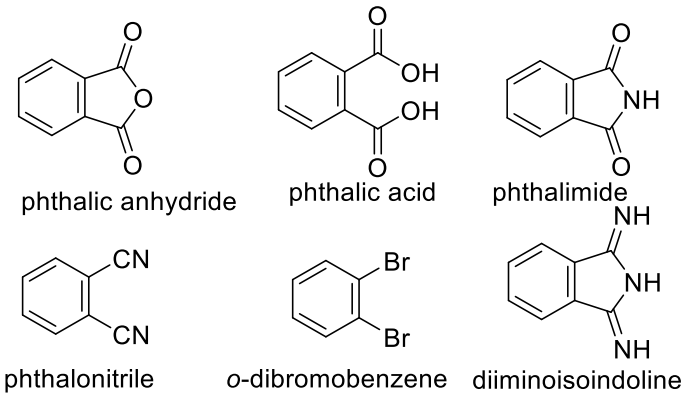

Figure 1.5. Commonly Used Precursors for Cyclotetramerization

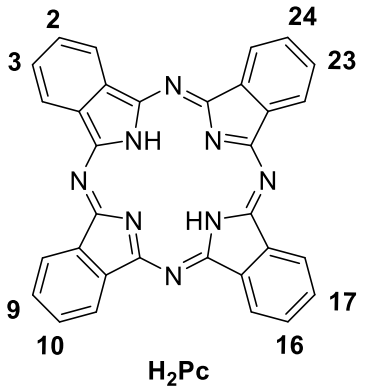

Figure 1.6. Peripheral Sites of Phthalocyanine

As can be seen in the Figure 1.6, metal free H_2Pc has eight peripheral sites (numbered) that can be used to attach solubilizing groups. Due to the high number of sites potentially suitable for functionalization, the tetramerization reaction of mono-substituted phthalocyanine precursors will yield a statistical mixture of four constitutional isomers: C_{4h}, C_{2v}, C_s, and D_{2h}. (Figures 1.7 & 1.8; *vide infra*). This issue can be resolved by filling all peripheral sites to yield an octasubstituted Pc.

The use of non-peripheral sites enforces regioselectivity due to steric interactions between the substituents (Figure 1.7). 3-Substituted phthalonitriles have been used to produce the C_{4h} isomer selectively[12] and exclusively.[13,14] The C_{4h} isomer is one which possess a 90° proper rotation axis (C_n) and a perpendicular reflection (h) plane of symmetry (i.e., mirror plane in center of Pc). Use of 4-substituted phthalonitrile yields a mixture of the isomers shown in Figure 1.8 with little selectivity, since the substituents have limited steric impact on the tetramerization process.

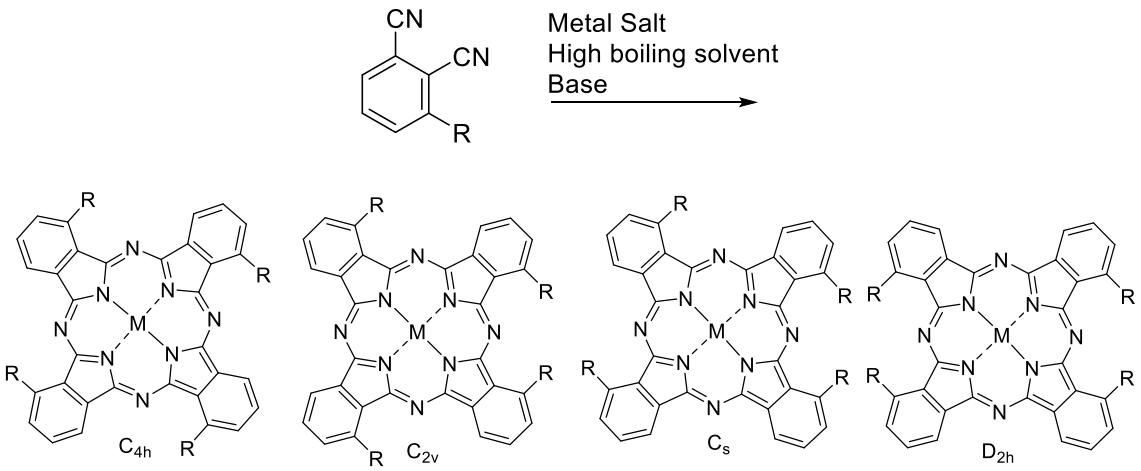

Figure 1.7. Structure and Symmetries of Pc Constitutional Isomers Derived from 3-substituted Phthalonitrile

Modification of substituents or specific ratios of precursor reagents can improve the formation of one or two of these isomers for the case of 4-substituted phthalonitrile, though separation is still a challenge. Another design strategy has been to link two phthalonitriles together to enforce specific regiochemical relationships upon their inclusion in the final phthalocyanine (Figure 1.9).[15] The drawback of producing isomers that are difficult to separate is often less severe for potential application of such an inseparable mixture than the obstacles of having to functionalize the Pc after it has formed via the cyclotetramerization reaction. Phthalocyanine macrocycle functionalization often requires harsher reaction conditions, there can be solubility issues with the initial macrocycle, and yields are typically lower compared to analogous functionalization of the monomer.

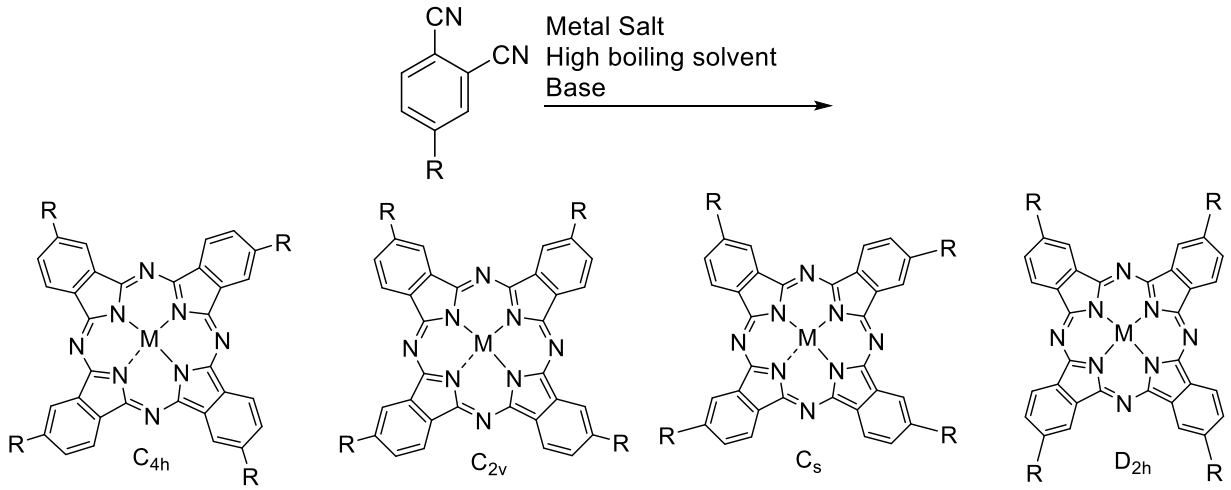

Figure 1.8. Structure and Symmetry of Pc Prepared from 4-Substituted Phthalonitriles

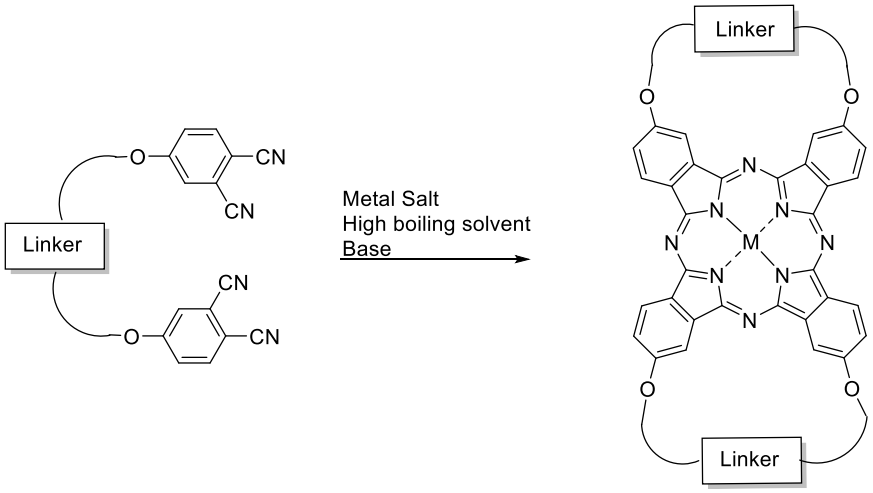

Figure 1.9. Linker Use in Phthalocyanine Synthesis

In academic laboratory syntheses, phthalonitriles are preferred as starting materials for cyclotetramerization due to better yields, while in industrial settings the use of phthalic anhydrides helps mitigate costs. The cyclotetramerization step requires the condensation reaction to occur around a metal template in a high boiling, polar solvent such as *N,N*-dimethylaminoethanol. Formation of non-metalated H_2Pc can be achieved using Linstead's method, viz. employing a Li, Na, or Mg metal alkoxide as the metal template to form the Pc, then removing the metal through addition of dilute acid.

Tomoda[16,17] and coworkers showed that catalytic quantities of strong, non-nucleophilic bases (such as DBU or DBN) act as a proton sponge for the alcohol. This generates an alkoxide *in situ* and enables the formation of the Pc under mild reaction conditions. They proposed that the mechanism involves an alkoxide ion acting as a nucleophile (**I**), forming the alkoxyisoindole intermediate (**II**) that can then cyclize rapidly creating the product phthalocyanine (**VII**, Scheme 1.2). The alkoxide is removed at the end of the cyclization and acts as a reducing reagent that stabilizes the newly formed Pc.

Phthalocyanines have been specifically functionalized to act as absorption dyes for dye-sensitized solar cells, electron transport, and binding partners for biomolecules. A major challenge in the synthesis of a functionalized Pc, particularly for use in biological systems, is the construction of an unsymmetrical Pc that incorporates a single "handle" by which the Pc can be anchored to other molecules. A practical way to access a specific mono-substituted isomer is to use a functionalized resin. The phthalonitrile or other precursor is attached to a resin which is then allowed to undergo the tetramerization reaction with at least three equivalents of the other precursor. The undesired tetramerization products that are formed in solution and are not attached to the resin can be washed away, allowing the resin-bound tetramer to be cleaved separately and isolated. This methodology has been used in this dissertation research for its simplicity and efficiency.

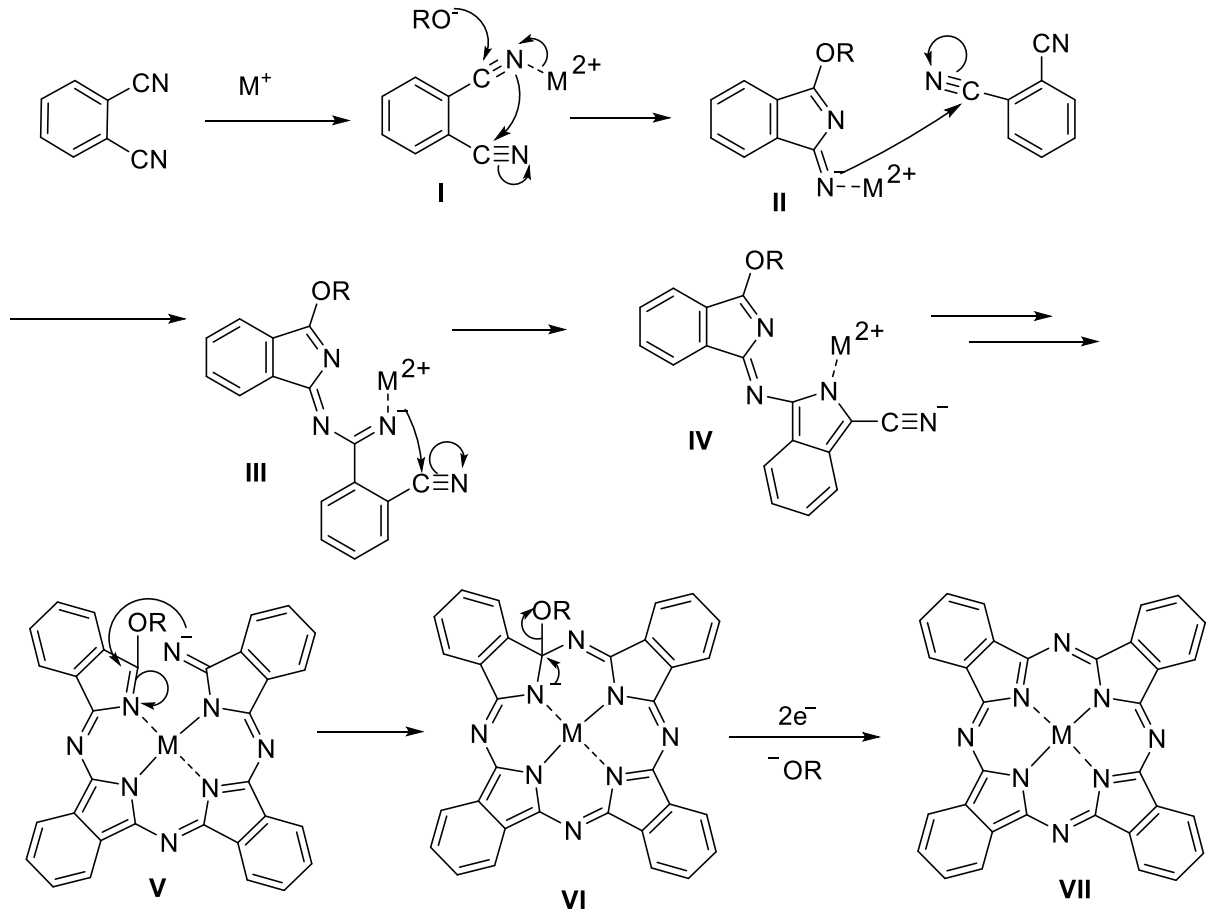

Scheme 1.2. Suggested Mechanism for Cyclotetramerization

1.3. Quinazolines – Type I Inhibitors of EGFR

The *erb* B receptor tyrosine kinase family consists of four homologous proteins: EGFR (*erbB*1), *erbB*2, *erbB*3, and *erbB*4. The protein is comprised of three distinct domains: the extracellular domain, the transmembrane domain, and the intracellular domain where tyrosine phosphorylation occurs. The extracellular domains of these proteins bind many structurally similar growth factors.[18] Upon epidermal growth factor (EGF), one of many growth factors, binding to the kinase, a complexation of receptors occurs that activates the intercellular kinase domain (Figure 1.10). This, in turn, leads to the autophosphorylation of tyrosine residues that form a tail at the C-terminus; thereby

regulating a range of cellular processes including cell proliferation, organ development, growth, and ion transport.[19] Kinase regulation of cell growth has been linked to certain types of cancers, and makes EGFR a promising target to inhibit cancer cell proliferation.[20]

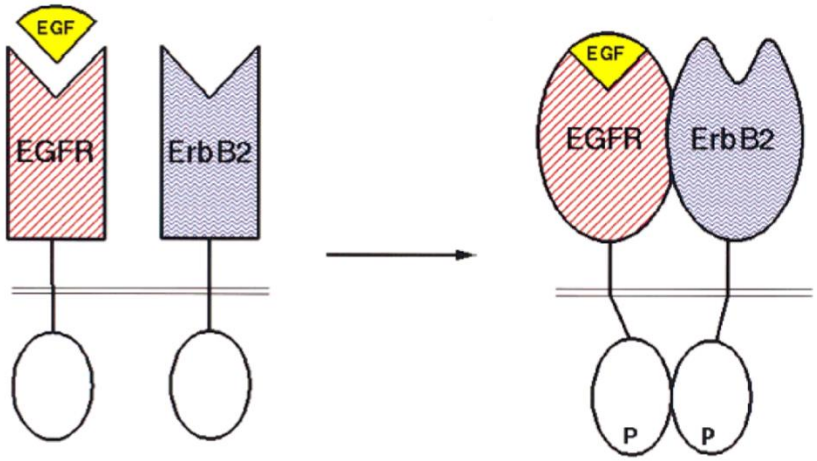

Figure 1.10. Binding of EGF to Erb B2 Protein and Dimerization.[18] Reprinted with Permission from Ref. 18. Copyright ® 1997 John Wiley & Sons.

Cohen's Nobel prize winning purification and elucidation of the EGF structure led to an understanding of how the receptor protein controls cellular functions.[19,20] This boosted research into the inhibition of these processes.[20] Monoclonal antibodies and small molecule probes have been intensely investigated vis-à-vis either the binding of the EGF receptor-moiety or competing with adenosine triphosphate (ATP) in the active site in order to decrease EGFR activity.[21]

Fry and coworkers designed a quinazoline based inhibitor (Figure 1.11, **2**) that gave an IC_{50} of 29 pM against EGFR from a cancer cell line, A-431.[22] The identification of this lead compound was the forerunner to the development of many quinazoline drugs for cancer treatment. The quinazoline core is normally connected to a phenyl ring through an amine or ether linkage. The phenyl ring is commonly functionalized with

either an unsaturated functionality or halogens to facilitate hydrophobic interactions in the active site. Typically, there are solubilizing groups attached to the quinazoline core that improve effectiveness.

Over time, patients reported a wide range of reactions to these drugs and some had no therapeutic response. For others, there was a loss of drug efficacy over time. Research into this variation in patient response showed that quinazoline-based inhibitors, while effective, are dependent upon a point mutation at codon 858 with leucine being replaced by an arginine (L858R).[23-26] The presence of this mutation (Figure 1.12), that can be confirmed by biopsy before prescription, allowed the first approved drugs (e.g. Gefitnib, Erlotinib) to be used as effective EGFR inhibitors (Figure 1.11).

Observation that some patients acquired resistance to treatment with quinazoline-based EGFR inhibitors led to the discovery of a second mutation in which the “ATP gatekeeper threonine” is mutated into methionine (T790M).[24] The bulkier methionine restricts interaction of the inhibitor within the binding pocket, causing a widening of the pocket which allows ATP to replace the inhibitor in the pocket, reducing the inhibitor effectiveness.

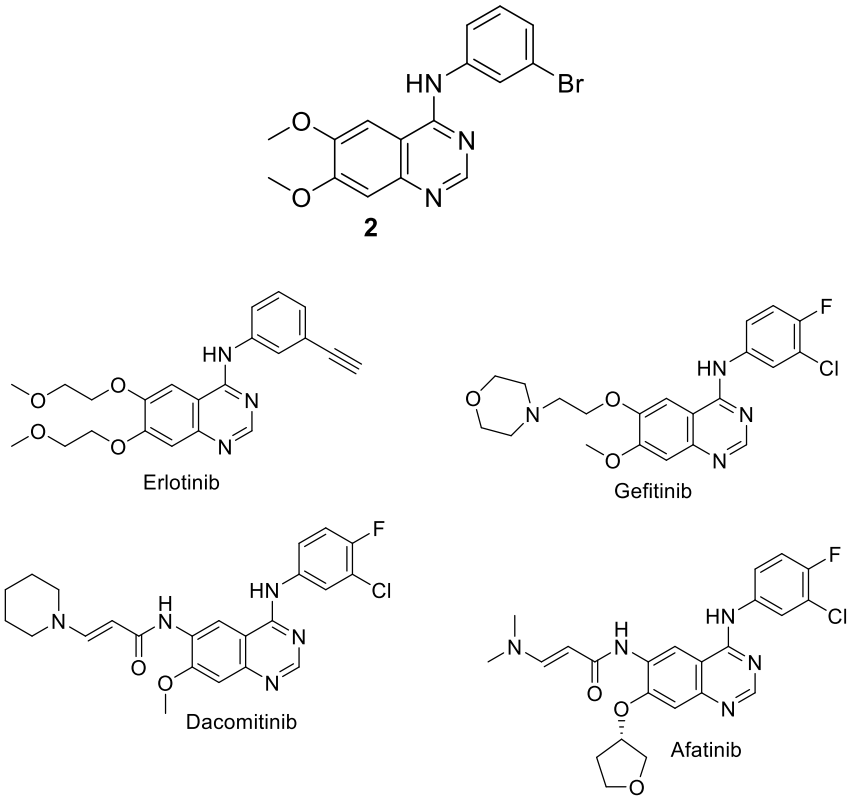

Figure 1.11. Quinazoline Inhibitors of EGFR

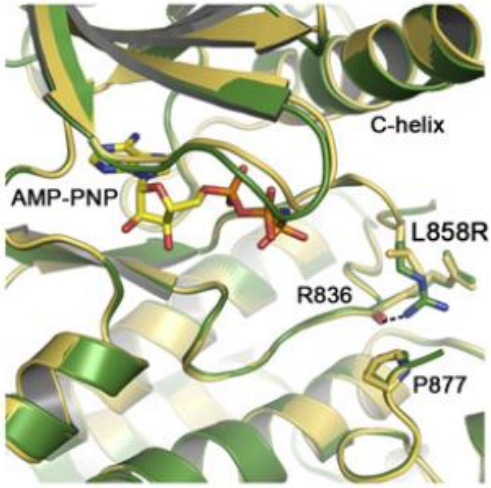

Figure 1.12. Crystal Structure of EGFR with ATP Analog AMP-PNP. Green: L858R Mutant; Yellow: Wild Type.[27] Reprinted with Permission from Ref. 27. Copyright ® 2007 Cell Press.

The crystal structure of EGFR bound to a quinazoline[28,29] inhibitor (Figure 1.13) revealed a cysteine residue outside of the binding pocket (C797/C773). Incorporation of

a Michael-acceptor into the structurally matching position of an inhibitor could be expected to lead to a covalent bonding with C797 that will retain the inhibitor in the active site, in spite of the acquired mutation (as in Dacomitinib and Afatinib, Figure 1.11).[24]

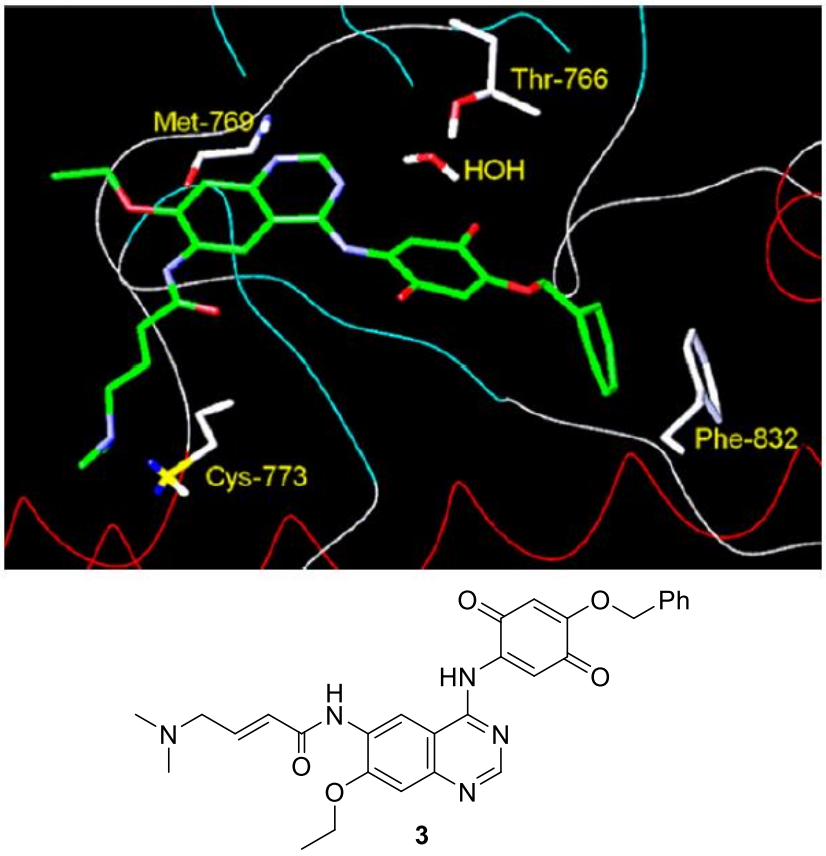

Figure 1.13. Crystal Structure of Quinazoline Probe (**3**) bound to ATP binding site at EGFR binding site.[30] Reprinted with Permission from Ref. 30. Copyright ® 2007 Elsevier

Detailed research has revealed the mechanism behind quinazoline effectiveness in treating EGFR overexpression,[29] providing insights into the structural features required in inhibitors. The two nitrogens in the pyrimidine aromatic ring (Figure 1.14) interact through hydrogen bonding with methionine 793/769 (*N1*) or threonine 766/780 mediated by water (*N3*). The quinazoline also is positioned in the hinge region of the

kinase, this occupation can be achieved by other nitrogen-containing heterocycles (e.g. pyrrolopyrimidine) though not as well. The 4-phenyl group fits into the hydrophobic pocket of the active site through interactions with the side chains of Leu788, Met766, Thr790, and Glu792.[27,29] Inhibitors with secondary amine groups linking the quinazoline and benzene rings are generally more potent than those with an ether linkage. Varying substituents on the phenyl ring demonstrated considerable impact on inhibitory activity. Halogenation (usually chloro or bromo substituents) at the meta position is effective in increasing inhibitory activity. The para position can be fluorinated to improve the metabolic stability of the inhibitor or used as an attachment point, via metal-catalyzed coupling, to install a hydrophobic ring that interacts with the back pocket region which is available in the inactive form of the kinase.

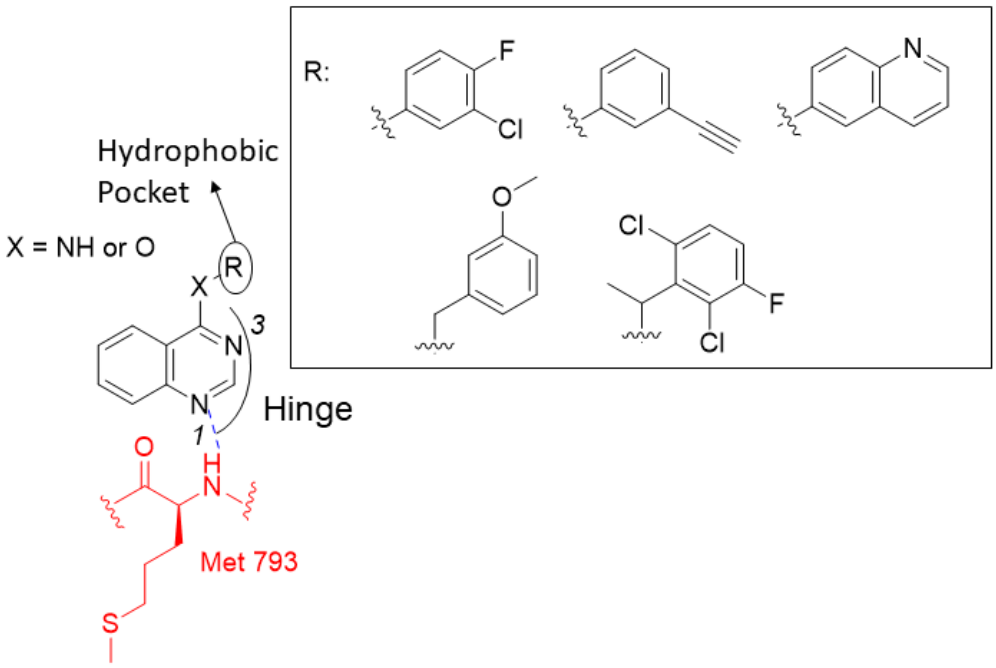

Figure 1.14. Quinazoline Structure Relation to Kinase and Variations. Adapted from *Source*: Eur. J. Med. 2017, **142**, 131-151

Type-I inhibitors can only bind to the activated, EGF-complexed form of the EGFR kinase. The active site features a binding pocket for ATP, between β-sheets of the N-lobe and α helicies of the C-lobe (Figure 1.15 or Figure 1.12, *vide supra*). Allosteric binding sites have been targeted with type-II inhibitors in an effort to increase efficiency. The back pocket is the allosteric site for the kinase and can only be reached in the inactive form of the enzyme. This extension into the back pocket is often used to facilitate a dual inhibitor for both EGFR activity and *erbB*2 complexation amplification, which is the second most common acquired mutation, with 12% of patients affected by it (versus T790M at 50 – 60%).[31] These inhibitors attach to the kinase at the allosteric site (*vide supra*) in either the inactive or active form of EGFR, depending on their structure.[23]

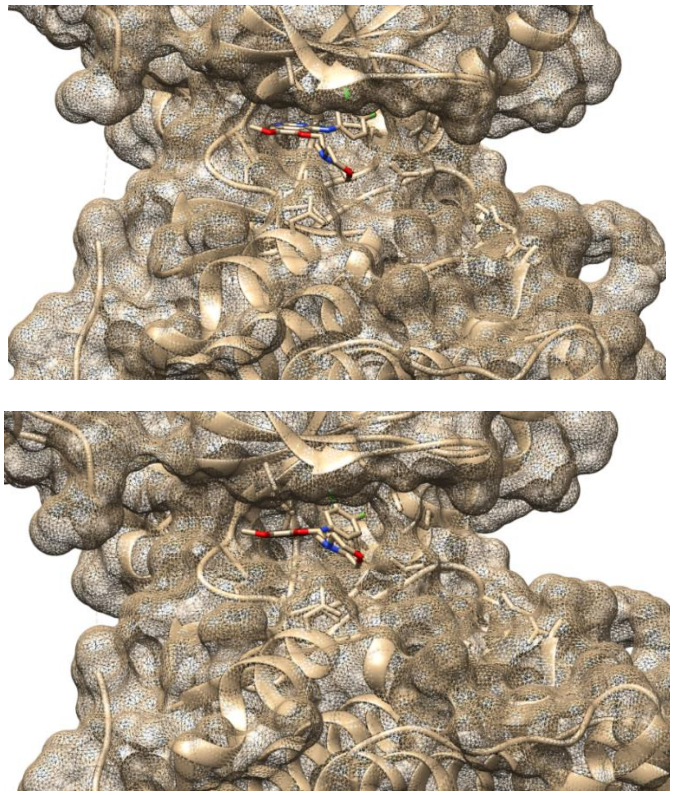

Figure 1.15. Active L858R Mutated EGFR with Gefitinib. PDB file: 2ITZ. N-Lobe at top of frame, C-lobe at bottom of frame.

1.4. Design of a Phthalocyanine – Quinazoline Conjugate Sensor:

The need to determine patient viability for treatment using EGFR inhibitors necessitates a biopsy to determine whether they possess the necessary mutation in exon 19 or 21,[32] as well as to address the commonly acquired mutation of T790M.[29] A goal to minimize the need for tumor biopsy and generally simplify the therapeutic treatment plan screening has inspired us to develop of a NIR fluorescent probe that is selective for EGFR overexpression and can be used to easily identify and track patient response to inhibitor drugs.

On a more general note, the development of a NIR fluorescent sensing platform for this specific kinase would also bring about a more general approach towards selective fluorescent detection of any specific protein (or other biomacromolecular target). The goal of this research is to develop a general design strategy toward a probe that, on binding to EGFR, would yield a quantitative measurement of emission via NIR fluorescence monitoring. Further, in a continuation of this development, introduction of a stronger-binding tyrosine kinase inhibitor (TKI) to a fluorescent probe-protein (probe-kinase) complex would promote displacement of the probe giving clear *in vitro* indication of the potential TKIs effectiveness in the patient. This will ultimately enable development of a simple fluorescent platform for rapid and reliable *in vitro* screening of the patient's response to specific TKI treatment. Due to the simplicity of the fluorescent monitoring, such a screening could be expediently done in the point-of-care setting.

Our strategy uses the well-studied, and widely used quinazoline-based, type-I inhibitor as the core for the probe. Variation of the quinazoline has been shown to affect binding affinity and crystallographic data,[28] along with computational docking

studies,[24,30] show that the 6-position points outside of the ATP binding pocket allowing for interaction with the solvent (Figure 1.15, *vide supra*). Fluorescent response would be achieved by utilizing a previously synthesized,[33] unsymmetric ZnPc (Scheme 1.3) that features three water-solubilizing triethylene glycol groups. A lysine amide would serve as a lynchpin for the probe, linking via the ε-amino group and a diamide of fumaric acid to the quinazoline, and linking to the Pc via the α-amino group and a p-hydroxybenzamide. The lysine would also serve as a point of attachment to the Rink amide resin that would yield a primary amide upon cleavage from the resin. A previously described[34] (but seldom used) process of Pc aggregation/de-aggregation in aqueous media will be employed as a signal generation mechanism. The main novelty of this research project is in the combination of the general (target independent) mechanism of fluorescent signal generation with specificity of the probe binding to a target biopolymer molecule, and practical demonstration of this unprecedented design concept.

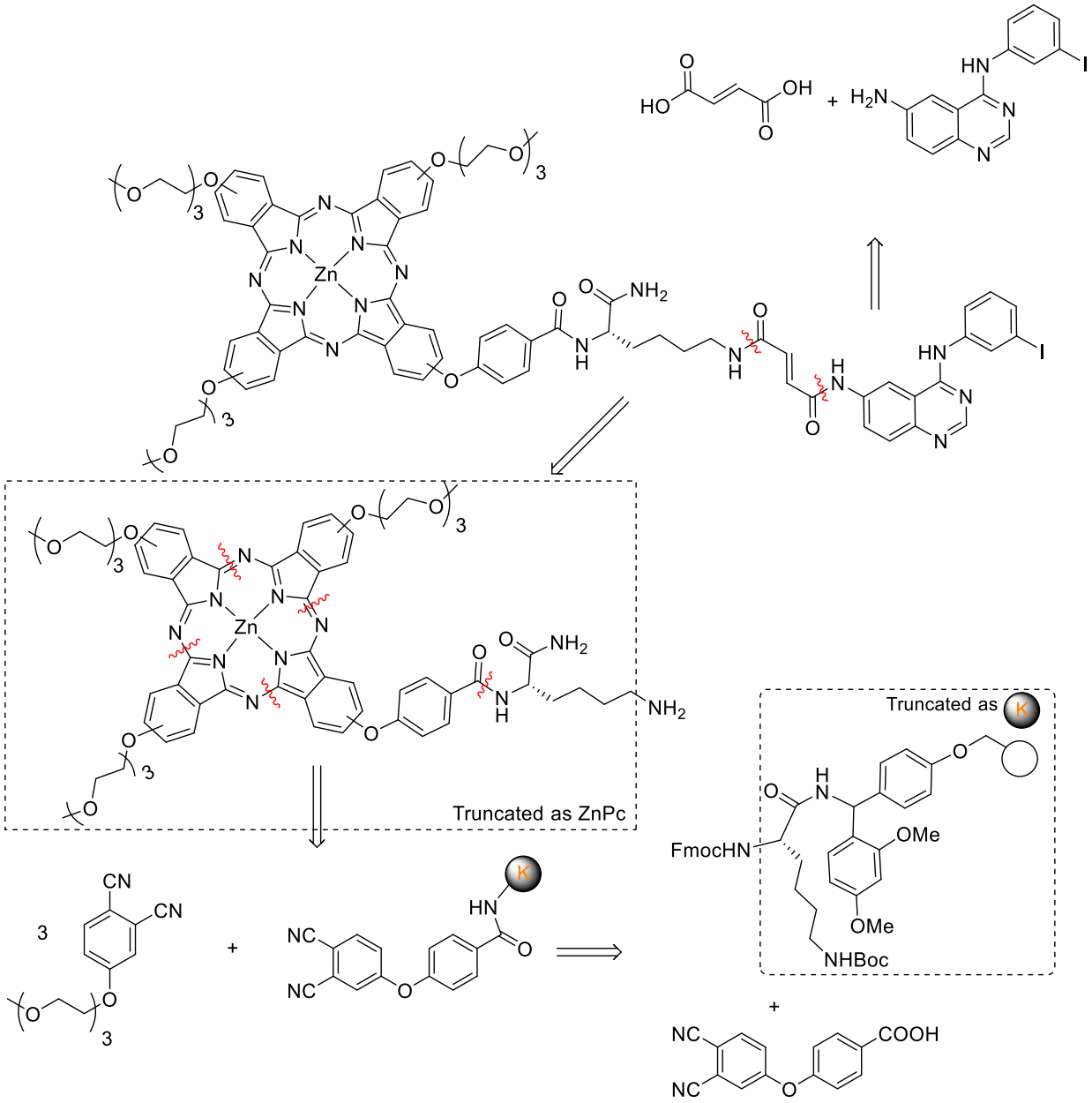

Scheme 1.3. Design and Retrosynthetic Analysis of Conjugated Probe and EGFR Inhibitor

1.5. Notes

1. Gonzalez de Castro, D.; Clarke, P. A.; Al-Lazikani, B.; Workman, P., Personalized cancer medicine: molecular diagnostics, predictive biomarkers, and drug resistance. *Clinical Pharmacology & Therapeutics* **2013,** *93* (3), 252-259.

2. Manna, D.; Ghosh, R., Effect of radiofrequency radiation in cultured mammalian cells: A review. *Electromagnetic Biology and Medicine* **2016,** *35* (3), 265-301.

3. Hammer, R. P.; Owens, C. V.; Hwang, S.-H.; Sayes, C. M.; Soper, S. A., Asymmetrical, Water-Soluble Phthalocyanine Dyes for Covalent Labeling of Oligonucleotides. *Bioconjugate Chemistry* **2002,** *13* (6), 1244-1252.

4. Braun, A. a. T., J., Über die Produkte der Einwirkung von Acetanhydrid auf Phthalamid. *Berichte der Deutschen Chemischen Gesellschaft* **1907,** *40*, 2709 - 2714.

5. de Diesbach, H.; von der Weid, E., Quelques sels complexes des o-dinitriles avec le cuivre et la pyridine. *Helvetica Chimica Acta* **1927,** *10* (1), 886-888.

6. Fukuda, T.; Kobayashi, N., UV-Visible Absorption Spectroscopic Properties of Phthalocyanines and Related Macrocycles. In *Handbook of Porphyrin Science*, Kadish, K. M.; Smith, K. M.; Guilard, R., Eds. World Scientific: Singapore, 2010; Vol. 9, pp 1-644.

7. Güzel, E.; Günsel, A.; Bilgiçli, A. T.; Atmaca, G. Y.; Erdoğmuş, A.; Yarasir, M. N., Synthesis and photophysicochemical properties of novel thiadiazole-substituted zinc (II), gallium (III) and silicon (IV) phthalocyanines for photodynamic therapy. *Inorganica Chimica Acta* **2017,** *467*, 169-176.

8. Saka, E. T.; Durmuş, M.; Kantekin, H., Solvent and central metal effects on the photophysical and photochemical properties of 4-benzyloxybenzoxy substituted phthalocyanines. *Journal of Organometallic Chemistry* **2011,** *696* (4), 913-924.

9. Göksel, M.; Durmuş, M.; Atilla, D., A comparative study on photophysical and photochemical properties of zinc phthalocyanines with different molecular symmetries. *Journal of Porphyrins and Phthalocyanines* **2012,** *16*, 895-906.

10. Dumoulin, F.; Durmuş, M.; Ahsen, V.; Nyokong, T., Synthetic pathways to water-soluble phthalocyanines and close analogs. *Coordination Chemistry Reviews* **2010,** *254* (23), 2792-2847.

11. Göksel, M.; Durmuş, M.; Atilla, D., Amino-functionalized water-soluble zinc phthalocyanines: Synthesis, photophysical, photochemical and protein binding properties. *Journal of Photochemistry and Photobiology A: Chemistry* **2013,** *266*, 37-46.

12. Hanack, M.; Schmid, G.; Sommerauer, M., Chromatographic Separation of the Four Possible Structural Isomers of a Tetrasubstituted Phthalocyanine: Tetrakis(2-ethylhexyloxy)phthalocyaninatonickel(II). *Angewandte Chemie International Edition in English* **1993,** *32* (10), 1422-1424.

13. Leznoff, C. C.; Hu, M.; McArthur, C. R.; Qin, Y.; van Lier, J. E., The syntheses of 2,9,16,23- and 1,8,15,22-tetrahydroxyphthalocyanines. *Canadian Journal of Chemistry* **1994,** *72* (9), 1990-1998.

14. Hu, M.; Brasseur, N.; Yildiz, S. Z.; van Lier, J. E.; Leznoff, C. C., Hydroxyphthalocyanines as Potential Photodynamic Agents for Cancer Therapy. *Journal of Medicinal Chemistry* **1998,** *41* (11), 1789-1802.

15. Ongarora, B. G.; Zhou, Z.; Okoth, E. A.; Kolesnichenko, I.; Smith, K. M.; Vicente, M. G. H., Synthesis, spectroscopic, and cellular properties of α-pegylated cis-A2B2- and A3B-types ZnPcs. *Journal of Porphyrins and Phthalocyanines* **2014,** *18* (10n11), 1021-1033.

16. Haruhiko, T.; Shojiro, S.; Shojiro, O.; Shinsaku, S., Synthesis of Phthalocyanines From Phthalonitrile With Organic Strong Bases. *Chemistry Letters* **1980,** *9* (10), 1277-1280.

17. Haruhiko, T.; Shojiro, S.; Shinsaku, S., Synthesis of Metallophthalocyanines From Phthalonitrile With Strong Organic Bases. *Chemistry Letters* **1983,** *12* (3), 313-316.

18. McInnes, C.; Sykes, B. D., Growth factor receptors: Structure, mechanism, and drug discovery. *Peptide Science* **1997,** *43* (5), 339-366.

19. Zeng, F.; Harris, R. C., Epidermal Growth factor, from gene organization to bedside. *Seminars in Cell & Developmental Biology* **2014,** *28*, 2-11.

20. Mendelsohn, J.; Baselga, J., The EGF receptor family as targets for cancer therapy. *Oncogene* **2000,** *19* (56), 6550-6565.

21. Zhang, X.; Gureasko, J.; Shen, K.; Cole, P. A.; Kuriyan, J., An Allosteric Mechanism for Activation of the Kinase Domain of Epidermal Growth Factor Receptor. *Cell* **2006,** *125* (6), 1137-1149.

22. Fry, D. W.; Kraker, A. J.; McMichael, A.; Ambroso, L. A.; Nelson, J. M.; R., L. W.; Conners, R. W.; Bridges, A. J., A Specific Inhibitor of the Epidermal Growth Factor Receptor Tyrosine Kinase. *Science* **1994,** *265* (5175), 1093-1095.

23. Jia, Y.; Yun, C.-H.; Park, E.; Ercan, D.; Manuia, M.; Juarez, J.; Xu, C.; Rhee, K.; Chen, T.; Zhang, H.; Palakurthi, S.; Jang, J.; Lelais, G.; DiDonato, M.; Bursulaya, B.; Michellys, P.-Y.; Epple, R.; Marsilje, T. H.; McNeill, M.; Lu, W.; Harris, J.; Bender, S.; Wong, K.-K.; Jänne, P. A.; Eck, M. J., Overcoming EGFR(T790M) and EGFR(C797S) resistance with mutant-selective allosteric inhibitors. *Nature* **2016,** *534*, 129 - 143.

24. Castelli, R.; Nicole, B.; Cavazzoni, A.; Bonelli, M.; Vacondio, F.; Ferlenghi, F.; Callegari, D.; Silva, C.; Rivara, S.; Lodola, A.; Digiacomo, G.; Fumarola, C.; Alfieri, R.; Petronini, P. G.; Mor, M., Balancing reactivity and antitumor activity: heteroarylthioacetamide derivateds as poten and time-dependent inhibitors of EGFR. *European Journal of Medicinal Chemistry* **2019,** *162*, 507-524.

25. Wang, S.; Song, Y.; Liu, D., EAI045: The fourth-generation EGFR inhibitor overcoming T790M and C797S resistance. *Cancer Letters* **2017,** *385*, 51-54.

26. Paez, J. G.; Jänne, P. A.; Lee, J. C.; Tracy, S.; Greulich, H.; Gabriel, S.; Herman, P.; Kaye, F. J.; Lindeman, N.; Boggon, T. J.; Naoki, K.; Sasaki, H.; Fujii, Y.;

Eck, M. J.; Sellers, W. R.; Johnson, B. E.; Meyerson, M., EGFR Mutations in Lung Cancer: Correlation with Clinical Response to Gefitinib Therapy. *Science* **2004,** *304* (5676), 1497-1500.

27. Yun, C.-H.; Boggon, T. J.; Li, Y.; Woo, M. S.; Greulich, H.; Meyerson, M.; Eck, M. J., Structures of Lung Cancer-Derived EGFR Mutants and Inhibitor Complexes: Mechanism of Activation and Insights into Differential Inhibitor Sensitivity. *Cancer Cell* **2007,** *11* (3), 217-227.

28. Shewchuk, L.; Hassell, A.; Wisely, B.; Rocque, W.; Holmes, W.; Veal, J.; Kuyper, L. F., Binding Mode of the 4-Anilinoquinazoline Class of Protein Kinase Inhibitor: X-ray Crystallographic Studies of 4-Anilinoquinazolines Bound to Cyclin-Dependent Kinase 2 and p38 Kinase. *Journal of Medicinal Chemistry* **2000,** *43* (1), 133-138.

29. Han, W.; Du, Y., Recent Development of the Second and Third Generation Irreversible Epidermal Growth Factor Receptor Inhibitors. *Chemistry & Biodiversity* **2017,** *14* (7), e1600372.

30. Wissner, A.; Fraser, H. L.; Ingalls, C. L.; Dushin, R. G.; Floyd, M. B.; Cheung, K.; Nittoli, T.; Ravi, M. R.; Tan, X.; Loganzo, F., Dual irreversible kinase inhibitors: Quinazoline-based inhibitors incorporating two independent reactive centers with each targeting different cysteine residues in the kinase domains of EGFR and VEGFR-2. *Bioorganic & Medicinal Chemistry* **2007,** *15* (11), 3635-3648.

31. Milik, S. N.; Lasheen, D. S.; Serya, R. A. T.; Abouzid, K., A. M., How to train your inhibitor: Design strategies to overcome resistance to Epidermal Growth Factor Receptor inhibitors. *European Journal of Medicinal Chemistry* **2017,** *142*, 131-151.

32. Adams, V. R.; Harvey, R. D., Histological and genetic markers for non-small-cell lung cancer: Customizing treatment based on individual tumor biology. *American Journal of Health-System Pharmacy* **2010,** *67* (1_Supplement_1), S3-S9.

33. Erdem, S. S.; Nesterova, I. V.; Soper, S. A.; Hammer, R. P., Mono-amine Functionalized Phthalocyanines: Microwave-Assisted Solid-Phase Synthesis and Bioconjugation Strategies. *Journal of Organic Chemistry* **2009,** *74* (24), 9280-9286.

34. Nesterova, I. V.; Erdem, S. S.; Pakhomov, S.; Hammer, R. P.; Soper, S. A., Phthalocyanine Dimerization-Based Molecular Beacons Using Near-IR Fluorescence. *Journal of the American Chemical Society* **2009,** *131* (7), 2432-2433.

Chapter 2. Phthalocyanine Fragment: Precedents and Synthesis

2.1. Zinc Phthalocyanine - Previous Work and Approaches to Synthesis

Previous studies[1,2] have demonstrated an increase in the emission of selectively functionalized Pcs, upon specific binding to biological molecules. Nesterova *et al*. prepared a “3+1” ZnPc, functionalized with one lysine residue and three triethylene glycol ether substituents (Figure 2.1), conjugated to a palindromic oligonucleotide sequence, and demonstrated an increase in fluorescence upon binding (dimerizing) to a complementary DNA chain, compared to the unbound Pc conjugate.[2] The self-aggregation properties of Pcs, combined with their increase in emission upon de-aggregation caused by binding to biopolymers, lends this class of compounds to serve as a signal transducing component of fluorescent sensors for biological molecules. This “turn-on” response is highly sought after in probe design, as it is easier to observe the appearance of a bright spot, than to look for a dim or dark spot, a so-called “turn-off” response. Phthalocyanines appear to not show a large change in emission due to non-specific binding with biological species. Such non-specific interactions are so transient that they do not induce de-aggregation of the Pc aggregates. Currently, there are no commercially available dyes with such inherent emissive behavior dependent on specific binding interactions.

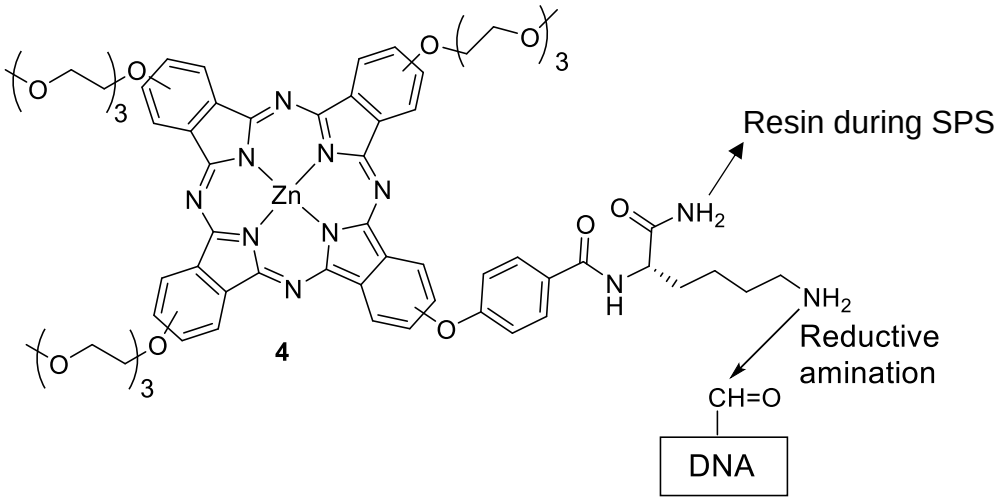

Figure 2.1. Zinc Phthalocyanine[1] for DNA Conjugation of Erdem *et al.*

Phthalocyanine synthesis is nominally a straightforward tetracyclization reaction (Scheme 2.1). However, in order to facilitate the formation of a required probe (also suitable for quantitative analysis), the Pc cannot be C_4 symmetric, but must possess only one quadrant that will be used to incorporate a specific binder to the target protein. In practice, formation of an unsymmetric Pc typically follows one of two strategies. The first strategy is a solution based method (Scheme 2.1) but the isolation of one isomer needs tedious chromatography. Chromatographic separation of Pc isomers is typically time-consuming and arduous due to the structural similarity of the isomers, arising from statistical condensation. The solution phase route is considered more expedient in the synthesis of the desired Pc but the ease of synthesis is contrasted with the effort to purify it. The second strategy is the solid phase synthesis (SPS) of the Pc which requires incorporating a mode of attachment to the resin that will not affect the ultimate probe performance. A resin-based synthesis (Scheme 2.2) enables the facile separation of the non-bound isomers, by washing the resin, prior to cleavage of the desired, resin-bound isomer. The attachment to the resin adds reaction steps to the synthesis,

including the protection/deprotection of functional groups that, if left unprotected, would not survive the reactions involving linkage to/detachment from the resin. These types of reactions are specific to each type of resin that could be used. Some are ether / ester based while others are amine / amide based.

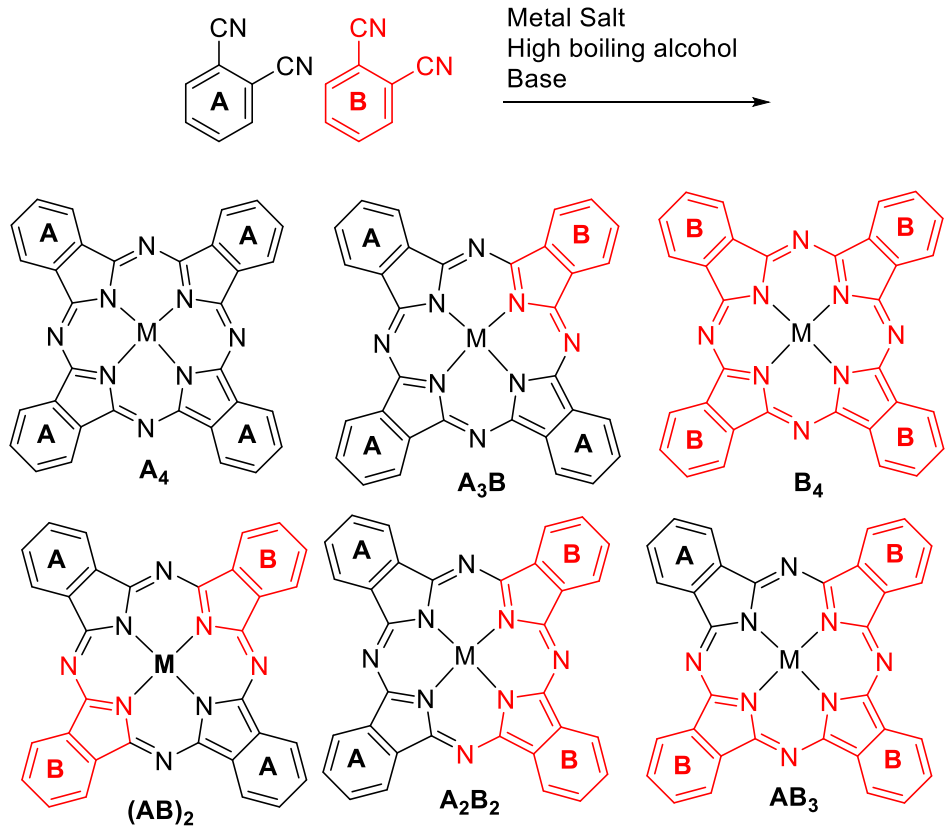

Scheme 2.1. Pcs via Statistical Condensation of Phthalonitriles

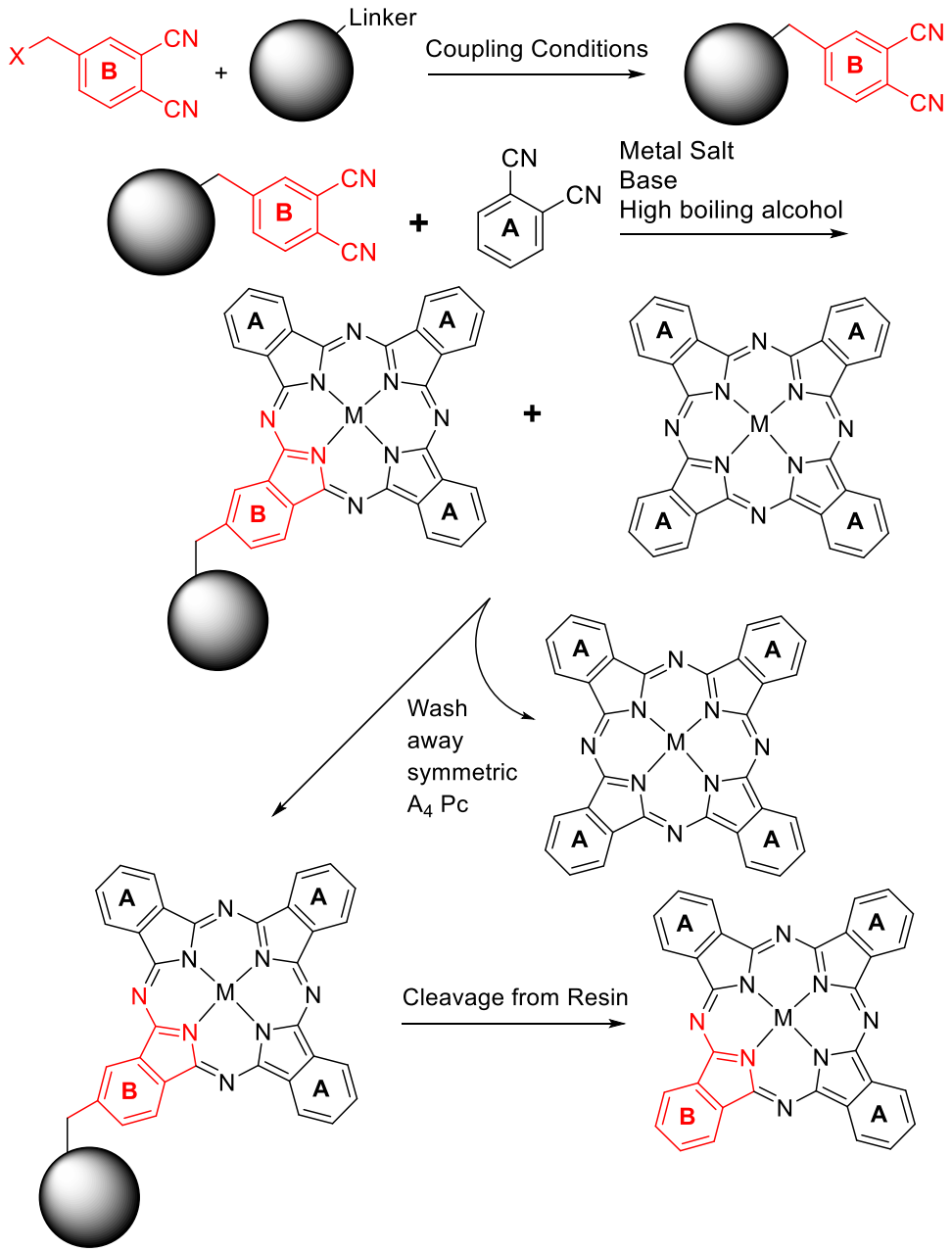

Scheme 2.2. Resin-Bound Formation of Phthalocyanine

The resin-bound synthesis of an unsymmetric Pc was first reported by Leznoff and coworkers in 1982.[3] Their synthesis was plagued by long (4 – 5 days) Soxhlet extractions to effectively wash away the unwanted symmetric Pc from the resin, and ultimately to extract the cleaved unsymmetric Pc from the resin.[4] Recovery from the resin was not good and additional purification of the extract, by chromatography, was

necessary. In a successful collaborative effort between Soper and Hammer groups (formerly at the LSU Department of Chemistry) to improve this synthesis, Erdem *et al*.[4] used a polyethylene glycol (PEG) resin rather than Leznoff's polystyrene, resulting in a more facile purification.

They also found[1] that microwave irradiation decreased the reaction time for Pc formation to less than an hour, and increased the crude yield by a factor of 2-3 compared to the same reaction performed by heating the reaction mixture in an oil bath for 24 hours. Their Pc (Figure 2.1, *vide supra*) was formed by condensation between triethylene glycol substituted phthalonitriles and a *p*-hydroxybenzoic acid functionalized phthalonitrile, that acted as the linkage point to a lysine residue. The use of a lysine residue (Figure 2.2) afforded three sites for functionalization: one to the resin through the lysine amide group; another to the benzoic acid phthalonitrile through the α-amino group, and lastly, the ε-amino group was used to conjugate the resultant Pc to their selected DNA-strand.

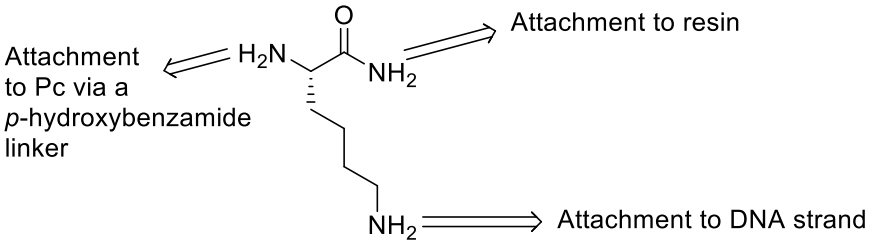

Figure 2.2. Lysine Lynchpin of Erdem *et al.*[1]

In designing the probe in the current work (Scheme 2.3), we embraced the Pc of Erdem *et al.*, as it has many elements that would serve well toward the overall goal of monitoring kinase activity. The lysine residue affords a hinge for the connection of the kinase probe and the Pc. Triethylene glycol monomethyl ether substituents would

enable solubility in aqueous and organic media due to their amphiphilic nature and had been shown to facilitate the transport of molecules through the cell lipid bilayer.[5-7] The latter capability is needed for intracellular studies, as the ATP binding site of EGFR is located inside the cell membrane. The fumarate moiety, along with the lysine side chain, provides a sufficient length linker between the Pc and quinazoline “anchor” group as well as acts as a Michael acceptor for a native cysteine residue that resides outside of the binding pocket of the kinase, thus presenting the possibility of covalent binding.

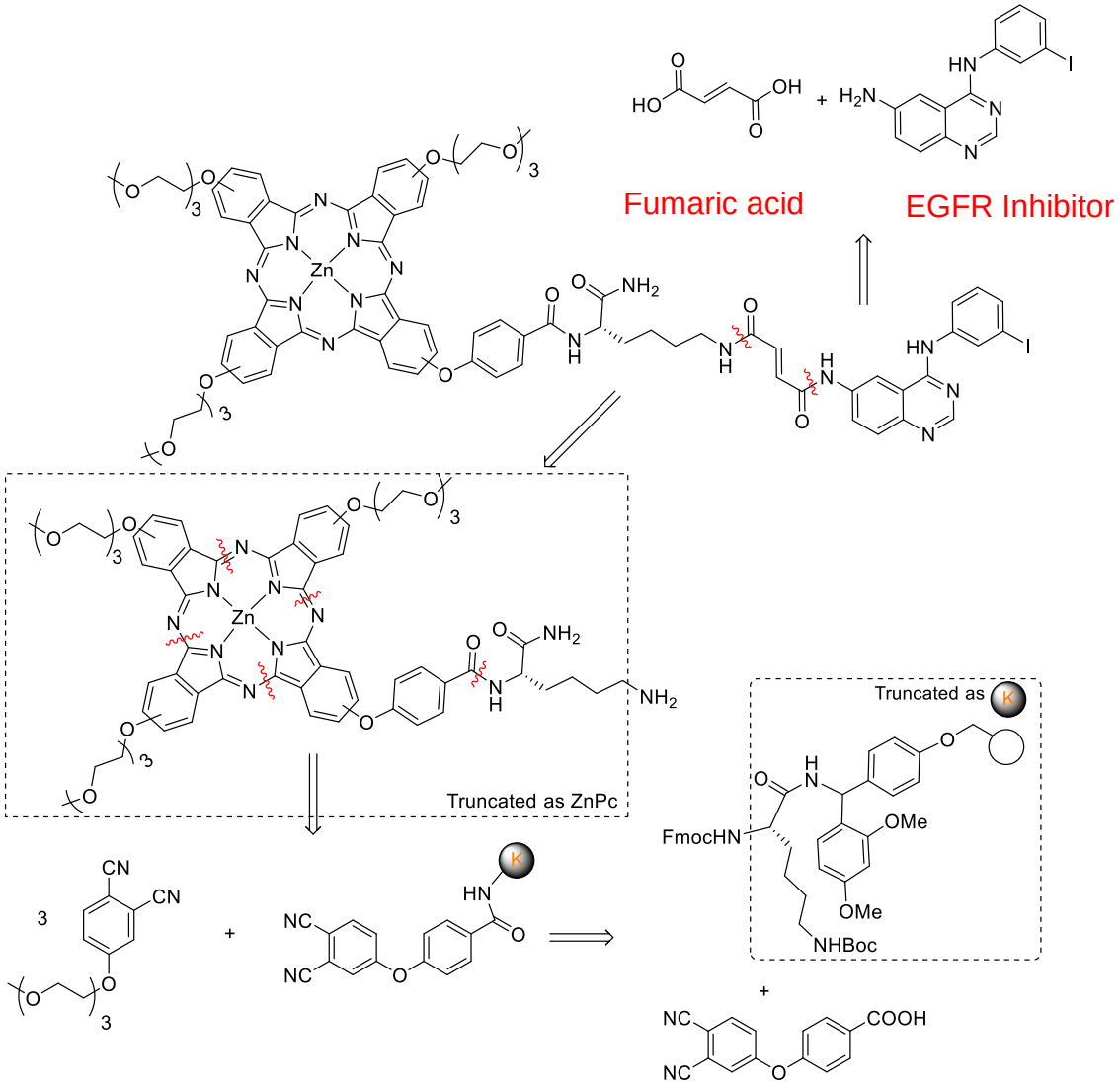

Scheme 2.3. Current Zinc Phthalocyanine Quinazoline Probe Design and Retrosynthetic Analysis

2.2. Synthesis and Data

2.2.1. Phthalonitriles

According to our retrosynthetic analysis, we required two different phthalonitriles: one functionalized for attachment to the resin, and one functionalized with a solubilizing group. Following the methods developed by the Soper and Hammer labs at LSU Chemistry,[1] we started from 4-nitrophthalonitrile, **5**, chosen for the compound's susceptibility to S_NAr type reactions which afforded the desired phthalonitriles in high yield. The water solubilizing triethylene glycol (TEG) group was incorporated to produce compound **6**.[4] In parallel, we also prepared phthalonitrile **7**[8] bearing a carboxylic acid (Scheme 2.4) as a means of attachment onto the resin.

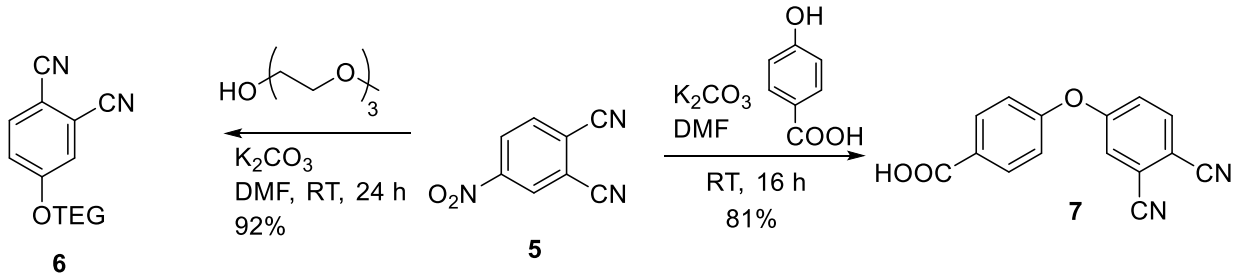

Scheme 2.4. Synthesis of Phthalonitrile Building Blocks **6** and **7** Required for Synthesis of Pc.

Challenges confronted in the formation and characterization of the ZnPc structure (*vide infra*) led us to consider an alternative modified synthetic route to Pc using disubstituted phthalonitriles (Scheme 2.5), which would allow avoiding constitutional isomers of the resultant Pc, and to simplify the resultant NMR spectra. The proposed synthesis of disubstituted phthalonitriles[9] started from 4,5-dichlorophthalic acid, that was first converted to its anhydride, **9**. Condensation with

formamide gave the 4,5-dichlorophthalimide, **10**. The imide was then formally dehydrated to give the requisite 4,5-dichlorophthalonitrile, compound **12**. Unfortunately, this synthesis was not as straightforward as we initially expected. Purification issues, during our execution of this scheme, were protracted enough that Pc formation via SPS, identification, and coupling issues (*vide infra*) were resolved before the formation of the disubstituted phthalonitrile was complete. Fortunately, during the course of this work, a local source was willing to donate 4,5-dichlorophthalonitrile (**12**) originally considered prohibitive due to cost ($159.00 / 5 g). The commercially-sourced material was thus in-hand, to make the octasubstituted Pc if desired.

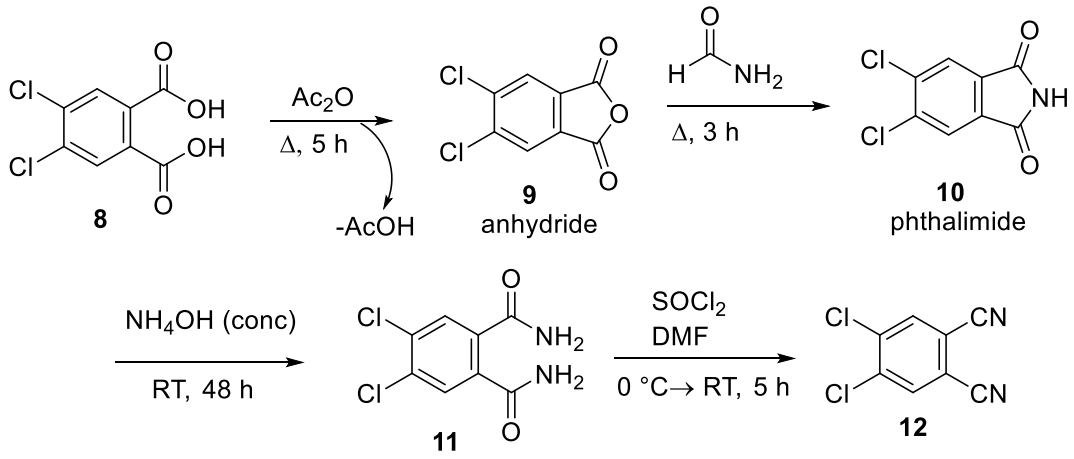

Scheme 2.5. Disubstituted Phthalonitrile Synthesis[9]

2.2.2. Symmetric Zinc Phthalocyanine Solution Synthesis

As a control, the fully symmetric Pc, with four triethylene glycol solubilizing groups, was easily synthesized. This was done using phthalonitrile **6** and $Zn(OAc)_2$ in DMF and *n*-butanol (Scheme 2.6).

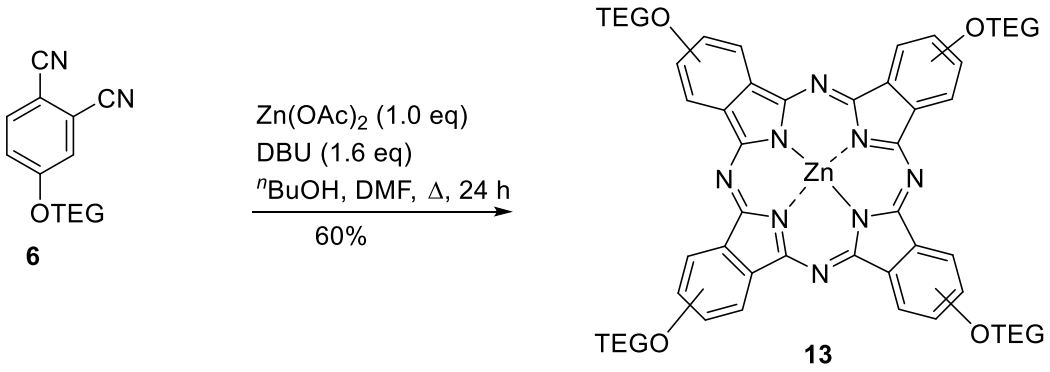

Scheme 2.6. Symmetrical Pc Formation

2.2.3. Resin Functionalization in Preparation for Synthesis of Unsymmetric Pc

Attention was next directed toward the attachment of phthalonitrile **7** to the resin (Scheme 2.7). Rink amide resin was employed in order to render a primary amide upon cleavage from the resin (Scheme 2.3, *vide supra*). Following the literature precedent,[1] the ***ε***-(4-methyltrityl) (Mtt) protected lysine residue was attached to the Rink amide resin through standard peptide coupling conditions, using the guanidinium reagent hexafluorophosphate benzotriazole tetramethyl uronium (HBTU) and the additive hydroxybenzotriazole (HOBt; Figure 2.3, Scheme 2.7). Unreacted amine was capped via acetylation and the resin's loading capacity was estimated by removal of the Fmoc protecting group from the α-amino group of lysine and measuring the absorbance of the filtrate at 300 nm.[1] The Fmoc group removal enabled further functionalization of the lysine by the benzoic acid functionalized phthalonitrile **7**.

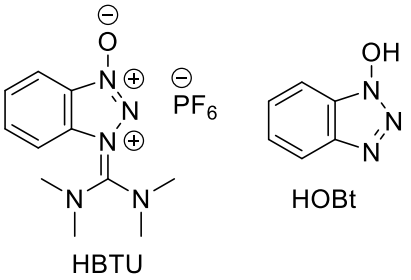

Figure 2.3. Structures of HBTU and HOBt

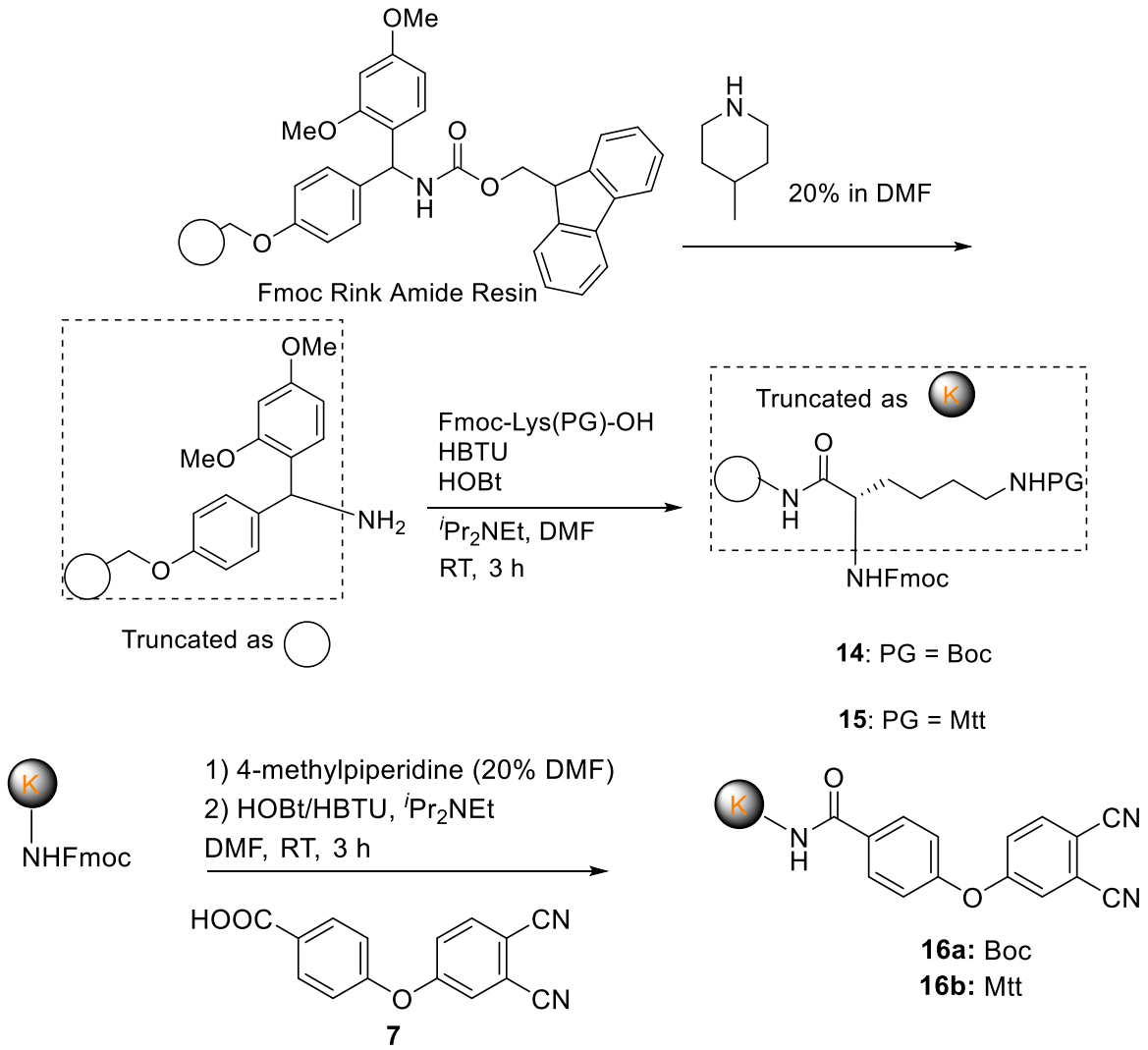

Scheme 2.7. Rink Amide Resin Functionalization with a Phthalonitrile **7**

Erdem *et al.* chose the Mtt group for protection of the lysine ε-amino group instead of Boc, to minimize the possibility of *n*-butanol transcarbamylation which would

have resulted in an uncleavable ε-amine protecting group (Scheme 2.8). Since transcarbamylation was not an issue in our situation due to the use of DMF instead of *n*-butanol as the main solvent, we pursued the *tert*-butyloxycarbonyl (Boc) protecting group for N-ε-Lys in parallel. In our approach, the unreacted amino group on the Lys(Boc) functionalized resin **14** were not capped, as was done previously by Erdem, but we used the Kaiser ninhydrin test[10] to monitor for the presence of free amine on the resin to determine when the reaction was complete.

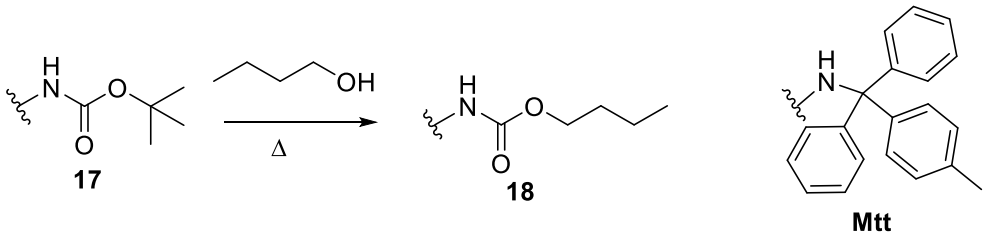

Scheme 2.8. Transcarbamylation of ε-Amine and Mtt Structure

2.2.4. Solid Phase Synthesis of the Unsymmetric Pc

2.2.4.1 Overview of the Previous Work

Erdem *et al.* showed that microwave irradiation vastly improved yields and reduced reaction time for the cyclotetramerization reaction to form the Pc **4**.[1] They used a Rink amide resin with a loading capacity of 0.52 mmol/g and attached the Fmoc-Lys(Mtt)-OH through guanidinium activation, using HBTU/HOBt, with subsequent capping of unreacted amine functionality on the resin with acetic anhydride. They found that capping of the resin was necessary to reduce site-site interactions between resin beads to minimize yields of congeners of the Pc.[4,11,12] Cleavage of the Fmoc group afforded the free α-amine of lysine which reacted with carboxylic phthalonitrile **7**,

activated using the HBTU/HOBt conditions. Resin loading was determined by cleaving the Fmoc group from a small amount of Fmoc-Lys(Mtt)-resin (~50 mg) and measuring the absorption of the fluorene-containing filtrate at 300 nm. Following attachment of the phthalonitrile monomer, the Pc was formed by addition of the second monomer (**6**), zinc metal salt, and using microwave irradiation at 850 W to maintain a temperature of 150 °C for 40 minutes. The resin was then washed thoroughly with hot *n*-butanol and dichloromethane to remove the symmetrical Pc then the resin was suspended in a cleavage solution composed of dichloromethane (78%), trifluoroacetic acid (TFA, 20%), and triisopropylsilane (TIPS, 2%). This afforded the desired Pc in 15 – 27% yield, following purification by HPLC. The molecular formula of the product was verified by mass spectrometry using Matrix Assisted Laser Desorption Ionization (MALDI).

2.2.4.2. Zinc Phthalocyanine Synthesis on Solid Support – This Work

Our research began with attempts to replicate this earlier work. The microwave reactor available to us had two power settings: 800 W and 1600 W. In an effort to satisfy concerns for the safety of the instrument, the initial trial was run at 100 °C but with all other parameters as reported. No product was isolated. The reaction was repeated at 150 °C, with no improvement. Changes in heating source (oil bath) and power setting (up to 1600 W) did not afford the desired product. Employing a resin with a higher loading capacity (0.61 mmol/g) did not give any advantage, nor did the composition of the cleavage solution (increasing the TFA content to 95/2.5/2.5; TFA/CH_2Cl_2/TIPS). The product mixture from the reaction, run with the microwave set at 1600 W, was a complex mixture arising from degradation. This could have been attributed to the high TFA concentration, the higher wattage, or a combination of both. The masses recovered

from the reactions were only 7 – 12% of the starting material and the complex mixtures were difficult to characterize by NMR.

2.2.5. Zinc Phthalocyanine Formation in Solution

Due to difficulties encountered with the resin-bound synthesis, we began to investigate, in parallel, the formation of the Pc by solution-based statistical condensation (Scheme 2.9), followed by chromatographic isolation and purification of products. In this way, we were able to obtain the desired product in as much as 18% yield (on a 20 mg scale). Unfortunately, attempts to carry out this protocol on a larger scale met with limited success as the highest yielding reaction (150 mg) gave only a 6% yield of the Pc, **19**.

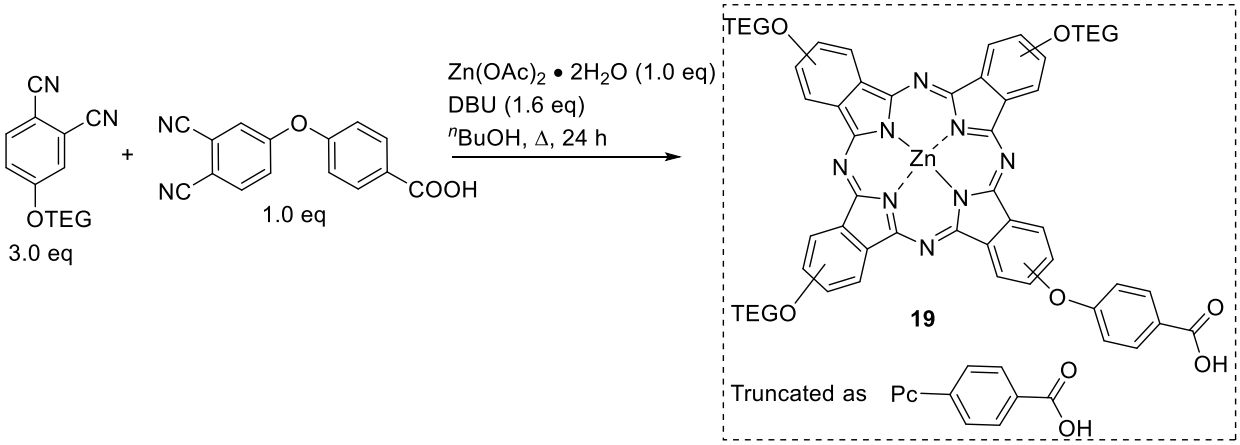

Scheme 2.9. Solution Synthesis of Benzoic Acid Functionalized Phthalocyanine **19**

Despite this low yield, we forged ahead with the material in hand. We were able to identify peaks in the proton NMR that integrated in appropriate ratios (3:1, TEG: Aromatic). A mono-protected bi-functional linker, of similar length to lysine, was found in *N*-Boc-1,6-hexanediamine. This diamine was chosen over lysine, as the amines were sufficient to link the Pc and our inhibitor. The additional amide functionality, used

previously for attachment to the solid support, was redundant in the current context. The synthesis (Scheme 2.10) started with the conversion of the benzoic acid functionalized Pc **19** to the corresponding acid chloride. The acylating agent was reacted with *N*-Boc-1,6-hexanediamine to yield **21,** after isolation via preparative TLC. The low yield and difficulty extracting **21** from the silica gel led us to abandon this route.

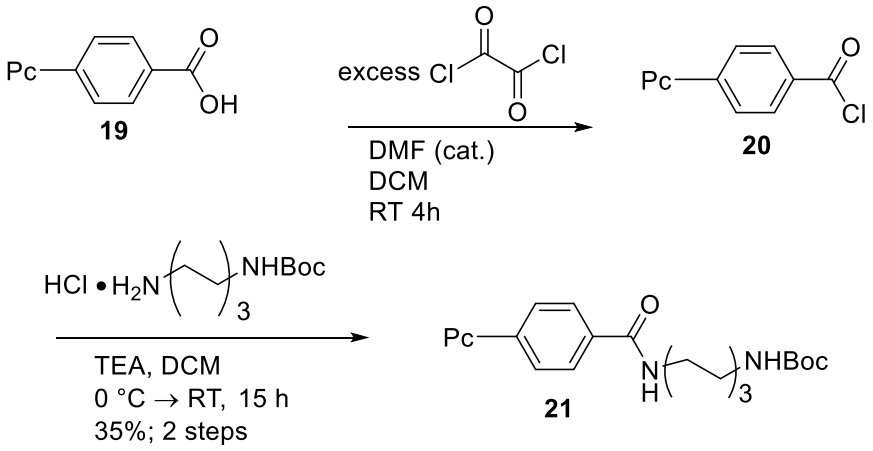

Scheme 2.10. Acid Chloride Mediated Amide Bond Formation

2.2.6. Return to Synthesis on the Solid Support: Solvent and Metal Salt Studies

With the solution phase synthesis also proving challenging, we turned back to looking at modifying reaction parameters in the SPS. *N*-Methylpyrrolidone (NMP) was chosen for its similarity to DMF in structure and properties. However, while DMF degrades to dimethylamine and carbon monoxide on heating; NMP does not. NMP proved an excellent solvent for swelling the resin and, as such, promised high interaction of all surface area to facilitate Pc formation. Unfortunately, little product was isolated. Following cleavage of the product from the resin (TFA/TIPS/CH_2Cl_2; 95%:2.5%:2.5%), the filtrate was a red-orange color, rather than the expected deep blue-green color characteristic of phthalocyanine. One reaction using NMP did provide a

green-colored material after washing the resin with DMF, dichloromethane, and methanol, but we found it difficult to completely remove the solvent. The ^{1}H NMR spectrum of the green colored material showed mostly unreacted phthalonitrile **6**, along with unidentified impurities. Closer inspection of the literature showed that high concentrations (>70%) of TFA could degrade the Pc during detachment from the resin;[1] this had been a mistake.

Careful analysis of the previous procedures revealed some preference for using anhydrous zinc salts, rather than the dihydrate, in a dry solvent. We therefore switched to an available anhydrous zinc salt [$Zn(OTf)_2$], instead of $Zn(OAc)_2 \cdot 2H_2O$, in order to probe the impact of water on the reaction (Scheme 2.11). A small-scale reaction gave a crude yield of 93% of a green solid. The cleavage cocktail was reverted back to [20:78:2 TFA/DCM/TIPS] giving more consistent yields. Less TFA simplified workup procedures and prevented degradation of the Pc. Upon purification by column chromatography, a blue-green solid was obtained in 21% yield. The solid demonstrated satisfactory ^{1}H NMR and high resolution mass spectrometry using electron spray ionization (HRMS-ESI) giving the $[M+2H]^{2+}$ peak for compound **4.**

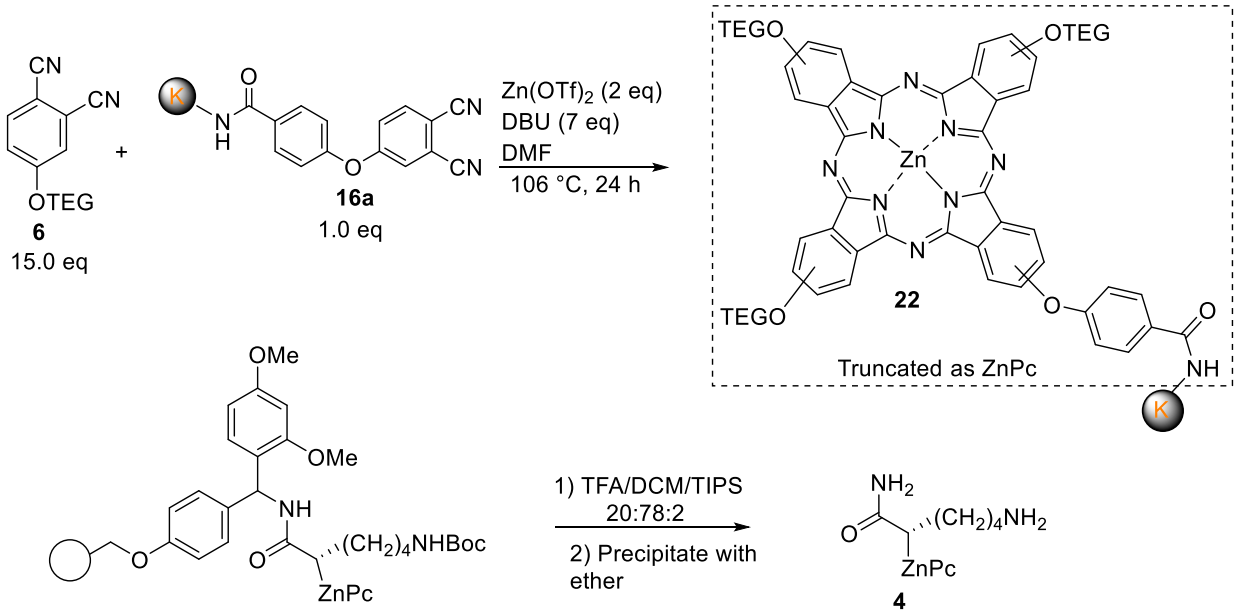

Scheme 2.11. Anhydrous Zinc (II) Triflate Phthalocyanine Reaction

In a subsequent development, the triflate salt was replaced with the anhydrous acetate salt under the above conditions, with the addition of *n*-butanol to act as the catalytic alkoxide to start the formation of the cyclotetramerization. This gave a 51% yield upon cleavage and isolation, though the elemental analysis was not satisfactory, in spite of filtering to remove any inorganic impurities. Mass spectrometry of the product detected the $[M+2H]^{2+}$ dication peak and the Pc could be purified by silica gel chromatography to yield satisfactory NMR spectra. Use of a large batch of resin gave insight into the effect of TFA concentration on the cleaved product. Refrigerated resin-bound ZnPc-NH_2 (**22**) was periodically cleaved using a stock cleavage solution; that was later found to have a much higher TFA concentration than initially made. The HRMS data showed appearance of a peak around *m/z* 1426 that could be assigned to the "A_2B_2" congener, possessing 2 resin bound phthalonitriles (**16a**) that required higher TFA concentration to be cleaved. This product was formed due to site-site interaction that has been well documented in polymer resin synthesis.[4,11] Nuclear magnetic

resonance experiments were conducted on the Pc **4** solid in deuterated dimethylformamide. The ^{1}H spectrum showed satisfactory integration and peak profiles for the desired "AB_3" congener. The absorbance spectrum of the product, as a solution in methanol, was recorded (Figure 2.4). There were the two expected maxima corresponding o the Soret and Q bands. The fluorescent spectrum of the ZnPc compound **4** displayed a narrow emission band with a small Stokes shift, which was nearly mirror symmetrical to the Q-band in the absorption spectrum.

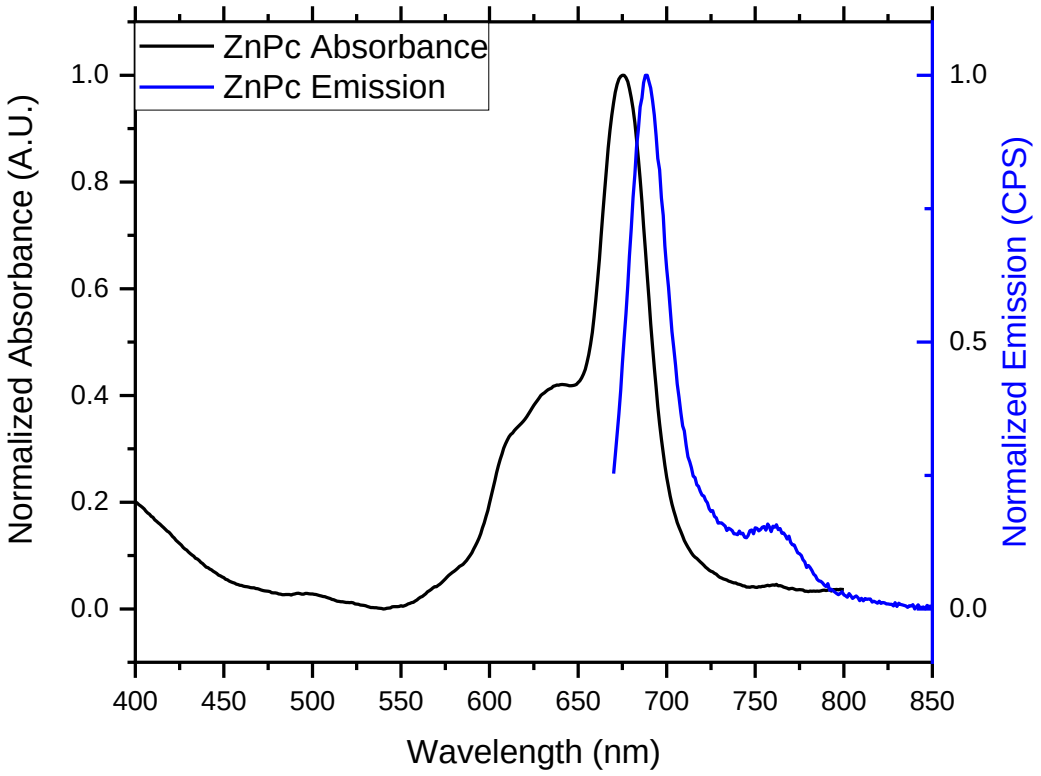

Figure 2.4. Photoluminescent Spectra of the Q-Band Region of Zinc Phthalocyanine (**4**) at 63 μM in MeOH

We also carried out more detailed studies of the influence of water-methanol solvent composition on the aggregation state of ZnPc **4**. As expected, in 100%

methanol there was a Q-band at approx. 676 nm (Figure 2.4). This bathochromically shifted Q-band corresponds to non-aggregated state of Pc chromophore. Upon increasing fraction of water (PBS buffer), we observed gradual disappearance of the non-aggregated state absorption band, and rise of the hypsochromically shifted absorption band corresponding to aggregated state of the ZnPc chromophore. Upon aggregation in aqueous conditions, Pc compounds tend to form H aggregates resulting from face-to-face stacking of the planar hydrophobic Pc units.[13] Formation of H-aggregates makes the lowest energy S_0-S_1 transition symmetry forbidden, and produces the bathochromic shift of the absorption band. In addition, H-aggregates are characterized by significantly lower extinction coefficients, associated with much lower absorbance values. Such changes were indeed observed in the case of ZnPc compound **4** (Figure 2.5) providing a convincing evidence that this new molecule can indeed act as a signal generating/transducing elements for our sensor design. Satisfied that we had finally obtained the Pc macrocycle and observed its aggregation/de-aggregation behavior in aqueous-organic media, we shifted our attention toward the design and preparation of the quinazoline “anchor”, as well as coupling it to the ZnPc unit. These attempts will be described in Chapter 3.

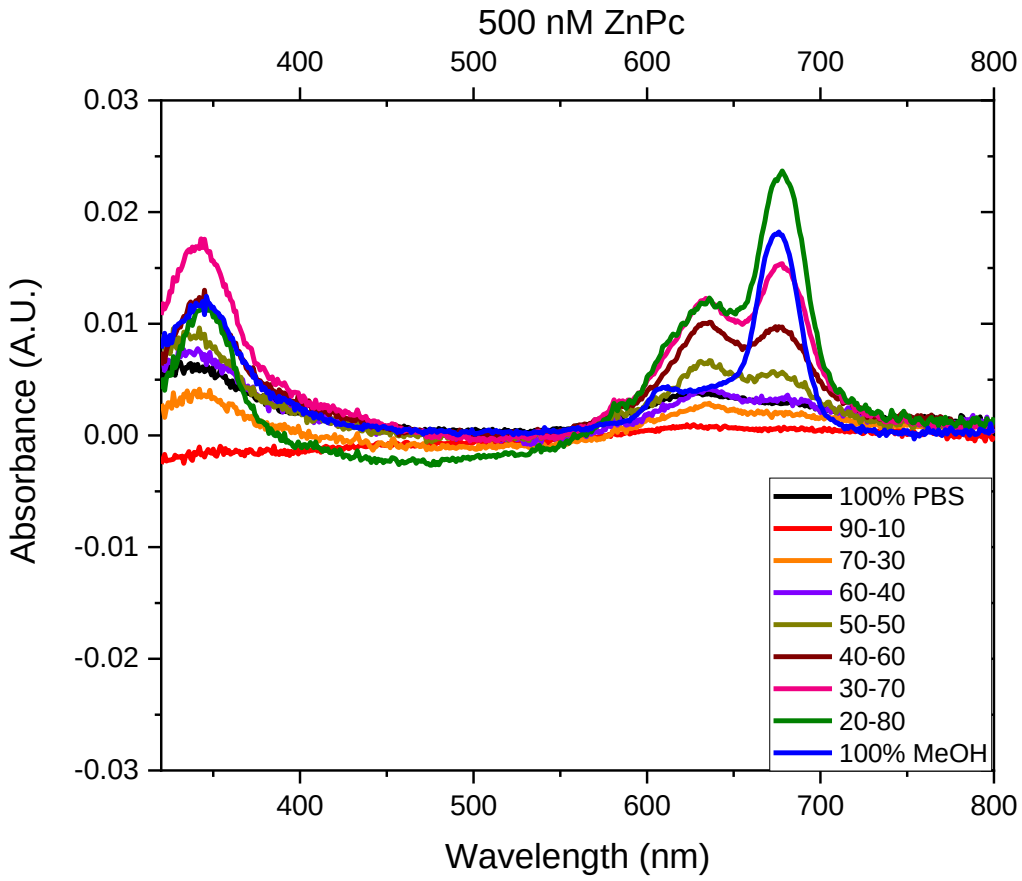

Figure 2.5. Absorption of ZnPc **4** Dependent upon Solvent at 500 nM in Phosphate Buffered Saline vs MeOH

2.3. Notes

1. Erdem, S. S.; Nesterova, I. V.; Soper, S. A.; Hammer, R. P., Mono-amine Functionalized Phthalocyanines: Microwave-Assisted Solid-Phase Synthesis and Bioconjugation Strategies. *Journal of Organic Chemistry* **2009,** *74* (24), 9280-9286.

2. Nesterova, I. V.; Erdem, S. S.; Pakhomov, S.; Hammer, R. P.; Soper, S. A., Phthalocyanine Dimerization-Based Molecular Beacons Using Near-IR Fluorescence. *Journal of the American Chemical Society* **2009,** *131* (7), 2432-2433.

3. Leznoff, C. C.; Hall, T. W., The synthesis of a soluble, unsymmetrical phthalocyanine on a polymer support. *Tetrahedron Letters* **1982,** *23* (30), 3023-3026.

4. Erdem, S. S.; Nesterova, I. V.; Soper, S. A.; Hammer, R. P., Solid-Phase Synthesis of Asymmetrically Substituted “AB3-Type” Phthalocyanines. *Journal of Organic Chemistry* **2008,** *73* (13), 5003-5007.

5. Ongarora, B. G.; Hu, X.; Verbern-Sutton, S. D.; Garno, J. C.; Vicente, M. G. H., Synthesis and Photodynamic Activity of Pegylated Cationic Zn(II)-Phthalocyanines in HEp2 Cells. *Theranostics* **2012,** *2* (9), 850-870.

6. Liu, J.-Y.; Jiang, X.-J.; Fong, W.-P.; Ng, D. K. P., Highly photocytotoxic 1,4-dipegylated zinc(II) phthalocyanines. Effects of the chain length on the in vitro photodynamic activities. *Organic & Biomolecular Chemistry* **2008,** *6* (24), 4560-4566.

7. Bai, M.; Lo, P.-C.; Ye, J.; Wu, C.; Fong, W.-P.; Ng, D. K. P., Facile synthesis of pegylated zinc(II) phthalocyanines via transesterification and their in vitro photodynamic activities. *Organic & Biomolecular Chemistry* **2011,** *9* (20), 7028-7032.

8. Synak, A.; Gil, M.; Organero, J. A.; Sánchez, F.; Iglesias, M.; Douhal, A., Fast to Ultrafast Dynamics of Palladium Phthalocyanine Covalently Bonded to MCM-41 Mesoporous Material. *Journal of Physical Chemistry C* **2009,** *113* (44), 19199-19207.

9. Wöhrle, D.; Eskes, M.; Shigehara, K.; Yamada, A., A Simple Synthesis of 4,5-Disubstituted 1,2-Dicyanobenzenes and 2,3,9,10,16,17,23,24-Octasubstituted Phthalocyanines. *Synthesis* **1993,** *1993* (02), 194-196.

10. Chan, W. C.; White, P. D., *Fmoc Solid Phase Peptide Synthesis A Practical Approach*. Oxford University Press: New York, 2000.

11. Shi, R.; Wang, F.; Yan, B., Site–Site Isolation and Site–Site Interaction – Two Sides of the Same Coin. *International Journal of Peptide Research and Therapeutics* **2007,** *13* (1), 213-219.

12. Poeylaut-Palena, A. A.; Mata, E. G., Unravelling the olefin cross metathesis on solid support. Factors affecting the reaction outcome. *Organic & Biomolecular Chemistry* **2010,** *8* (17), 3947-3956.

13. Liu, W.; Jensen, T. J.; Fronczek, F. R.; Hammer, R. P.; Smith, K. M.; Vicente, M. G. H., Synthesis and Cellular Studies of Nonaggregated Water-Soluble Phthalocyanines. *Journal of Medicinal Chemistry* **2005,** *48* (4), 1033-1041.

Chapter 3. Synthesis of Quinazoline Inhibitor and Conjugation to Phthalocyanine Fragment

3.1. Quinazoline-Based Inhibitor Selection and Design

The identification of epidermal growth factor (EGF) and, later, isolation and purification of the receptor by Stanley Cohen, transformed researchers' understanding of how the overexpression of epithelial cell growth related to certain cancers.[1,2] Fry *et al.* made the key discovery of a quinazoline-based inhibitor[3] of EGFR in 1994. There have been many designs and structure-activity relationship studies to determine aspects of inhibitor structure that most influence their activity.

Crystallographic data of the EGFR (and related kinase proteins) show a high degree of conservation of the ATP binding site across protein tyrosine kinases.[4-6] The data for EGFR-quinazoline complexes (e.g. Figure 3.1) shows strong interactions between the side chains of active site residues and the quinazoline inhibitor. Notably, the pyrimidine nitrogens and the 4-anilino substituent, make the quinazoline molecule highly favorable as an effective binder of EGFR and related kinases.[6] These structures showed that the 6-position of the quinazoline (Scheme 3.1) is exposed to solvent (Figure 3.1) which facilitates inclusion of secondary binding sites[7] and could be harnessed to help monitor the binding through radiological[8,9] or emissive methods.[10,11]

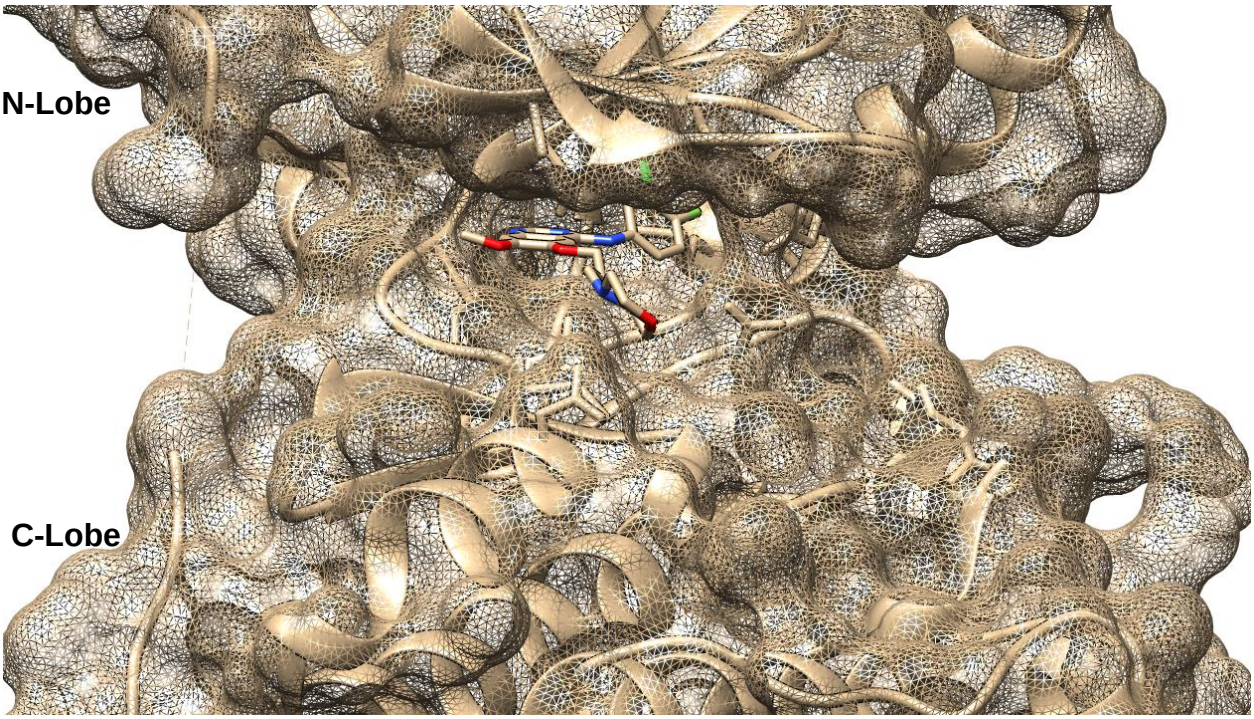

Figure 3.1. Gefitinib Inhibitor bound to L858R Mutant of EGFR. PDB File 2ITZ

Shaul *et al*.[8] described a straightforward synthesis (Scheme 3.1) of a quinazoline-based inhibitor, in their pursuit of an iodine bioprobe for the use in positron emission tomography (PET). They discovered that an acrylamide (**28**, intended to react with C797 near the active site and thereby increase efficacy) is readily metabolized *in vivo*, resulting in poor bioavailability of such inhibitors and increased cytotoxicity. However, the more hindered *N,N*-dimethylaminobut-2-enamide (compound **27**; red circle) was less likely to be consumed in metabolic pathways (before attaching to the ATP binding kinase via a Michael addition with C797), and showed little to no decrease in inhibition 8 hours after injection; giving an IC_{50} value of 5 nM against A431 cell lysates. A431 cells overexpress wild type EGFR and are traditionally used to test inhibitor efficiency.[8,12] Pal *et al.*[9] expanded on Shaul's work, substituting in the fumaric diamide linked morpholine "side chain" (compound **31**), in an effort to design a non-

invasive radiolabel for PET imaging of EGFR activity (Scheme 3.2). Compound **31** demonstrated an IC_{50} value of 0.6 nM *in vitro* and 0.096 μM in A431 cells.

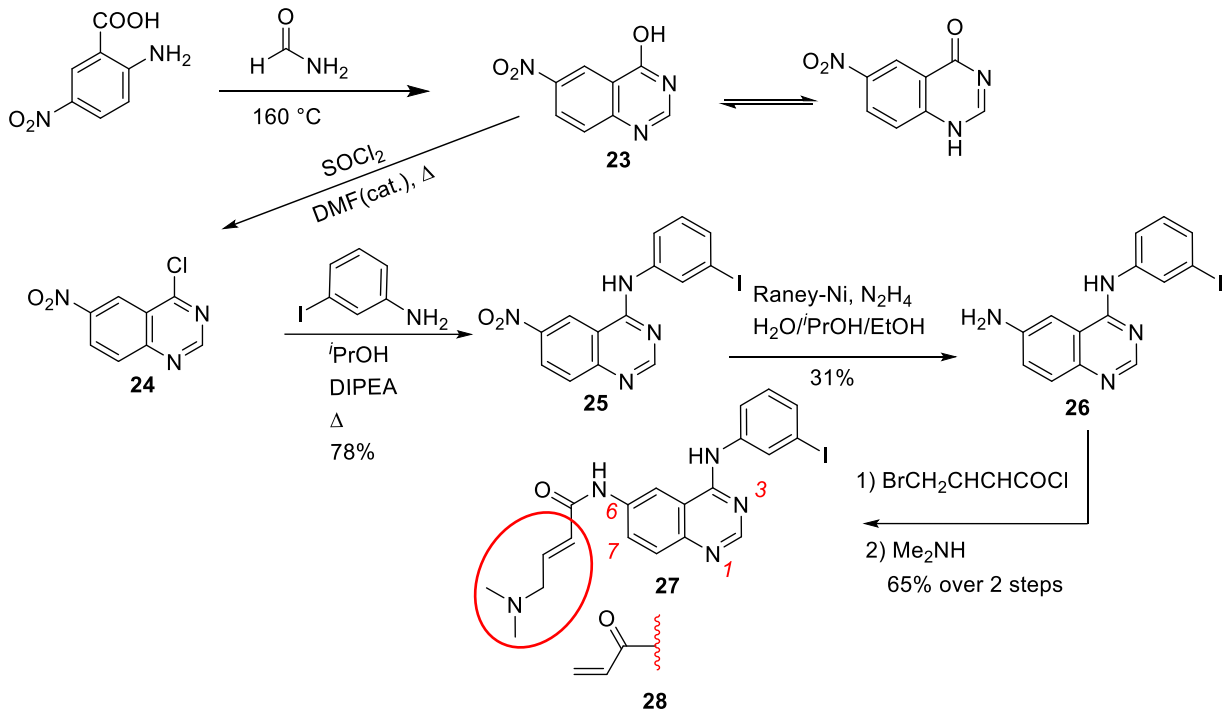

Scheme 3.1. Synthesis of Quinazoline **27** by Shaul *et al.*[8]

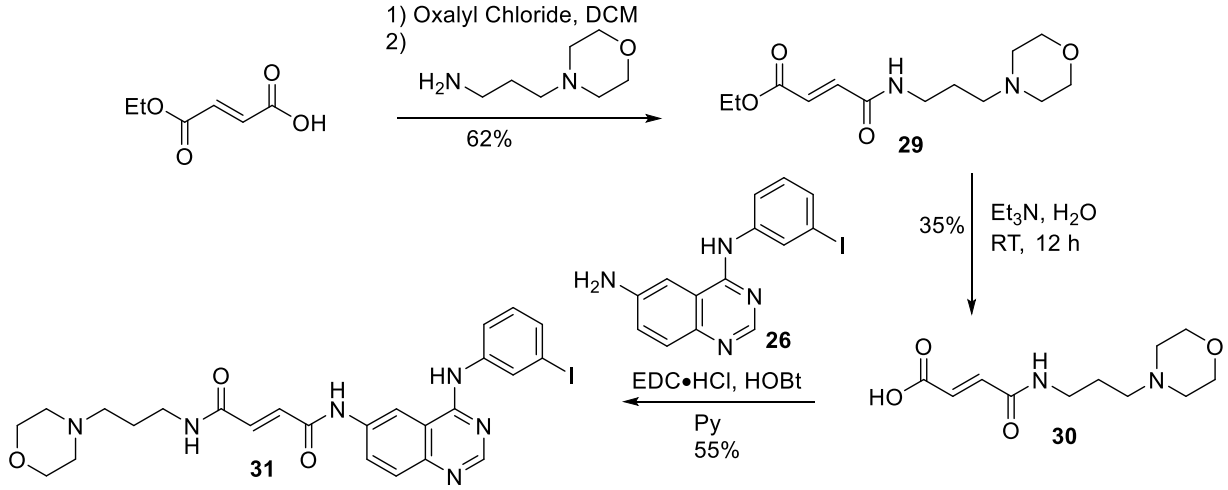

Scheme 3.2. PET Radiolabel Synthesis of **31** by Pal *et al.*[9]

Our goal is to design a probe with moderate binding affinity, that could be displaced by a more effective inhibitor, and simultaneously incorporate the zinc

phthalocyanine fluorophore (Schemes 3.3 & 2.3). The initial synthesis of the quinazoline portion of the probe would follow the work of Shaul[8] and Pal[9] in order to synthesize an irreversible binding probe. We envisioned use of a butenamide linker, anticipating higher selectivity toward EGFR and higher response values when the probe is bound to the kinase. By analogy to Pal's work, use of the (*E*)-butenoic acid would yield a ready point-of-attachment for our fluorophore. We envisioned (Scheme 3.3) an amidation reaction between fumaric acid and the aminoquinazoline. This aminoquinazoline could be formed from the reaction of the iodoaniline and the nitroquinazoline, followed by a chemoselective reduction of the nitro group. The nitroquinazoline could be formed by reaction of formamide with 5-nitroanthranilic acid.

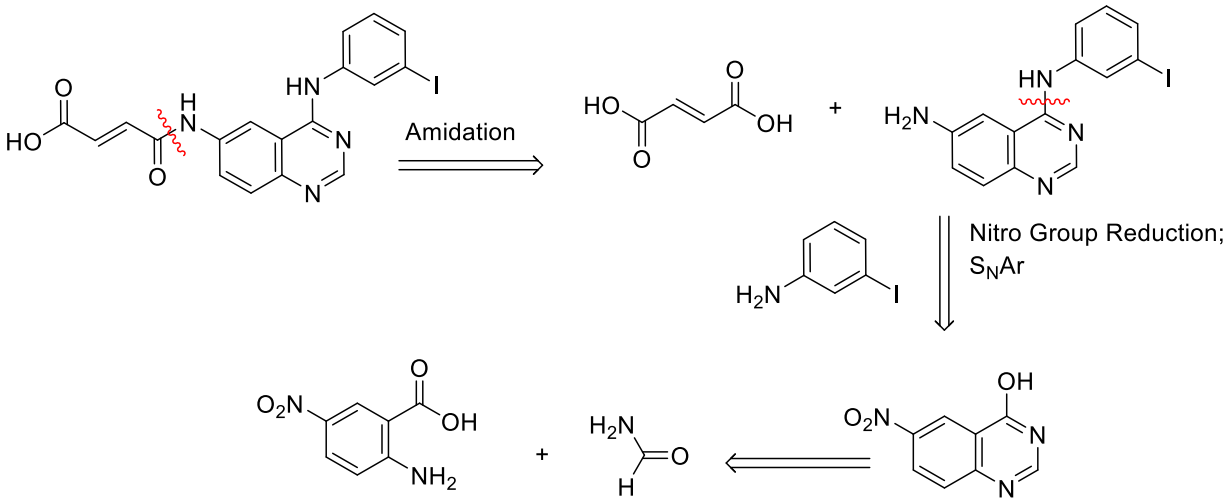

Scheme 3.3. Retrosynthetic Analysis of Quinazoline Inhibitor and Fumarate Linker

3.2. Synthesis of the Quinazoline

While Shaul gave experimental details to carry out the synthesis from **24** to their final product **27**; they referred to earlier literature reports for the synthesis of **23** (Scheme 3.1).[13] A modern version of this synthesis was found in the paper Hou *et al.*[14] and enabled us to readily synthesize quinazolone **23** (Scheme 3.4). Reaction of the quinazolone with thionyl chloride appeared to be successful but difficulties were encountered in the workup. Hou *et al.*[14] advocated treatment with ice-cold methanol; in our experience this quenching was violently exothermic and caused hydrolysis of the product back to the quinazolone with isolation of only trace amounts of the desired chlorinated quinazoline, **24**. Shaul *et al.*[8] recommended removal of excess thionyl chloride through vacuum distillation; we found this to be effective. The residual material could be coupled with the 3-iodoaniline to afford the quinazoline (**25**); although, we added *N,N*-diisopropylethylamine (DIPEA, Hünig's Base) to facilitate this nucleophilic substitution.

In our hands, the real stumbling block in the synthesis of aminoquinazoline **26** was the chemoselective reduction of the nitro group; achieved in 31% yield by Shaul *et al.* In the present work, treatment of **25** with Raney nickel and hydrazine led to simultaneous reduction of the nitro group and cleavage of the Ar-I bond, giving compound **32** (Scheme 3.4) in 69% yield. Proton NMR spectra of the isolated product featured splitting patterns not consistent with starting material **25** or product **26**, exhibiting an extra aromatic signal.[8,9] Variations in the amount of hydrazine and Raney nickel, and reaction temperature, altered the yield of the dehalogenated compound **32**, but the desired product was never obtained. It is likely that the chemoselectivity

observed by Shaul *et al*. was a function of the quality and reactivity of the catalyst that was notably different to that obtained from Aldrich in 2015. Alternative reduction methodologies were then sought. An initial trial using palladium on carbon, and 25 psi of hydrogen gas, also gave the fully reduced product **32**, in 87% yield.

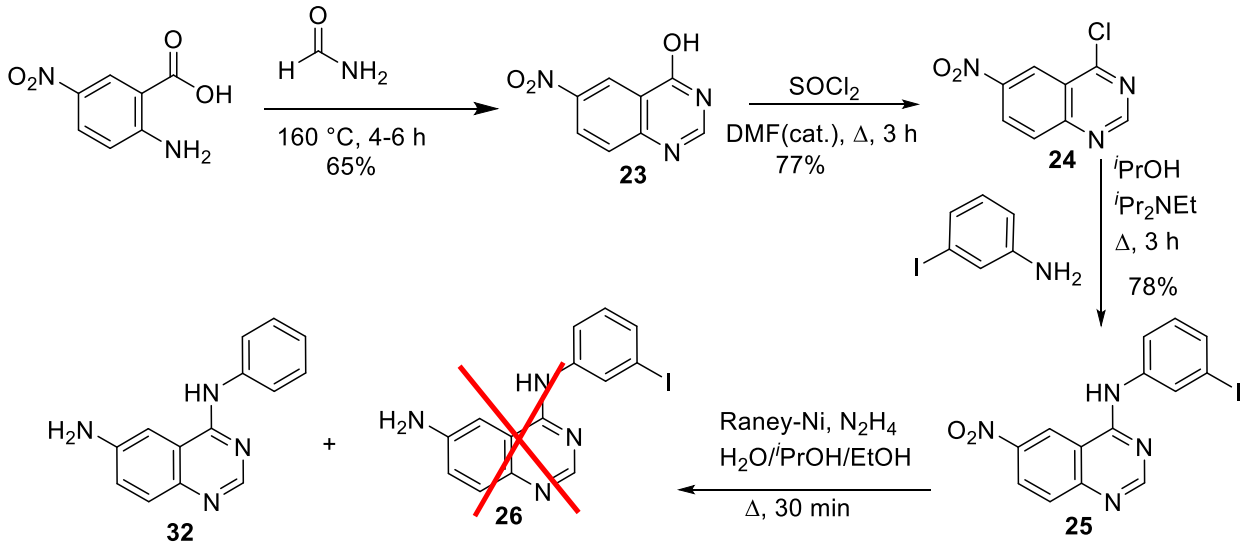

Scheme 3.4. Preliminary Attempts to Synthesize Quinazoline **26**

We found examples in literature which allowed reduction of the nitro group in the presence of an aryl-halogen bond. Van Dort *et al.*[15] reported the reduction of a nitrobenzonitrile **33** to iodoanline **34** with tin (II) chloride. Cao *et al*.[16] described the reduction of sterically hindered nitrobenzene **35** to afford aniline **36**. Even more relevant, Kulkarni *et al*.[17] reported reduction of the nitro group of quinazolone **37** to the corresponding amine **38** (Scheme 3.5). The examples in Scheme 3.5 proceeded in high yields, while preserving the aryl halide bond when it was present. We were delighted to find that use of five equivalents of $SnCl_2 \bullet 2H_2O$ yielded our desired quinazoline **26**. We then turned our research toward amide bond formation.

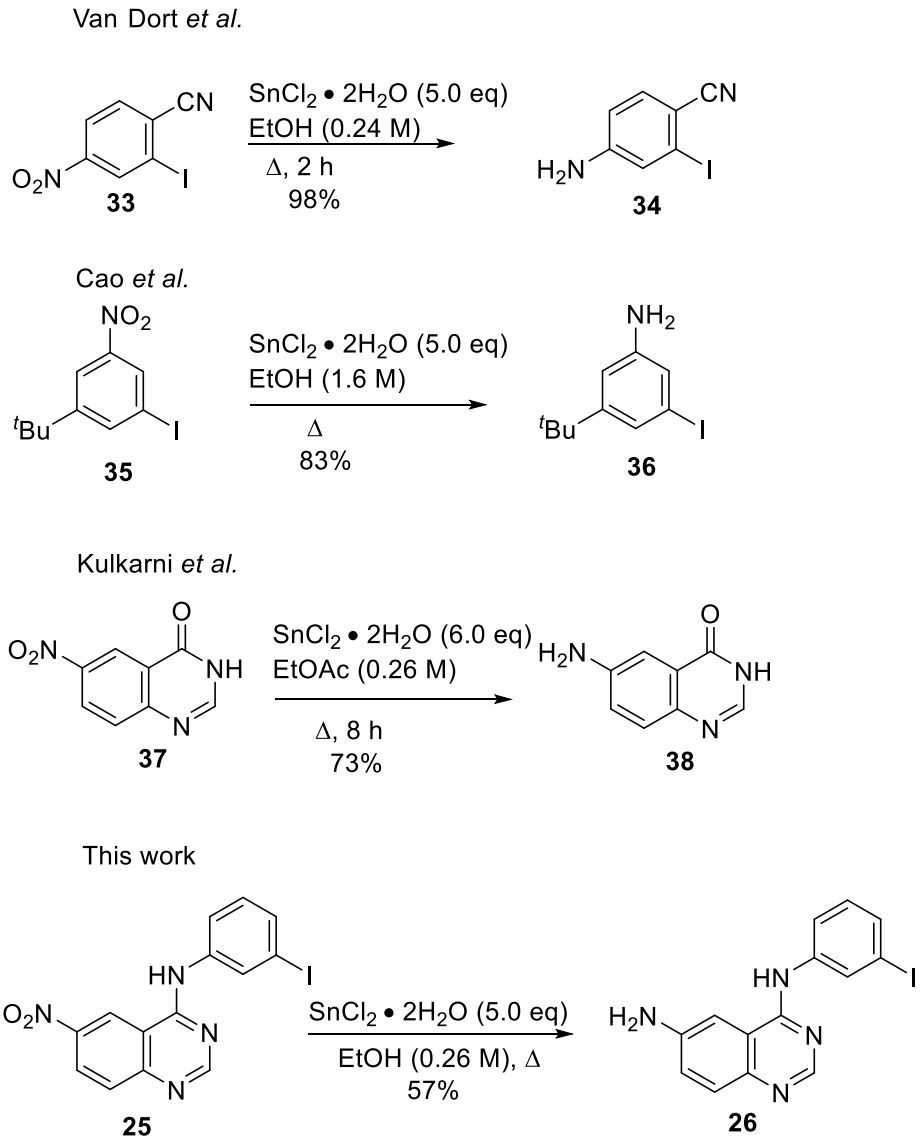

Scheme 3.5. Reduction of the Nitro Group with Tin (II) Chloride

3.3. Overview of Amide Bond Formation

Amide bond formation is a long-studied topic, particularly in the formation of peptides and other biologically active molecules.[18] The amide bond formation is normally precluded by the acid-base reaction (Scheme 3.6) between them; forming a salt. Amides are classically formed by the heating of a carboxylic acid and amine (typically above 200 °C) in order to overcome the lowered reactivity of the salt.[18,19]

These conditions are only feasible with thermally stable ammonia, primary, or secondary amines. Most compounds would decompose under these harsh conditions.

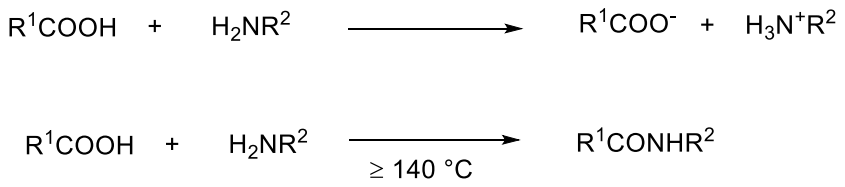

Scheme 3.6. Acid-Base Reaction Between Amine and Carboxylic Acid and High Temperature Amidation.[20]

The solution to this inherent problem is to make activated intermediates from the carboxylic acid. Common tactics include: derivatization to the acid chloride through common reagents (e.g., oxalyl chloride, thionyl chloride, phosphoryl chloride), formation or use of the acid anhydride (Schotten-Bauman conditions), or use of coupling reagents (e.g., carbodiimide, guanidinium, mixed anhydrides).[21] Many situations requiring amide bond formation do not easily lend themselves to use of these methods[18] and many "non-classical" methods have been developed. Use of organoboranes (in molar equivalents or catalytic amounts) or transition metal / organometallic catalysts have been used to form amides, often in high yield (Scheme 3.7).[18,22,23]

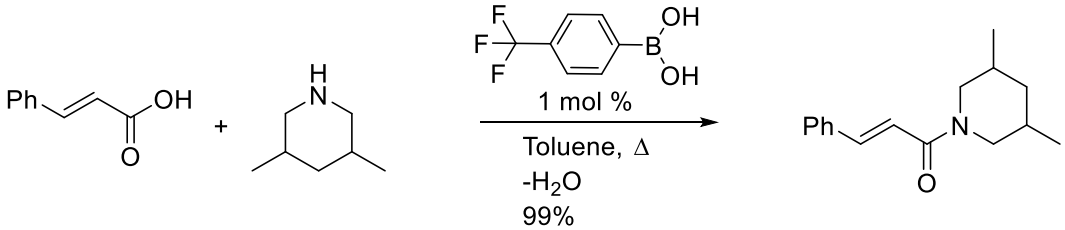

Scheme 3.7. Yamamoto *et al*. Amide Formation[22]

Application of assorted protocols to the butendioic acid system has been investigated by many researchers. Higuchi and Miki[24] showed, in 1961, that both

fumaric and maleic acid could form an amide bond with aniline in aqueous environment at 95 °C, facilitated by the secondary carbonyl group acting as a hydrogen bond director for the attack by the aniline (Scheme 3.8, no yields reported).

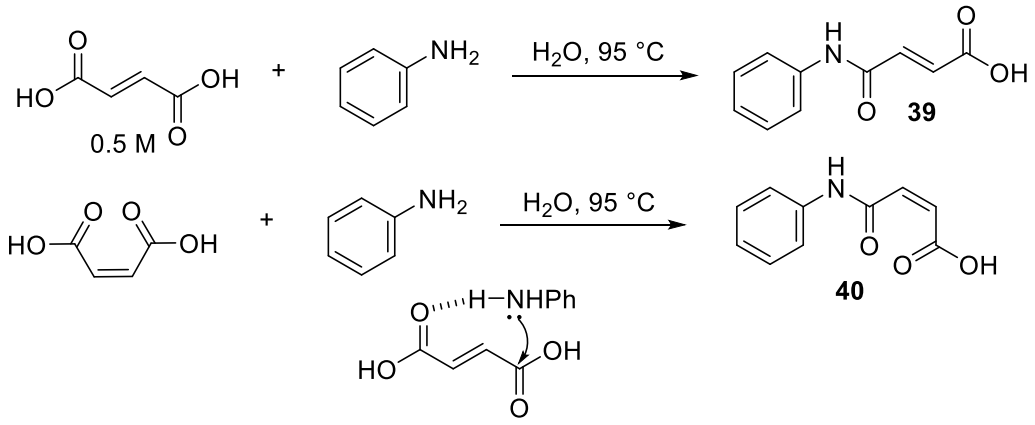

Scheme 3.8. Higuchi and Miki Amide Synthesis

Jha *et al.*[25,26] formed the maleiamide using maleic anhydride and fumaramide via an acid chloride intermediate (Scheme 3.9).

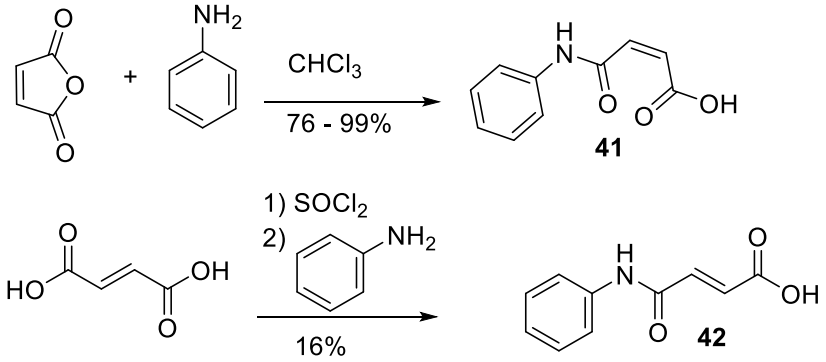

Scheme 3.9. Synthesis of But-2-endioic Amides by Jha, *et al.*

Ekblad *et al.*[27] used a similar approach to the two isomers but saw a marked increase in yield of the fumaramide to 41% (Scheme 3.10). Ekblad also showed that these conditions worked well with Rink amide resin to form the *cis* isomer of the

monomethyl amide derivative (**45**) which they found was a selective inhibitor for ADP-ribosyl transferase 10 (HOAt structure given in Table 3.3; *vide infra*).

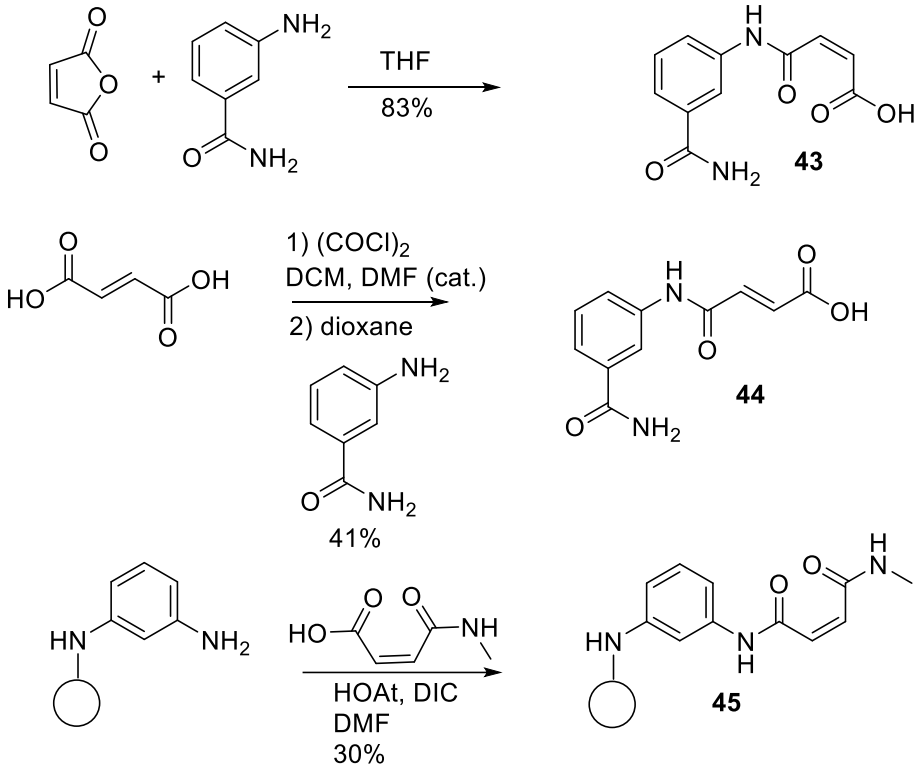

Scheme 3.10. Ekblad *et al.* Synthesis of Amides

On the basis of the widespread use of the acid chloride intermediate for coupling to fumaric acid, our initial synthetic strategy utilized a mono protected fumarate that could be coupled to either the quinazoline or the ε-amine of the lysine residue attached to our Pc.

3.4. Coupling of the Butenoic Acid

3.4.1 Quinazoline Coupling

With 6-amino quinazoline in hand, formation of the amide bond with monomethyl fumarate was performed. Initial reactions, via acid chloride intermediate, employed oxalyl chloride as the activator (Scheme 3.11) based on the success of Ekblad *et al*. Initially, only starting quinazoline could be recovered from the reaction mixture. Solubility issues were initially thought to be the cause of this failure. However, while attempts to increase solubility did not yield product, this did allow for increased recovery of the starting material. We also explored the use of dicyclohexylcarbodiimide (DCC) but again saw no amide. One DCC reaction seemed to produce product, according to TLC and NMR, but our inability to differentiate between **46** and the DCC-derived urea, on the basis of solubility, prevented product purification by chromatography.

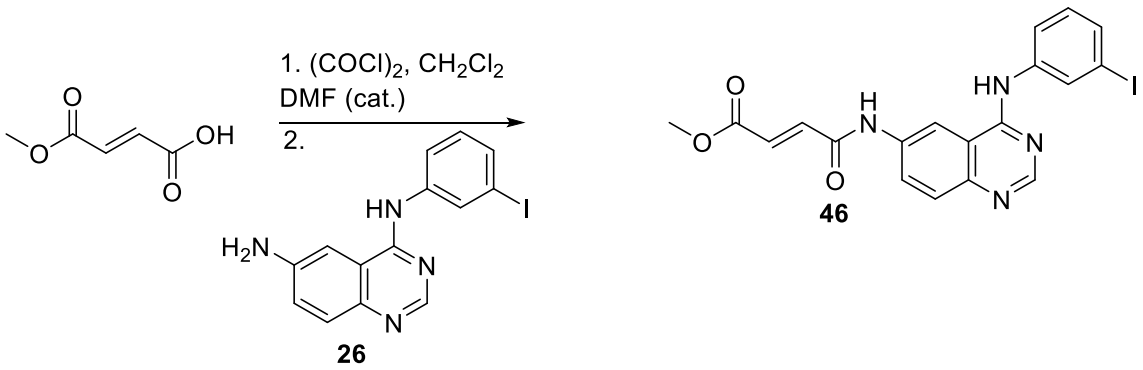

Scheme 3.11. Initial Fumarate Coupling to Quinazoline Attempt

To avoid wasteful consumption of the synthetically valuable aminoquinazoline (**26**) during the reaction optimization, 3-iodoaniline was chosen as a model system for the electron deficient aminoquinazoline (Scheme 3.12). Dicyclohexylcarbodiimide activation of methyl fumarate in THF/DMF (3:1), before addition of the aniline at room

temperature, led only to recovery of **26**. Addition of Hünig's base led to a complex mixture from which nothing particular could be isolated. Use of the acid chloride methodology was also unproductive (Scheme 3.12). We suspected that product may be forming but getting retained, or degraded, during silica gel chromatography. We hypothesized that increasing the size, and hydrophobicity, of the ester would facilitate handling.

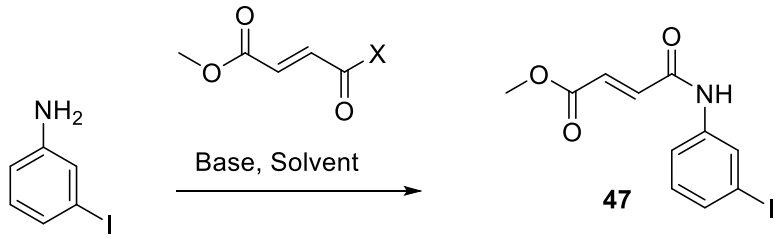

Scheme 3.12. Model System for Coupling Aniline with Monomethyl Fumarate

Accordingly, we ordered monoethyl fumarate while we investigated the synthesis of the *n*-butyl mono ester. Thus, fumaric acid was reacted with n-butanol (Scheme 3.13) using catalytic acid (sulfuric or *p*-tosic acid) and heated at reflux. The diester (**48a**) was observed as the major product.

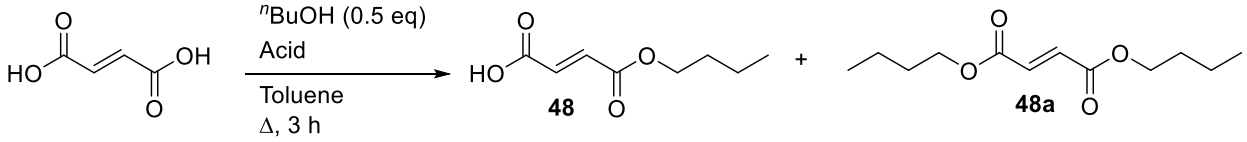

Scheme 3.13. Acid Catalyzed Esterification of Fumaric Acid

Ma *et al.*[28] had formed a monoester of fumaric acid, via opening of maleic anhydride and then isomerization of the double bond by a Lewis acid catalyst (Scheme 3.14). The first step was readily achieved by reacting *n*-butanol and maleic anhydride under basic conditions. However, isolation of the product from the isomerization reaction proved difficult. Nevertheless, the reaction yielded 2.6 g of the isomerized

monobutyl fumarate **50**, although the collected product still showed some presence of the *cis* isomer by NMR. We observed the proton NMR spectrum had an 82:18 *trans*/*cis* ratio giving the doublets from the *trans* isomer centered around 6.90 ppm with a coupling value of 15.6 Hz value while the *cis* isomer doublets are centered around 6.40 ppm with a coupling constant of 12.7 Hz.

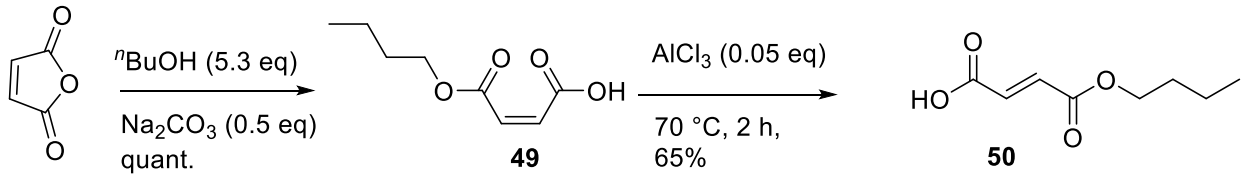

Scheme 3.14. Isomerization of Butenoic Esters

This butyl ester, **50**, was coupled with the aminoquinazoline **26**, through acid chloride activation, though the product was isolated in only 16% yield after silica chromatography purification and ^{1}H NMR verification (Scheme 3.15). Subsequent success with the commercially available monoethyl fumarate ester (*vide infra*) coupling led us to abandon the monobutyl fumarate strategy.

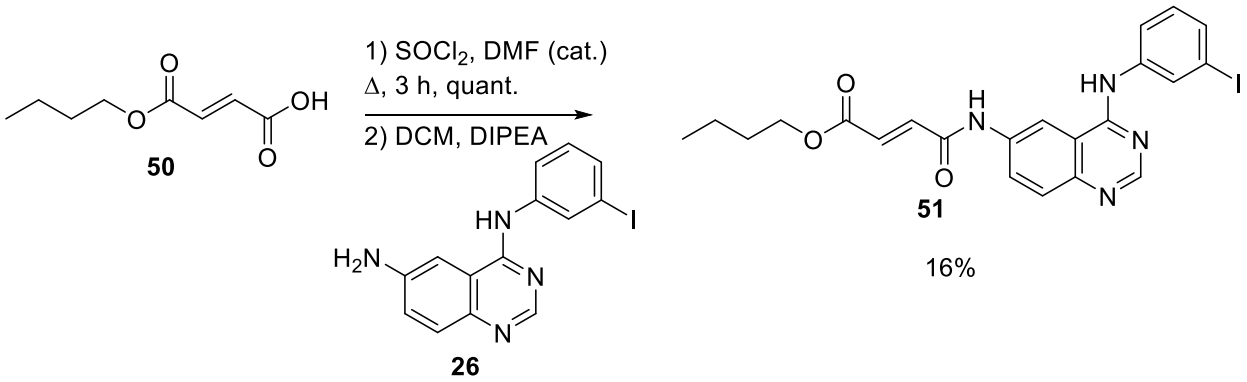

Scheme 3.15. Monobutyl Fumarate Coupling with Quinazoline.

Monoethyl fumarate was converted to its acid chloride then 6-aminoquinazoline **26** was introduced at low temperature, in the presence of a base, and in an initial

attempt, yielded 24% of amide **52** (Scheme 3.16). Unfortunately we were unable to reproduce this first experiment in any subsequent attempts.

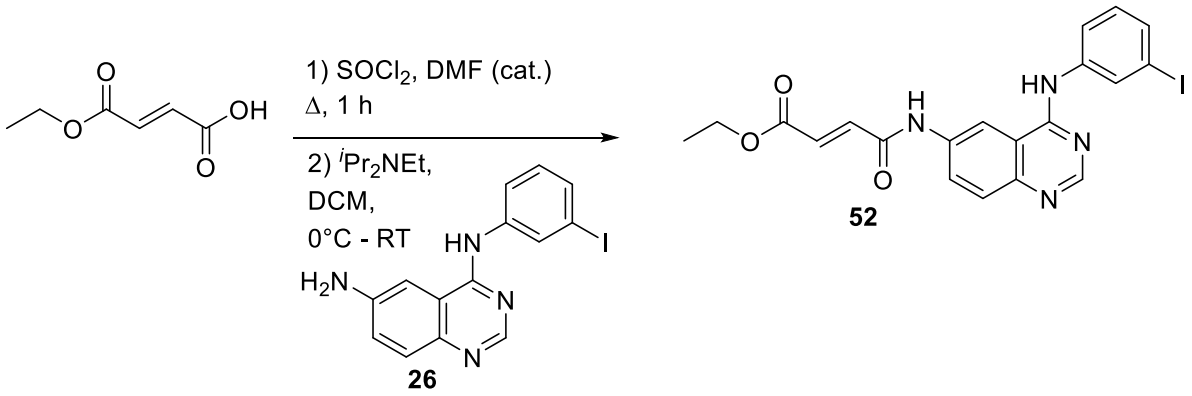

Scheme 3.16. Monoethyl Fumarate Coupling with Quinazoline

Concerns about the stability of the acid chloride to ambient moisture, low yield of amide product, and irreproducibility of the initial experiment prompted a change of coupling procedure. Previous experience of the guanidinium reagents (HBTU/HOBt) in adding the lysine residue onto the Rink amide resin (Chapter 2) and literature precedents[29-31] using coupling reagents for mono-protected butenoates encouraged us to explore this method. Our first trial (Table 3.2) afforded amide **52** in 68% yield after flash chromatography. Attempts to increase the solubility of reagents by use of DMF as solvent gave a disappointing 53% yield of crude product that was difficult to purify. In the next attempt, the reaction was carried out in dichloromethane (DCM), but halving the concentration; still the resultant solid was mostly unreacted quinazoline starting material. The reaction was repeated, allowing for the guanidinium activation reaction to occur for an hour at room temperature, while the coupling was conducted for 8 hours; unfortunately the reaction yielded only 8% of pure target product. In the next attempt, the reaction mixture was cooled to 0 °C before quinazoline addition while being allowed

to warm to room temperature yielding near quantitative mass recovery but only 22% product was obtained following column chromatography.

Table 3.1. Guanidinium-Mediated Amide Formation

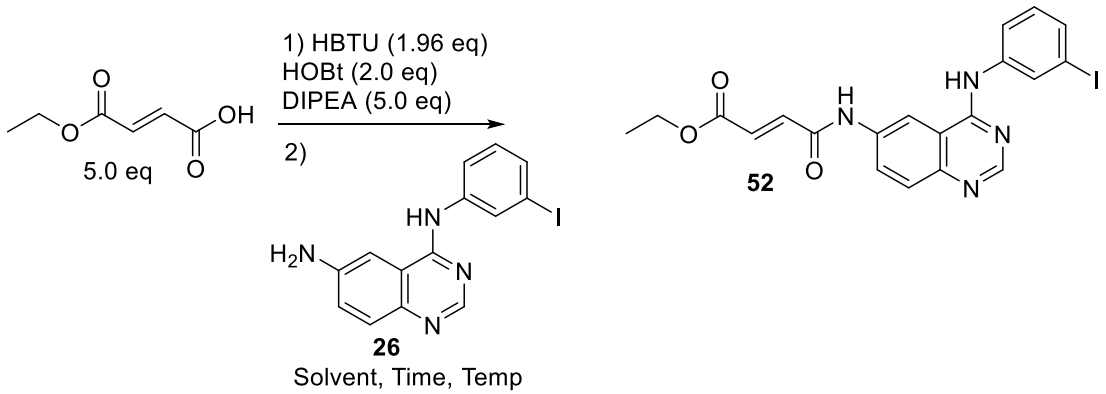

Entry	Solvent	Activation (A)/ Coupling (C)	Temperature (°C)	Reaction Outcome (% Yield/ Recovery)
1	DCM (dry,6.3 mM)	3 min (A) 1 h (C)	25	**52** (68)
2	DMF (wet, 11.5 mM)	5 min (A) 72 h (C)	25	**52** (53)
3	DCM (dry, 4.6 mM)	5 min (A) 20 h (C)	25	**26** (70)
4	DCM (dry, 4.6 mM)	1 h (A) 8.5 h (C)	25	**52** (8.6)
5	DCM (dry, 17.3 mM)	2 h (A) 17 h (C)	25 (A) 0 – 25 (C)	**52** (22)
6	DCM (dry, 9.2 mM)	1 h (A) 14 h (C)	25	**52** (37)
7	DCM (dry, 55.2 mM)	1 h (A) 24 h (C)	25 (A) 0 – 25 (C)	**52** (33)
8	DMF (dry, 34.5 mM)	14 h (A/C)	25	**52** (40)
9	DCM (dry, 11.5 mM	15 min (A) 23 h (C)	25 (A) 0 – 25 (C)	**52** (82)

We suggested that the cold temperature might have slowed the reaction, therefore the reaction was repeated at room temperature in DCM, which improved yield slightly. Solubility of the quinazoline was thought to be the cause of the low yield,

therefore, pure dry DMF was tried which yielded a modest yield of product similar to the reactions carried out in DCM at room temperature or at low temperatures. Lastly, noting the variation in concentration, the reaction was attempted in dry DCM at 11 mM reagent concentration, which finally gave a good yield after purification, which completed optimization of the reaction.

Having found the optimized conditions of the conjugation to form compound **52**, hydrolysis of the ethyl ester was then attempted using lithium hydroxide.[32] The reaction proceeded smoothly and gave the expected carboxylic acid with an average yield of 60% (Scheme 3.17).

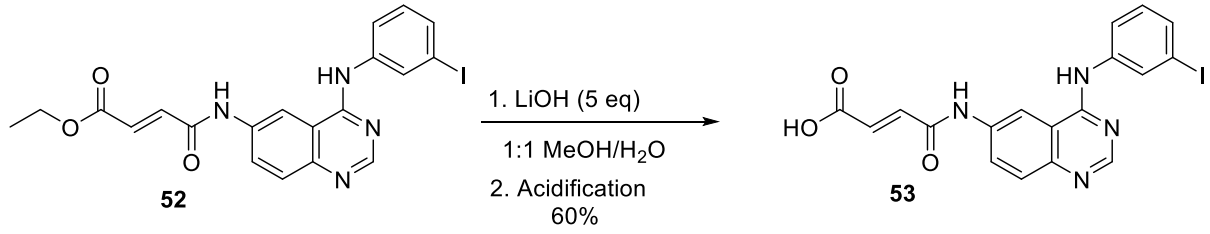

Scheme 3.17. Hydrolysis of Ethyl Ester **53**

3.4.2. Phthalocyanine Coupling with Fumarate-Quinazoline Conjugate

Concurrently, we attempted coupling between **4** and **53** through two methodologies. Activation of **53** (Scheme 3.18), into the corresponding acid chloride, followed by an attempt to react with ZnPc-NH_2 **4** did not lead to any product formation. Use of HBTU/HOBt, in wet dichloromethane or dimethylformamide gave a green precipitate, but mass spectrometry showed no evidence for the formation of the desired product. A test reaction between monoethyl fumarate and ZnPc-NH_2 **4** using the HBTU/HOBt reagents with the addition of *N,N*-4-dimethylaminopyridine (DMAP) as

base gave a crude product with a ^{1}H NMR spectrum that was consistent with the desired product, though we could not reproduce this initial result in subsequent attempts.

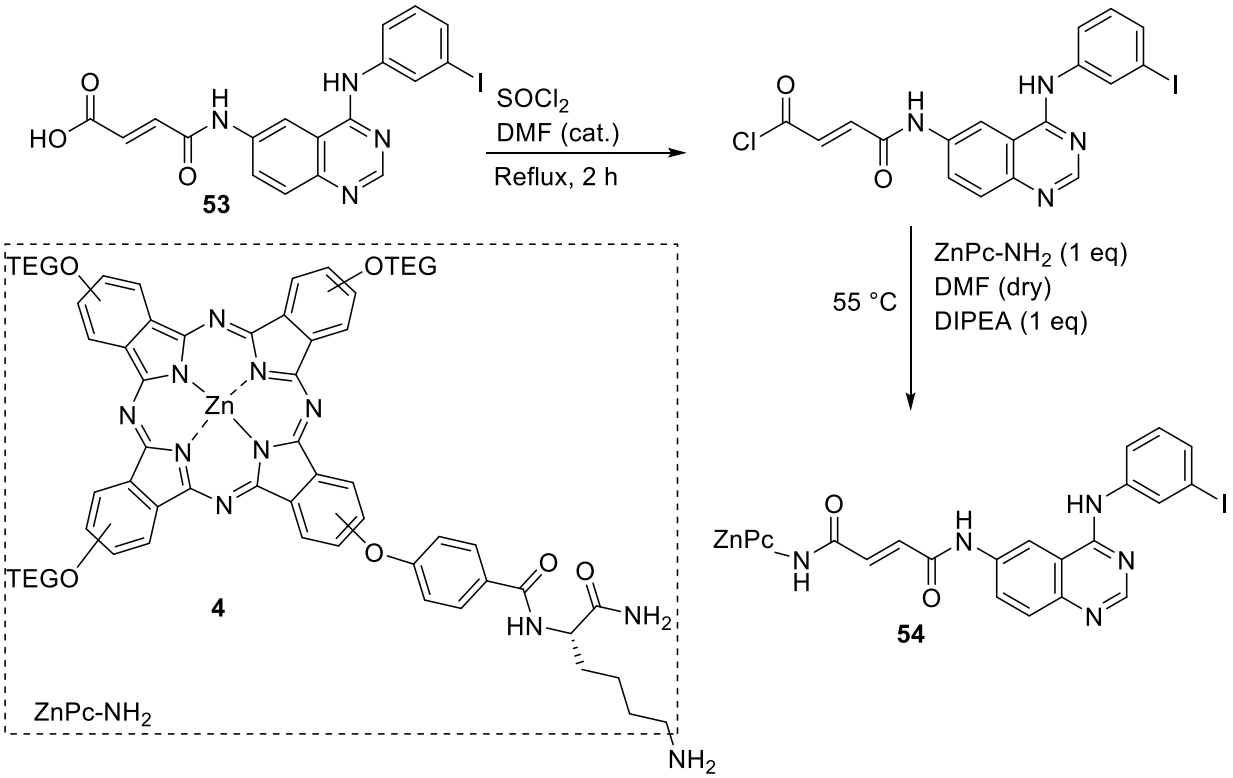

Scheme 3.18. Attempt of Acid Chloride Coupling Between ZnPc and Quinazoline Fragments

The coupling between ZnPc **4** and quinazoline **53** was then tested using a range of coupling reagents. The test reactions were conducted on a scale of 15 mg of ZnPc **4** with around 0.8 molar equivalents of carboxylic acid **53**, for about 24 hours. Initially, two parallel reactions were run (Table 3.3) testing the use of the activating reagents HBTU (guanidinium) or PyBOP (uronium). Mass spectrometry did not detect the desired coupling product in the crude product mixtures. Other peptide coupling reagents were investigated for their effectiveness in facilitating the coupling reaction. The DCC reaction did not lead to isolation of any product despite the use of 100% *i*-PrOH with formic acid.

Reactions using reagents TFFH, CDI, and HATU all gave a similar green precipitate as reaction product. These precipitates were investigated by MALDI mass spectrometry, but gave no evidence for the formation of the desired product and only showed evidence for the $[M]^+$ peak of the starting Pc.

Table 3.2. Zinc Phthalocyanine – Fumarate Coupling Trials and Coupling Reagents

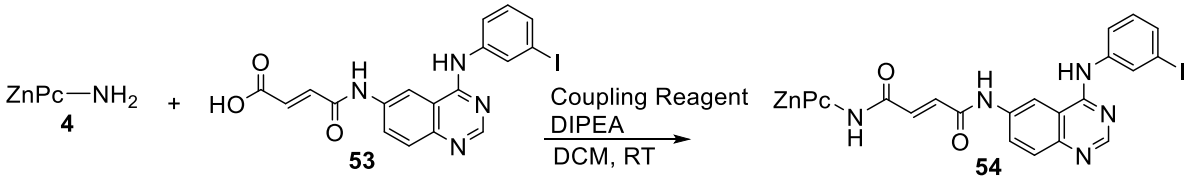

Entry	Coupling Agent	Carboxylic Acid **53** amount (mg)	Molar Equivalent **53**	Reaction Time
1	HBTU	5	0.9	22 h
2	PyBOP	5	0.9	26 h
3	DCC	4	0.7	17 h
4	CDI	4	0.7	17 h
5	TFFH	4	0.7	23 h
6	HATU	3	0.7	23 h

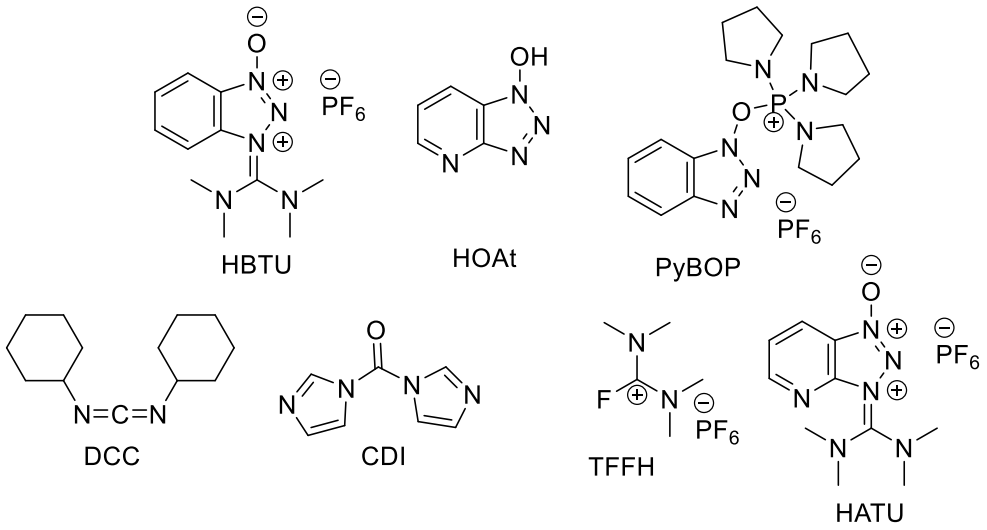

To avoid wasteful use of the valuable quinazoline **53** during the reaction conditions optimization, *trans*-cinnamic acid, **55**, was chosen as a model system for the

conjugated carboxylic acid in further studies. Various coupling reagents were again tested in the coupling reaction between ZnPc-NH_2 **4** and *trans*-cinnamic acid in pure, dry DMF.[33,34] We found that ACS-grade DMF additionally dried over 3 Å molecular sieves in a solvent system column satisfied this requirement for purity. The reactions using HBTU/HOBt, DCC, and DCC/HOBt were left to run at room temperature for 5 days; however, starting ZnPc-NH_2 **4** still was present by TLC after this time. The solutions were then heated to 80°C and were reacted for an additional 48 h. Ethyl ether was added to the reaction mixtures after cooling the mixture to room temperature, inducing precipitation. The precipitated solids were concentrated by centrifugation, isolated, washed with fresh ethyl ether, and dried under vacuum. Unfortunately, electrospray ionization mass spectroscopy did not show the expected molecular ion to support desired amide formation.

Table 3.3. Coupling Reagent Optimization

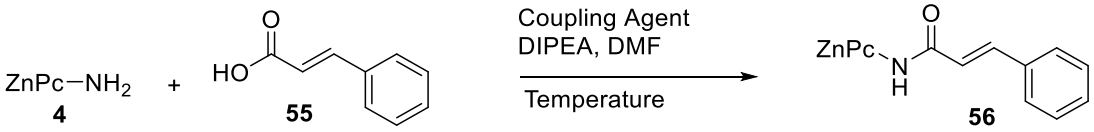

Entry	Coupling Reagent	Temperature (°C)	Solid Amount
1	HBTU/HOBt	25/ 80	N/A
2	DCC	25/ 80	2.7 mg
3	HOBt/ DCC	25/ 80	3.6 mg

A new test reaction (Scheme 3.19) between the fumaric acid-quinazoline conjugate **53** and *N*-Boc-1,6-hexanediamine using HBTU/HOBt gave a crude coupled product. In previous studies, we demonstrated that this amine could successfully react with ZnPc **19** (Scheme 2.10, **21**). Based on this information, we attempted coupling of the quinazoline and ZnPc using this guanidinium activation system in pure, dry DMF.

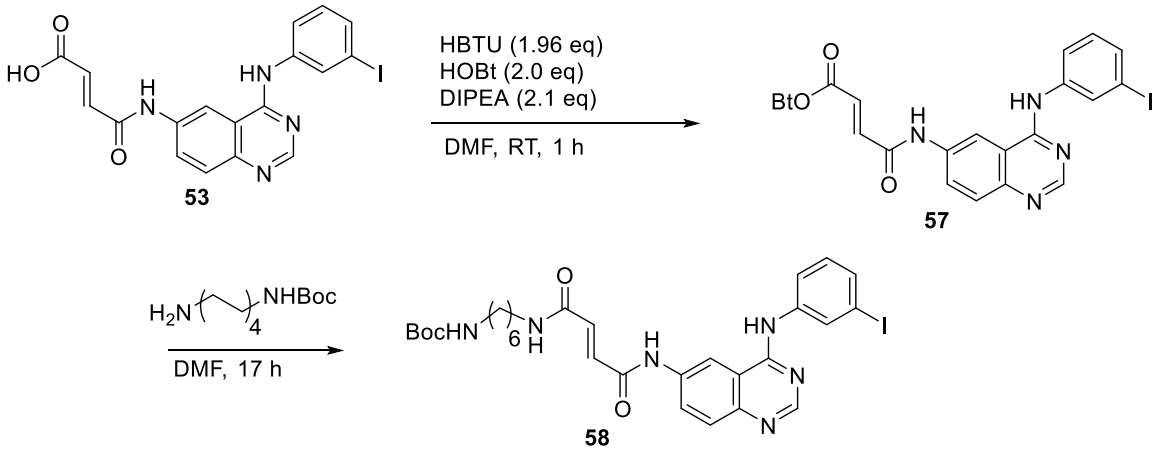

Scheme 3.19. Quinazoline Test Reaction

Using the air-free reaction technique, the ZnPc **4** fragment was finally coupled to the quinazoline **53** fragment using the HBTU/HOBt reagent system (Scheme 3.20) forming the compound **57** upon ultrasonication. It was identified by both TLC and color change (into red solution). The desired product **54** was verified by HRMS-ESI, showing the doubly charged $[M+2H]^{2+}$ ion and the proton NMR spectrum showed peaks that could be assigned to the Pc, fumarate double bond, and quinazoline fragments.

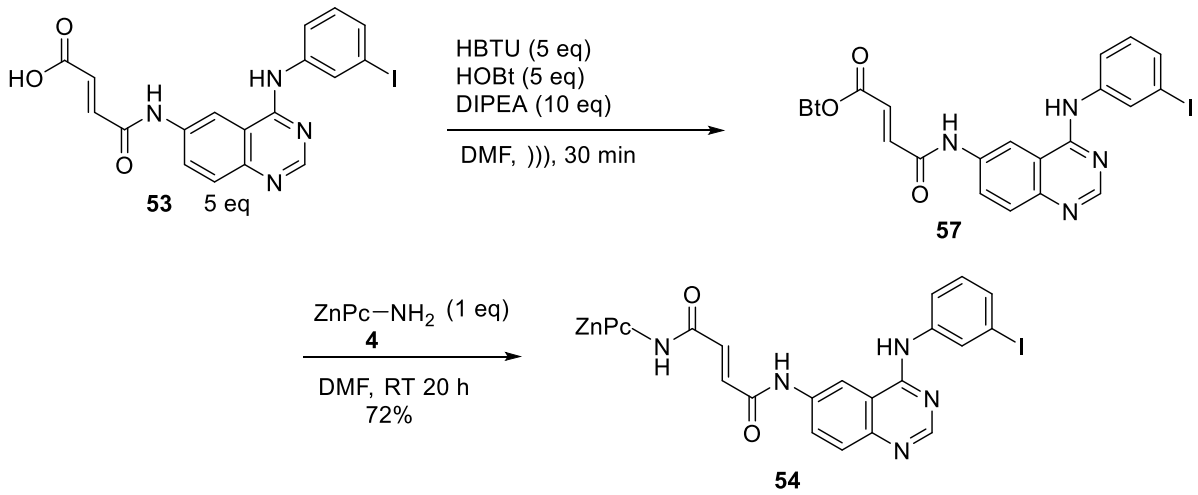

Scheme 3.20. Fumarate **53** Coupling to Zinc Phthalocyanine **4**

Absorbance and emission spectra were acquired for the coupled product (Figure 3.2). Not surprisingly, both UV absorption and emission spectra features of **54** were very similar to the initial ZnPc-NH_2 **4.** The observed Stokes shift was very slight (12 nm) showing almost no change between ground state and excited state geometries/ charge states. Using absorption spectroscopy, we also found that incorporation of the quinazoline fragment did not noticeably change the aggregation behavior of the Pc moiety in aqueous media that was previously observed for ZnPc-NH_2 **4** and described in the previous chapter (Figures 3.3 & 2.6). This observation was expected as Pcs typically do not greatly change their photophysical behavior after substituents undergo reaction.[35]

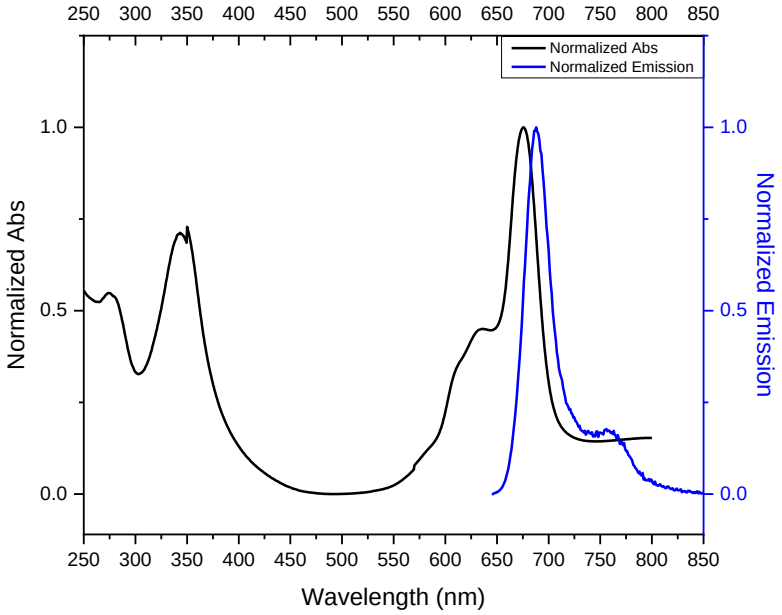

Figure 3.2. Absorption and Photoluminescence Spectra of ZnPc-Quinazoline Conjugate **54** (conc. 63 μM in MeOH)

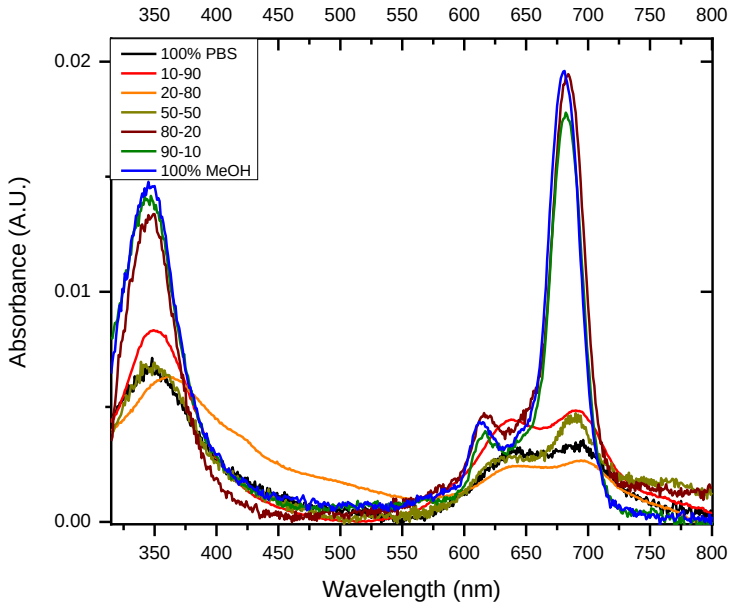

Figure 3.3. Change in Absorption Spectrum of Quinazoline Pc Conjugate **54** (conc. 500 nM) upon Varying Ration of Methanol to PBS Buffer.

3.5. Structural Variations in Quinazoline Fragment to Study the Structure-Activity Relationships and Kinase Binding – Current Developments

Having successfully coupled the quinazoline inhibitor to the Pc chromophore using the fumarate linker, we continued our synthetic studies towards variations both in the quinazoline unit and in the linker. First, attempts to structurally vary the linker were undertaken. This study was aimed at investigating the effect of the linker on the EGFR domain binding strength (due to the possibility of Michael type addition at the C=C bond in the binding pocket, see page 50 above, and related reversibility vs. irreversibility of the binding). In an attempt to change the geometry of C=C bond in the linker from *E* to *Z*, reaction of quinazoline with maleic anhydride in acetic acid (Scheme 3.21, **A**) was investigated and yielded the conjugate **58** in high yield (80 – 90%). Unfortunately, all attempts to couple the Z-butenoic acid **58** fragment and ZnPc-NH_2 **4** failed in all experimental trials and further attempts to reach the final product were abandoned due

to the increasingly short time scale and the pressure to produce synthetically viable analogs. We hypothesized that possibly some kind of steric effect (due to less favorable geometry of the Z-isomer) might be preventing from the formation of the amide bond due to the large size of the Pc.

Application of the same process to succinic anhydride in order to prepare a linker without an unsaturated C=C bond (Scheme 3.21, **B**) initially yielded no product. Replacement of acetic acid solvent with toluene along with increasing the reaction temperature to reflux condition did not yield any product according to TLC monitoring. Addition of DMAP was also ineffectual. Introducing the monomethyl ester of succinic acid instead of the anhydride and using HBTU/HOBt activation was successful and yielded 82% product **60** following purification (Scheme 3.21, **C**). Hydrolysis of the ester was accomplished using lithium hydroxide which gave pure carboxylic acid **59** product in quantitative yield after acidification. This fragment will be subsequently used for coupling with Zn-Pc chromophore **4** and will yield a critically important analog without C=C bond in the linker for comparative EGFR TK binding studies. The initial coupling attempts failed so far and the product has yet to be formed and may require alternative conditions than those that we have optimized here.

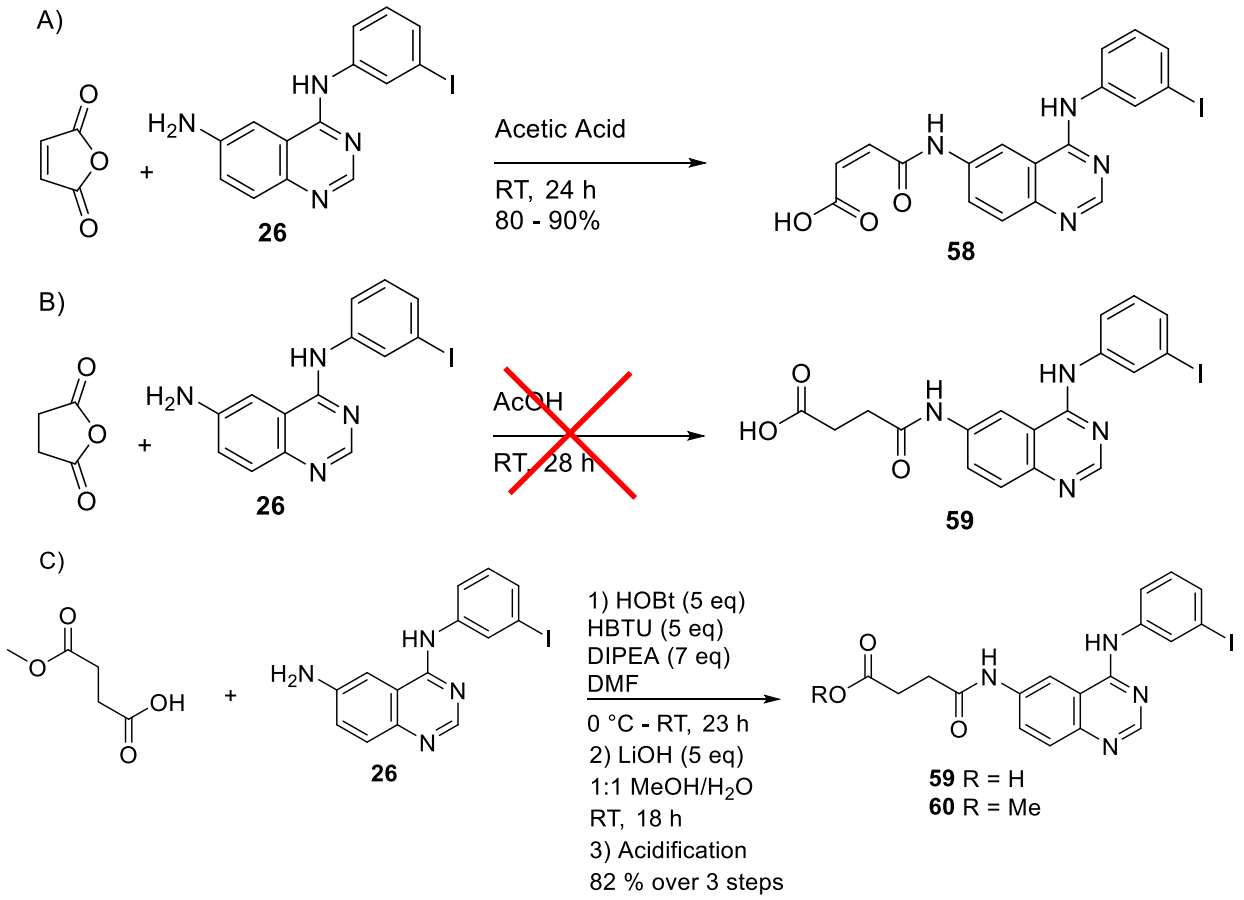

Scheme 3.21. Linker Structural Variations

In a closely related development, we attempted to vary the structure of the quinazoline fragment as a way to change affinity of its binding to EGFR. The halogenated aniline component was changed to 3-chloro-4-fluoroaniline to more closely mimic FDA approved inhibitors (Figure 1.11, Gefitinib) and the resultant nitroquinazoline **61** (Scheme 3.22) was successfully reduced to give aminoquinazoline **62**.

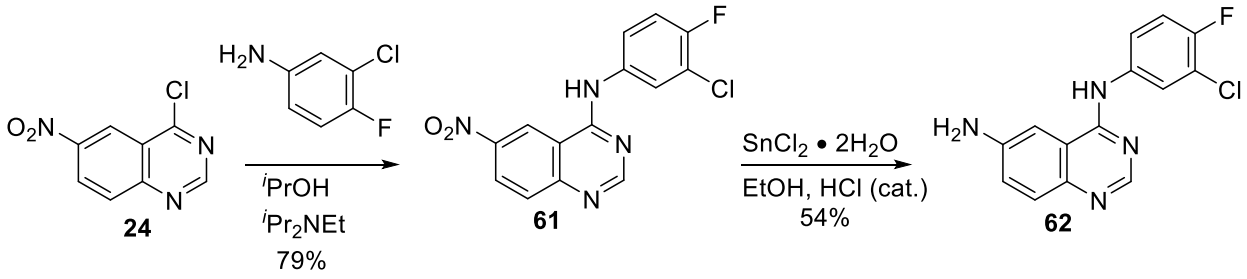

Scheme 3.22. Synthesis of the Structurally Modified Quinazoline Unit

Coupling of compound **62** to monoethyl fumarate was accomplished in moderate yield using the conditions developed for compound **52** and yielding target compound **63** after purification using silica gel chromatography. Ester hydrolysis was performed without issue and the resulting carboxylic acid was then successfully coupled to the ZnPc-NH_2 **4** to give a new probe **65** as a green solid (Scheme 3.23). The product exhibited the required $[M+2H]^{2+}$ molecular ion when investigated using HRMS-ESI it is currently being additionally purified prior to its use in kinase binding studies.

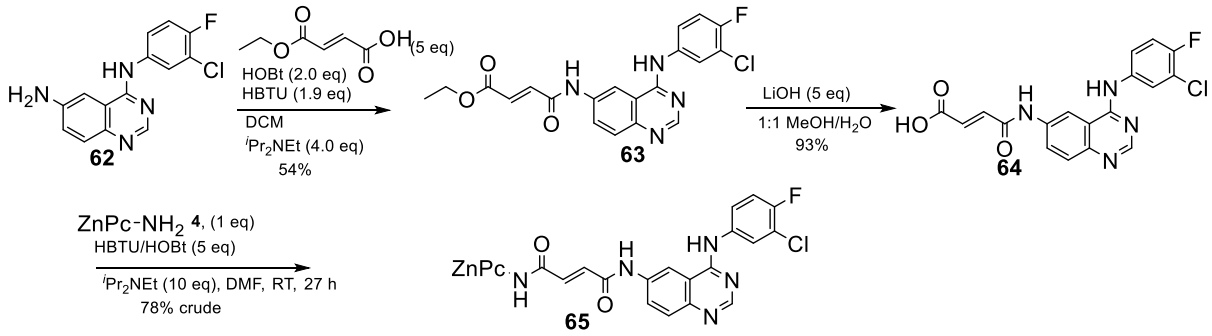

Scheme 3.23. Formation of a Structurally Altered Probe **65**

3.6. Notes

1. Mendelsohn, J.; Baselga, J., The EGF receptor family as targets for cancer therapy. *Oncogene* **2000,** *19* (56), 6550-6565.

2. Zeng, F.; Harris, R. C., Epidermal Growth factor, from gene organization to bedside. *Seminars in Cell & Developmental Biology* **2014,** *28*, 2-11.

3. Fry, D. W.; Kraker, A. J.; McMichael, A.; Ambroso, L. A.; Nelson, J. M.; R., L. W.; Conners, R. W.; Bridges, A. J., A Specific Inhibitor of the Epidermal Growth Factor Receptor Tyrosine Kinase. *Science* **1994,** *265* (5175), 1093-1095.

4. Zhang, H.-Q.; Gong, F.-H.; Li, C.-G.; Zhang, C.; Wang, Y.-J.; Xu, Y.-G.; Sun, L.-P., Design and discovery of 4-anilinoquinazoline-acylamino derivatives as EGFR and VEGFR-2 dual TK inhibitors. *European Journal of Medicinal Chemistry* **2016,** *109*, 371-379.

5. Zhang, X.; Gureasko, J.; Shen, K.; Cole, P. A.; Kuriyan, J., An Allosteric Mechanism for Activation of the Kinase Domain of Epidermal Growth Factor Receptor. *Cell* **2006,** *125* (6), 1137-1149.

6. Shewchuk, L.; Hassell, A.; Wisely, B.; Rocque, W.; Holmes, W.; Veal, J.; Kuyper, L. F., Binding Mode of the 4-Anilinoquinazoline Class of Protein Kinase Inhibitor: X-ray Crystallographic Studies of 4-Anilinoquinazolines Bound to Cyclin-Dependent Kinase 2 and p38 Kinase. *Journal of Medicinal Chemistry* **2000,** *43* (1), 133-138.

7. Castelli, R.; Nicole, B.; Cavazzoni, A.; Bonelli, M.; Vacondio, F.; Ferlenghi, F.; Callegari, D.; Silva, C.; Rivara, S.; Lodola, A.; Digiacomo, G.; Fumarola, C.; Alfieri, R.; Petronini, P. G.; Mor, M., Balancing reactivity and antitumor activity: heteroarylthioacetamide derivateds as poten and time-dependent inhibitors of EGFR. *European Journal of Medicinal Chemistry* **2019,** *162*, 507-524.

8. Shaul, M.; Abourbeh, G.; Jacobson, O.; Rozen, Y.; Laky, D.; Levitzki, A.; Mishani, E., Novel iodine-124 labeled EGFR inhibitors as potential PET agents for molecular imaging in cancer. *Bioorganic & Medicinal Chemistry* **2004,** *12* (13), 3421-3429.

9. Pal, A.; Glekas, A.; Doubrovin, M.; Balatoni, J.; Beresten, T.; Maxwell, D.; Soghomonyan, S.; Shavrin, A.; Ageyeva, L.; Finn, R.; Larson, S. M.; Bornmann, W.; Gelovani, J. G., Molecular Imaging of EGFR Kinase Activity in Tumors with 124I-Labeled Small Molecular Tracer and Positron Emission Tomography. *Molecular Imaging and Biology* **2006,** *8* (5), 262-277.

10. Yin, D. M.; Hammler, D.; Peter, M. F.; Marx, A.; Schmitz, A.; Hagelueken, G., Inhibitor-Directed Spin Labelling—A High Precision and Minimally Invasive Technique to Study the Conformation of Proteins in Solution. *Chemistry – A European Journal* **2018,** *24* (26), 6665-6671.

11. Quinn, S. D.; Srinivasan, S.; Gordon, J. B.; He, W.; Carraway, K. L.; Coleman, M. A.; Schlau-Cohen, G. S., Single-Molecule Fluorescence Detection of the Epidermal Growth Factor Receptor in Membrane Discs. *Biochemistry* **2019,** *58* (4), 286-294.

12. Ullrich, A.; Coussens, L.; Hayflick, J. S.; Dull, T. J.; Gray, A.; Tam, A. W.; Lee, J.; Yarden, Y.; Libermann, T. A.; Schlessinger, J.; Downward, J.; Mayes, E. L. V.; Whittle, N.; Waterfield, M. D.; Seeburg, P. H., Human epidermal growth factor receptor cDNA sequence and aberrant expression of the amplified gene in A431 epidermoid carcinoma cells. *Nature* **1984,** *309* (5967), 418-425.

13. Elderfield, R. C.; Williamson, T. A.; Gensler, W. J.; Kremer, C. B., Synthesis of Bz-Substituted Quinazoline and Antimalarials from them. A Contribution to the Chemistry of Quinazoline. *The Journal of Organic Chemistry* **1947,** *12* (3), 405-421.

14. Hou, X.; Zhang, J.; Zhao, X.; Chang, L.; Hu, P.; Liu, H., Design, Synthesis and Bioactivities Evaluation of Novel Quinazoline Analogs Containing Oxazole Units. *Chinese Journal of Chemistry* **2014,** *32* (6), 538-544.

15. Van Dort, M. E.; Robins, D. M.; Wayburn, B., Design, synthesis, and pharmacological characterization of a 4-[4,4-Dimethyl-3-(4-hydroxybutl)-5-oxo-2-thioxo-1-imidazolidinyl]-2-iodobenzonitrile as a high-affinity nonsteroidal androgen receptor ligand. *Journal of Medicinal Chemistry* **2000,** *43* (17), 3344 - 3347.

16. Cao, L.; Jiang, R.; Zhu, Y.; Wang, X.; Li, Y.; Li, Y., Synthesis of 1,2,3-Triazole-4-carboxamide-Containing Foldamers for Sulfate Recognition. *European Journal of Organic Chemistry* **2014,** *2014* (13), 2687-2693.

17. Kulkarni, S. S.; Singh, S.; Shah, J. R.; Low, W. K.; Talele, T. T., Synthesis and SAR optimization of quinazolin-4(3H)-ones as poly(ADP-ribose)polymerase-1 inhibitors. *European Journal of Medicinal Chemistry* **2012,** *50*, 264-273.

18. Pattabiraman, V. R.; Bode, J. W., Rethinking amide bond synthesis. *Nature* **2011,** *480*, 471.

19. Valeur, E.; Bradley, M., Amide bond formation: beyond the myth of coupling reagents. *Chemical Society Reviews* **2009,** *38* (2), 606-631.

20. Dunlap, F. L., The Production of Acylamines by the Interaction of Sodium Salts of Monobasic Acids and Amine Hydrochlorides. *Journal of the American Chemical Society* **1902,** *24* (8), 758-763.

21. Carey, F. A.; Sundberg, R. A., *Advanced Organic Chemistry Part B: Reaactions and Synthesis*. Springer Science+Business Media, LLC: 2007; Vol. 5th, p 1321.

22. de Figueiredo, R. M.; Suppo, J.-S.; Campagne, J.-M., Nonclassical Routes for Amide Bond Formation. *Chemical Reviews* **2016,** *116* (19), 12029-12122.

23. Ojeda-Porras, A.; Gamba-Sánchez, D., Recent Developments in Amide Synthesis Using Nonactivated Starting Materials. *The Journal of Organic Chemistry* **2016,** *81* (23), 11548-11555.

24. Higuchi, T.; Miki, T., Reversible Formation of Amides From Free Carboxylic Acid And Amine in Aqueous Solution. A Case of Neighboring Group Facilitation. *Journal of the American Chemical Society* **1961,** *83* (18), 3899-3901.

25. Jha, A.; Mukherjee, C.; Prasad, A. K.; Parmar, V. S.; Clercq, E. D.; Balzarini, J.; Stables, J. P.; Manavathu, E. K.; Shrivastav, A.; Sharma, R. K.; Nienaber, K. H.; Zello, G. A.; Dimmock, J. R., E,E,E-1-(4-Arylamino-4-oxo-2-butenoyl)-3,5-bis(arylidene)-4-piperidones: A topographical study of some novel potent cytotoxins. *Bioorganic & Medicinal Chemistry* **2007,** *15* (17), 5854-5865.

26. Jha, A.; Dimmock, J. R., Syntheses of 4-(3,5-Bisphenylmethylene-4-oxo-piperidin-1-yl)-4-oxo-but-2 Z -enoic Acid Arylamides as Candidate Cytotoxic Agents. *Synthetic Communications* **2003,** *33* (7), 1211-1223.

27. Ekblad, T.; Lindgren, A. E. G.; Andersson, C. D.; Caraballo, R.; Thorsell, A.-G.; Karlberg, T.; Spjut, S.; Linusson, A.; Schüler, H.; Elofsson, M., Towards small molecule inhibitors of mono-ADP-ribosyltransferases. *European Journal of Medicinal Chemistry* **2015,** *95*, 546-551.

28. Ma, Y.-L.; Zhou, R.-J.; Zeng, X.-Y.; An, Y.-X.; Qiu, S.-S.; Nie, L.-J., Synthesis, DFT and antimicrobial activity assays in vitro for novel cis/trans-but-2-enedioic acid esters. *Journal of Molecular Structure* **2014,** *1063*, 226-234.

29. Jones, R. A.; Rustidge, D. C.; Sarin, R., Pyrrole Studies. Part. 44.1 Synthesis of Potentially Biologically Active Pyrroloylanilines. *Synthetic Communications* **1993,** *23* (6), 771-777.

30. Götz, M. G.; James, K. E.; Hansell, E.; Dvořák, J.; Seshaadri, A.; Sojka, D.; Kopáček, P.; McKerrow, J. H.; Caffrey, C. R.; Powers, J. C., Aza-peptidyl Michael Acceptors. A New Class of Potent and Selective Inhibitors of Asparaginyl Endopeptidases (Legumains) from Evolutionarily Diverse Pathogens. *Journal of Medicinal Chemistry* **2008,** *51* (9), 2816-2832.

31. Miura, T.; Mikano, Y.; Murakami, M., Nickel-Catalyzed Synthesis of 1,3,5-Trisubstituted Hydantoins from Acrylates and Isocyanates. *Organic Letters* **2011,** *13* (14), 3560-3563.

32. Brimioulle, R.; Bach, T., Enantioselective Lewis Acid Catalysis of Intramolecular Enone [2+2] Photocycloaddition Reactions. *Science* **2013,** *342* (6160), 840-843.

33. Jad, Y. E.; Acosta, G. A.; Khattab, S. N.; de la Torre, B. G.; Govender, T.; Kruger, H. G.; El-Faham, A.; Albericio, F., Peptide synthesis beyond DMF: THF and ACN as excellent and friendlier alternatives. *Organic & Biomolecular Chemistry* **2015,** *13* (8), 2393-2398.

34. Heravi, M. M.; Ghavidel, M.; Mohammadkhani, L., Beyond a solvent: triple roles of dimethylformamide in organic chemistry. *RSC Advances* **2018,** *8* (49), 27832-27862.

35. Weijer, R.; Broekgaarden, M.; Kos, M.; van Vught, R.; Rauws, E. A. J.; Breukink, E.; van Gulik, T. M.; Storm, G.; Heger, M., Enhancing photodynamic therapy of refractory solid cancers: Combining second-generation photosensitizers with multi-targeted liposomal delivery. *Journal of Photochemistry and Photobiology C: Photochemistry Reviews* **2015,** *23*, 103-131.

Chapter 4. Spectroscopic and EGFR Binding Studies of the ZnPc-Quinazoline Conjugate

4.1. General Aggregation / De-aggregation Behavior of Pc Compounds as a Fluorescent Signal Generating Mechanism

In the previous chapters, we discussed some aspects of spectroscopic features of the ZnPc-NH_2 (**4**, Figure 2.5) and of the quinazoline-conjugate (**54**, Figure 3.3), related to its reversible aggregation or de-aggregation based on aqueous content of the solvent. Pcs intrinsically aggregate in aqueous conditions (with dimerization constant as high as 10^9) because of the attractive π-π interactions between Pc planar hydrophobic aromatic cores,[1] and form essentially non-fluorescent H-aggregates. Importantly, the propensity towards aggregation decreases when Pcs are associated with large biopolymers.[2-5] As a consequence of the de-aggregation, a Pc chromophore bound to a large biomolecule becomes fluorescent. Therefore, a turn-on fluorescent response upon Pc de-aggregation will happen over a dark background of aggregated, unbound Pc molecules and lead to an intrinsically high signal-to-background (S/B) ratio without the need to remove unbound species. Additionally, the Pc's characteristic NIR fluorescence will lead to further improvement of the S/B ratio[6-11] due to a lower photon absorption and scattering and reduced auto-fluorescence from both artificial[12] and biological environments.[8,13]

In this work, we functionalize a Pc fluorescent reporter with a small-molecule ("anchor") quinazoline group that can selectively bind to a target EGFR tyrosine kinase. In the absence of the specific target, the small "anchor" group would be unable to preclude Pc aggregation in aqueous conditions (as we demonstrated in Figure 3.3). In the presence of a target protein, however, interaction of the "anchor" with the target's

binding site would “pull” a sensor molecule (**54**) out of an aggregate, and thus turn the fluorescence on (Figure 4.1). This conceptually simple design relies on a general, protein-independent signal generation mechanism (Pc aggregation / de-aggregation), whereas the detection selectivity comes from a proper choice of a small-molecule binding group.

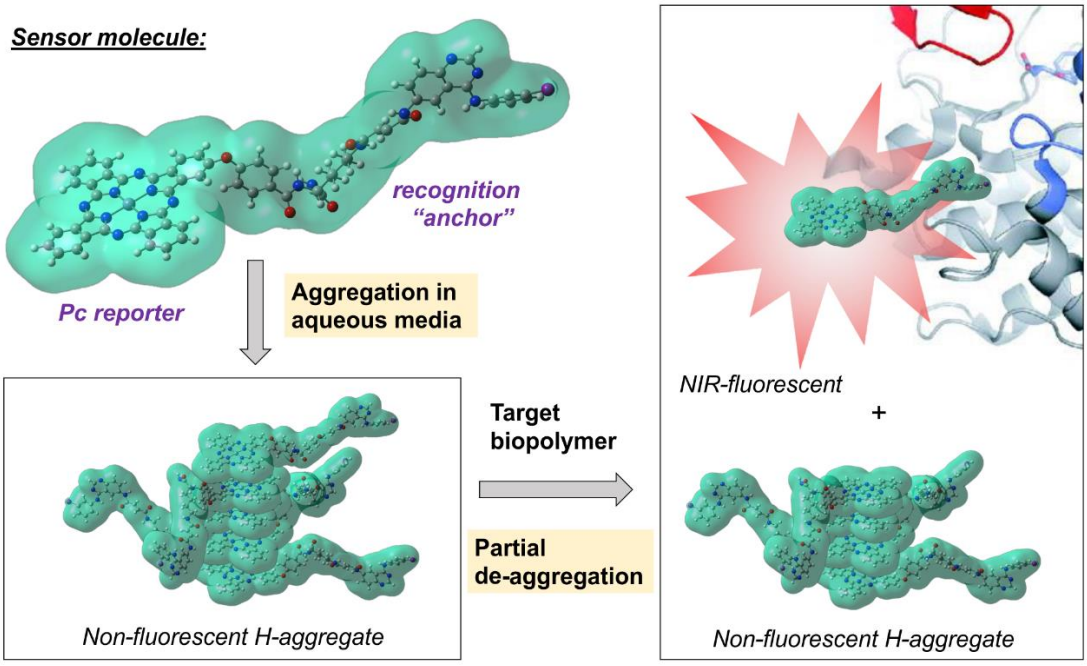

Figure 4.1. General Schematics of a Selective Fluorogenic Probe.

The EGFR kinase obtained from Sigma-Aldrich is derived from A431 cell lysates, which are grown from an epidermoid carcinoma, and have been demonstrated to have an IC_{50} as low as 0.05 nM when using Shaul’s quinazoline **27** (Scheme 3.1) or 0.6 nM with Pal’s compound **31** (Scheme 3.2).[14,15] We therefore began studies with the concentration of conjugated probe **54** at 20 nM, two orders of magnitude higher than the IC_{50} values reported for the related quinazolines. This was anticipated to provide a satisfactory ratio of aggregated / de-aggregated probe upon kinase binding. This was expected to serve as a “proof-of-concept,” as well as allow for detection of the de-

aggregated probe when it formed the probe-protein complex, presumably at a concentration above the sensitivity threshold of the instrument.

4.2. Buffer Considerations and Kinase Variables

The kinase kit described by Aldrich[16] (although no longer available from them) contained a 2-[4-(2-hydroxyethyl)piperazin-1-yl]ethanesulfonic acid (HEPES) buffer (50 mM HEPES, pH 7.4, 20 mM $MgCl_2$, 0.1 mM $MnCl_2$, and 0.2 mM Na_3VO_4), poly-Glu-Tyr substrate, ATP, EGFR (a positive control), and an enzyme-linked immunosorbent assay (ELISA) protocol using a mouse monoclonal anti-phosphotyrosine-peroxidase (a reporter for kinase activity). The glutamate-tyrosine polymeric substrate contains multiple tyrosine residues in a random distribution along the polymer backbone at approx. 4:1 Glu-Tyr ratio. The antibody is conjugated to horseradish peroxidase in a colorless solution which, upon reacting with *o*-phenylenediamine dihydrochloride, changes from colorless to an orange-yellow solution. The *o*-phenylenediamine is introduced as an indicator, after incubating the phosphorylated-tyrosine antibody, to afford the color change based on the activity of the kinase. The change in solution color can be quantified using UV/vis spectroscopy and referencing to a standard curve (typically using EGFR activity).The kit was designed to measure kinase inhibition by measuring the deviation from the standard activity of EGFR by introduction of the chosen inhibitor.

Based on previous research,[15-18] the HEPES buffer was chosen as our working buffer, as enzyme activity in this buffer has been shown to closely mimic *in vivo* conditions. Based on the procedure procured from Aldrich, we prepared a HEPES

buffer that contained HEPES, $MgCl_2$, $MnCl_2$, and Na_3VO_4. Sodium orthovanadate is added to inhibit ATP hydrolysis via ATPase enzymes.[19,20] Inclusion of the divalent metal chloride salts is necessary for the EGFR kinase to adopt its active conformation, in response to the presence of either metal ion.[21] Enzyme activation, in the presence of metal ion, reduced the preparation of components necessary to test the binding of our conjugate-Pc to the EGFR by removing the need to introduce an activating growth factor oligopeptide.[21,22]

As we initially were interested in the ability of our probe to bind to the active kinase, dissociate from the aggregate and display a fluorescent signal, we adjusted the EGFR lysate concentration in the buffer to yield a final concentration of 2 units of EGFR kinase in our sample solution, as the active kinase forms a dimer pair (see Chapter 1). After equilibration for an hour at room temperature, the absorbance and emission of the sample was measured and compared with controls containing only the conjugate-Pc **54** or only the kinase in buffer at the same concentrations.

4.3. Preliminary Spectroscopic and Binding Studies of ZnPc-Quinazoine Conjugate 54 in the Presence of EGFR

Initial tests followed the described procedure[16] but absorbance and emission spectra intensities were negligible (Figures 4.2 and 4.3), even up to concentrations of 500 nM of the conjugate **54**. At that concentration of conjugate **54**, absorption could be detected but it displayed spectroscopic characteristics of the H-aggregated Pc even upon introduction of the kinase, as evident by the hypsochromically shifted Q-band in absorption spectrum (Figure 4.2) and essentially no observable emission band (Figure 4.3).

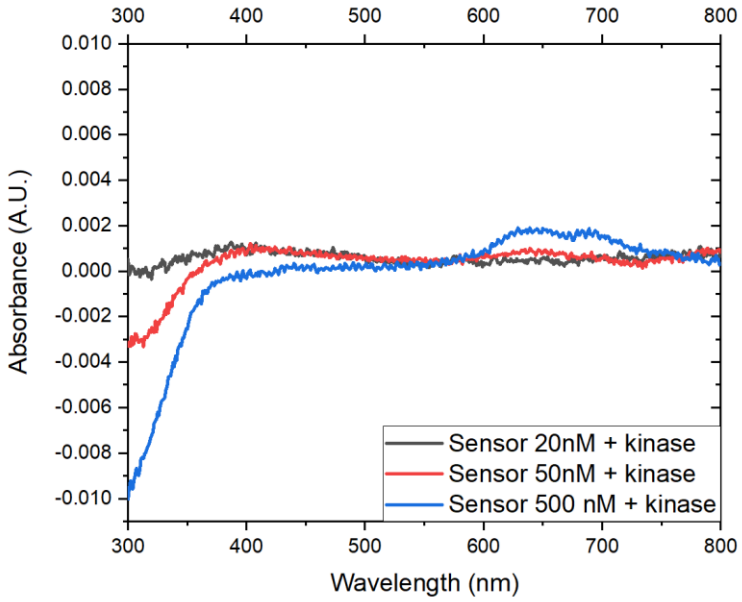

Figure 4.2. UV/Vis Absorbance Spectra of ZnPc-Quinazoline Conjugate **54** in the Presence of 2 units of EGFR Kinase in HEPES buffer (50 mM HEPES, pH 7.4, 20 mM $MgCl_2$, 0.1 mM $MnCl_2$, and 0.2 mM Na_3VO_4).

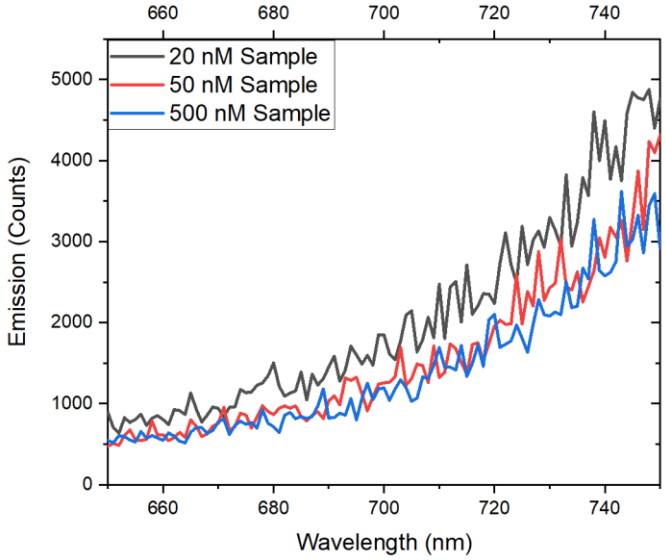

Figure 4.3. Emission Spectra of ZnPc-Quinazoline Conjugate **54** in the Presence of 2 units of EGFR Kinase in HEPES buffer (50 mM HEPES, pH 7.4, 20 mM $MgCl_2$, 0.1 mM $MnCl_2$, and 0.2 mM Na_3VO_4)

Work by Koland and Cerione in 1990,[21] showed that a higher manganese (II) ion concentration (up to 10 mM) might be needed to induce the EGFR kinase to adopt its active conformer. Thus, we increased the Mn^{2+} concentration to 10 mM (from 0.1 mM) in

order to facilitate conformationally-induced binding of our Pc to the active kinase. Preparation of the buffer using this increased manganese (II) concentration met with difficulties but we were able to counteract this issue by the addition of the $MnCl_2$, after adjusting the pH. The absorption spectrum of **54** in this buffer was measured, although still no signal was observed (Figure 4.4).

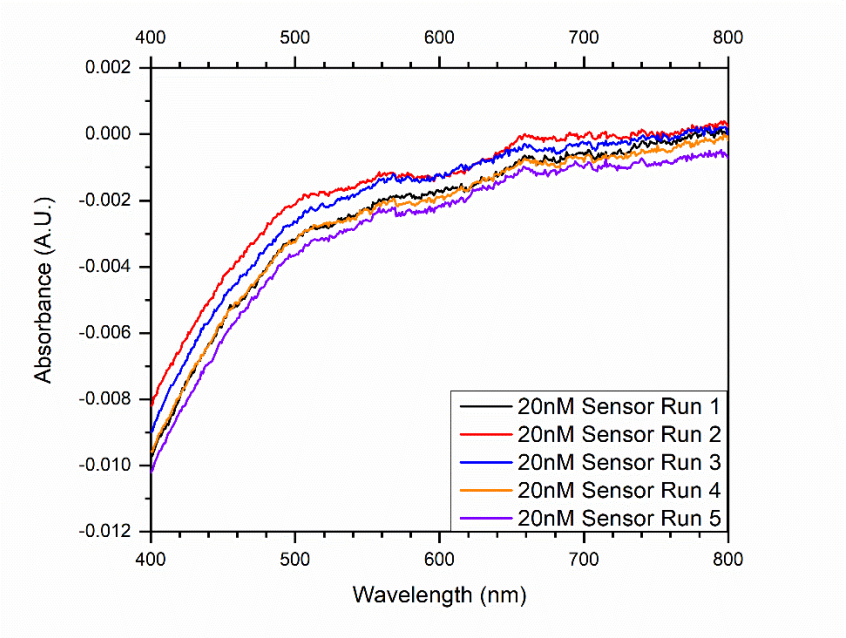

Figure 4.4. Zinc-Quinazoline Conjugate **54** with 10 mM Mn^{2+} in HEPES Buffer with 2 units of Kinase (12 Minutes per run).

Attempts to vary probe concentration and buffer constituents still did not afford observable absorption spectra. Upon further testing of the Cary 5000 UV/vis spectrometer, it was found that the instrument was out of tune which greatly hindered its ability to record consistent spectra at low absorbance values. As an alternative at that time, we focused our research on emission characterization. In order to facilitate probe de-aggregation, introduction of an appropriate amount of DMSO into the buffer conditions was investigated without the introduction of the expensive EGFR kinase. We found that additions of small amounts of dimethyl sulfoxide (<10% DMSO) to the

aqueous buffer did not noticeably alter the emission spectrum, but above 10% v/v, marked increase in emission was observed which we attributed to the de-aggregation of the probe **54** (Figure 4.5). The emission band also saw a slight hypsochromic shift, as the percent composition of DMSO in the buffer increased.

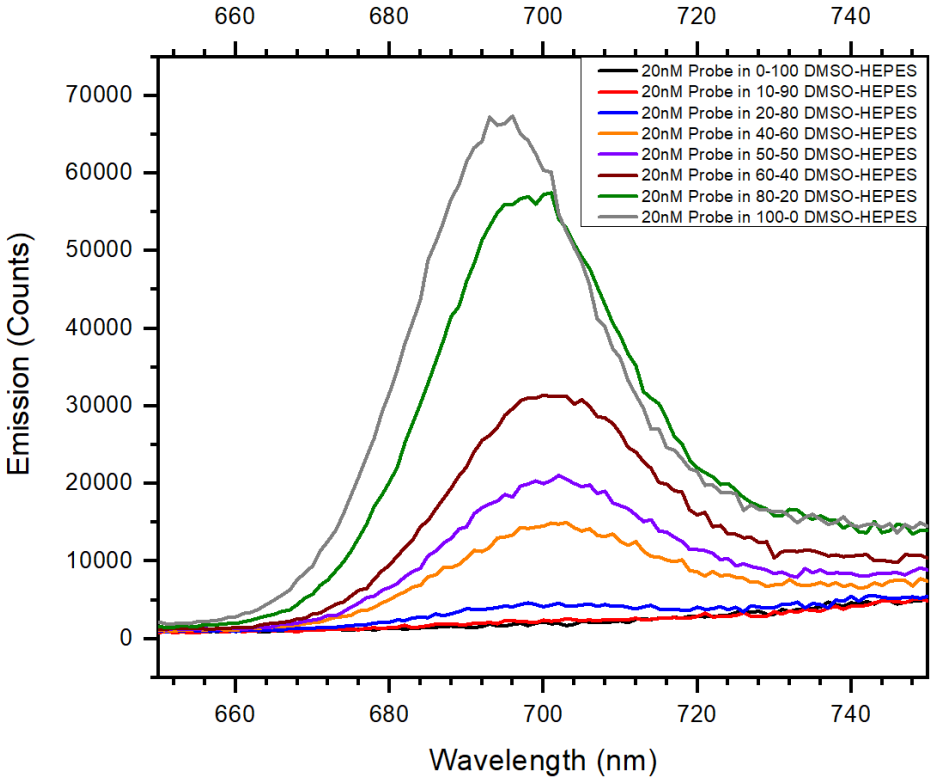

Figure 4.5. Emission Spectra of ZnPc-Quinazoline Conjugate **54** in DMSO-HEPES Solution upon Varying DMSO Fraction

These preliminary results gave us some hope that the sensor **54** would show the expected behavior, at least based on the ability to cause its reversible aggregation / de-aggregation based on the medium composition. However, the need to work with expensive and temperature-sensitive EGFR kinase and carry out spectroscopic experiments at the threshold of the equipment sensitivity prompted us to look for external collaboration. At this juncture, we then turned to our collaborators at Northern Illinois University, Dr. Irina Nesterova and her students, Zane LaCasse and Tanya

Sheth, who were able to optimize the kinase sensing conditions and obtain the highly encouraging proof-of-concept results described below.

4.4. Turn-On Fluorescent Detection of Active EGFR Tyrosine Kinase with ZnPc-Quinazoline Conjugate 54

The above spectroscopic studies of the ZnPc-quinazoline conjugate **54** indicated that it was suitable for NIR turn-on sensing. Thus, it exhibited a high extinction coefficient (78,400 cm^{-1} M^{-1}) and a strong NIR emission from the non-aggregated state (quantum yield 12.5 % in DMSO). Importantly, although it was soluble in aqueous media, it showed an extensive aggregation as could be seen from the hypsochromic shift of the Q-band in absorption spectrum (Figure 4.7, red trace). As a consequence, **54** was non-fluorescent in aqueous solutions (Figure 4.6, red trace). When de-aggregated, ZnPc-quinazoline conjugate **54** exhibits strong NIR fluorescence (black trace). Likewise de-aggregated ZnPc-quinazoline conjugate **54** displays a large absorbance near 676 nm (Figure 4.7, black trace).

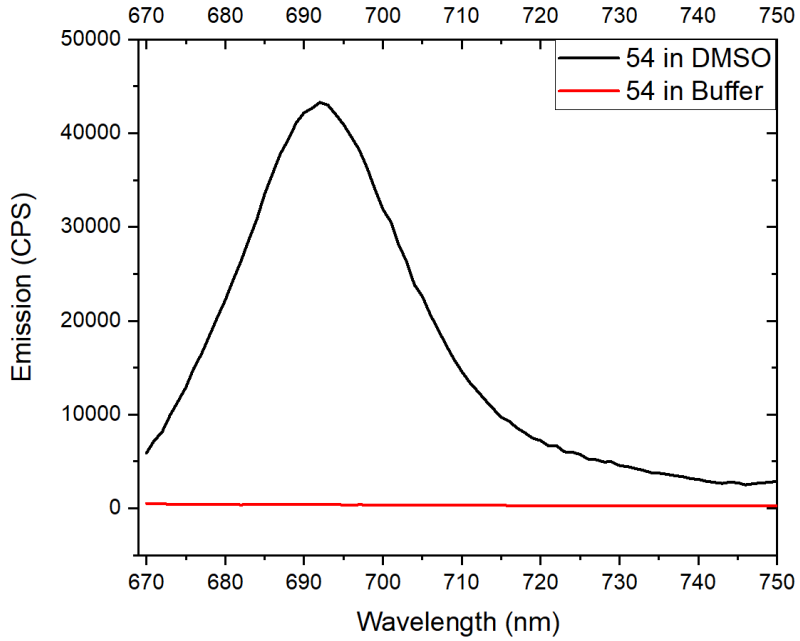

Figure 4.6. Emission Spectra of ZnPc-Quinazoline Conjugate **54** in DMSO vs 10% DMSO in Aqueous Buffer. Concentration of **54** 400 nM, Excited at 665 nm.

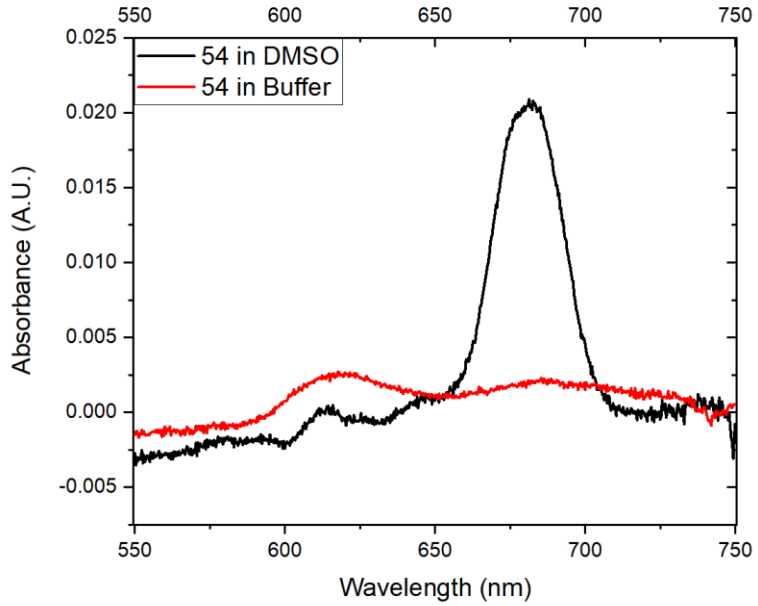

Figure 4.7. Absorption Spectra of ZnPc-Quinazoline Conjugate **54** in DMSO vs 10 % DMSO in aqueous buffer. Concentration of **54** 400 nM.

To determine the conjugate sensor **54** response towards EGFR, we exposed it to low-nanomolar concentrations of the kinase in aqueous solutions. Addition of EGFR

resulted in an immediate appearance of the fluorescent emission with a maximum at 692 nm. As expected, the emission intensity increased upon increasing EGFR concentration (Figure 4.8).

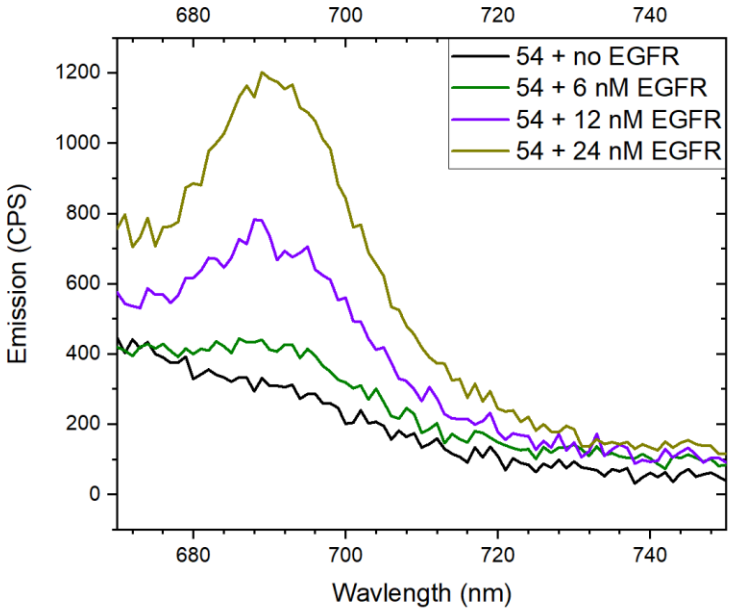

Figure 4.8. Emission Spectra of ZnPc-Quinazoline Conjugate **54** Upon Varying Cocentration of EGFR Kinase in HEPES Buffer. Concentration of **54** 400 nM, Excitationt at 665 nm.

The observed behavior was consistent with our hypothesis that the Pc's emission was restored in the presence of EGFR. We attribute the turn-on fluorescent response to de-aggregation of the phthalocyanine reporter upon quinazoline "anchor" binding to the EGFR kinase site. We confirmed this assumption through comparison of the absorption spectra of **54** in the presence of EGFR and without the enzyme. In aqueous solution, the Q-band (black trace in Figure 4.9) was hypsochromically shifted indicating an extensive H-aggregation. Addition of EGFR resulted in appearance of the bathochromically shifted "non-aggregated" Q-band at 680 nm (blue trace in Figure 4.9) indicating that at least a fraction of the Pc chromophore population became not

aggregated in the presence of EGFR. Exposing the conjugate **54** to control protein BSA did not induce this bathochromic shift seen with EGFR, indicating a selectivity for EGFR.

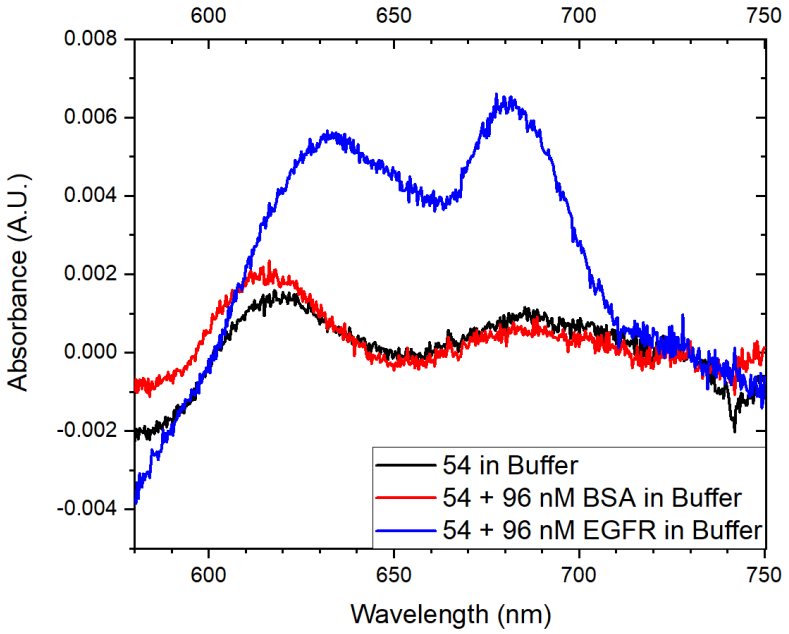

Figure 4.9. Absorption Spectra of ZnPc-Quinazoline Conjugate **54** in HEPES Buffer with Either BSA or EGFR Additions. Concentration of **54** 400 nM.

To demonstrate and confirm the selective response of the conjugate sensor **54** towards EGFR, we exposed **54** to various concentrations of BSA protein. There was no fluorescence detected in the presence of any amount of BSA protein indicating that Pc emission was not restored, even upon adding exceedingly high concentrations of BSA (Figure 4.10).

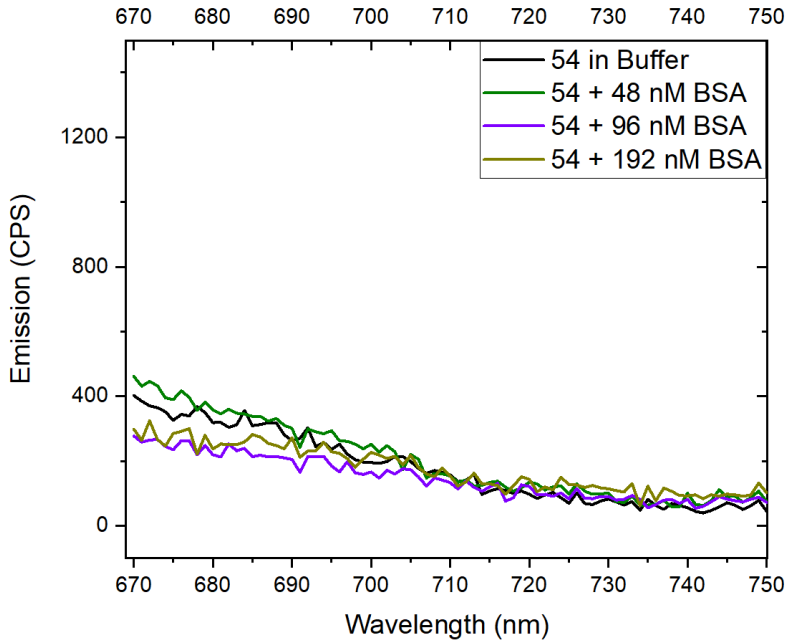

Figure 4.10. Emission Spectra of ZnPc-Quinazoline Conjugate **54** with Varying Concentrations of BSA Protein in HEPES Buffer. Concentration of **54** 400 nM, Excitation at 665 nm.

These groundbreaking experiments confirmed a conceptually novel simple design for selective and sensitive fluorogenic sensors for biopolymers (specifically, EGFR tyrosine kinase). This design yields NIR fluorescent systems that turn on upon binding to a specific protein target and furnish S/B ratios that are significantly higher than other reported long-wavelength fluorescent probes.[23] The turn-on response is based on the Pc aggregation/de-aggregation mechanism, and thus independent on the specific protein target. Binding selectivity results form including a well characterized small-molecule inhibitor fragment into the sensor's structure. While other sensors with specificity driven by inhibitor-based domains are known,[9,24-29] our approach offers an intrinsic turn-on response (with high S/B ratio over dark background), which does not require any washing steps, and does not suffer from non-target reactivity in biological environments ultimately leading to simplified analytical protocols.[30] The selective turn-on

fluorescent sensor for EGFR kinase illustrated that Pc's aggregation / de-aggregation mechanism provides a perfect balance between the possibility to affect this process via binding to a specific biopolymer target while remaining unaffected by non-specific binding. Therefore, this approach can offer broad capabilities in designing fluorogenic sensors not only for EGFR kinase but also for various protein targets.

4.5. Future Directions

Based on the success of this probe, we are currently investigating the photophysical properties of compounds which vary in the nature and position of halogenation (**54** vs **65**) and presence of the Michael acceptor (**54** vs **66**) (Figure 4.11).

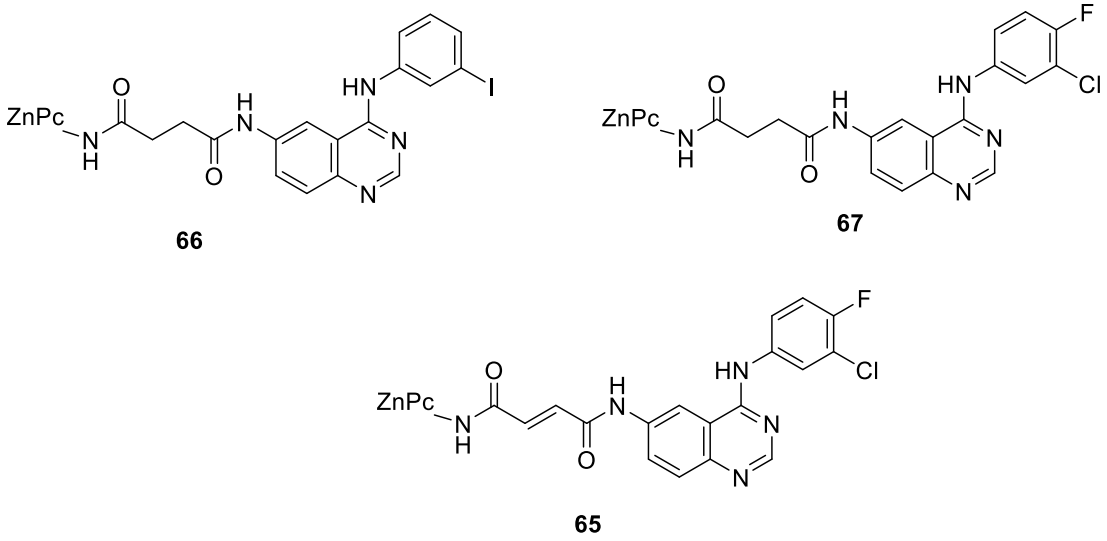

Figure 4.11. Structural Analogs of ZnPc-Quinazoline Conjugate **54**

The goal of monitoring TKI treatment and determining potential TKI effectiveness using this probe-protein complex system necessitates the ability for the probe to bind reversibly to the protein. The current structure could potentially prevent this binding reversibility due to the presence of the C=C double bond (Michael acceptor). Thus, the

development of the saturated analogs **66** and **67** of the probe (which lack this double bond) would allow us to investigate the use of our system in both monitoring treatment outcomes and helping predict new molecular design of inhibitors. The synthesis of the new sensor molecules would follow the schemes described previously (see Chapter 3). The behavior of these three probes would give us better insight into the generality of the aggregation / de-aggregation, turn-on fluorescent mechanism, and will enable developing practical fluorescent-based assays for kinase inhibitor screening.

4.5. Notes

1. Lebedeva, N. S., Aggregation properties of water-soluble metal p hthalocyanines: effect of ionic strength of solution. *Russian Chemical Bulletin* **2004,** *53* (12), 2674-2683.

2. Duan, W.; Smith, K.; Savoie, H.; Greenman, J.; Boyle, R. W., Near IR emitting isothiocyanato-substituted fluorophores: their synthesis and bioconjugation to monoclonal antibodies. *Organic & Biomolecular Chemistry* **2005,** *3* (13), 2384-2386.

3. Nesterova, I. V.; Verdree, V. T.; Pakhomov, S.; Strickler, K. L.; Allen, M. W.; Hammer, R. P.; Soper, S. A., Metallo-Phthalocyanine Near-IR Fluorophores: Oligonucleotide Conjugates and Their Applications in PCR Assays. *Bioconjugate Chemistry* **2007,** *18* (6), 2159-2168.

4. Nesterova, I. V.; Erdem, S. S.; Pakhomov, S.; Hammer, R. P.; Soper, S. A., Phthalocyanine Dimerization-Based Molecular Beacons Using Near-IR Fluorescence. *Journal of the American Chemical Society* **2009,** *131* (7), 2432-2433.

5. Nesterova, I. V.; Bennett, C. A.; Erdem, S. S.; Hammer, R. P.; Deininger, P. L.; Soper, S. A., Near-IR single fluorophore quenching system based on phthalocyanine (Pc) aggregation and its application for monitoring inhibitor/activator action on a therapeutic target: L1-EN. *Analyst* **2011,** *136* (6), 1103-1105.

6. Soper, S. A.; Mattingly, Q. L.; Vegunta, P., Photon burst detection of single near-infrared fluorescent molecules. *Analytical Chemistry* **1993,** *65* (6), 740-747.

7. Williams, D. C.; Soper, S. A., Ultrasensitive Near-IR Fluorescence Detection for Capillary Gel Electrophoresis and DNA Sequencing Applications. *Analytical Chemistry* **1995,** *67* (19), 3427-3432.

8. Frangioni, J. V., In vivo near-infrared fluorescence imaging. *Current Opinion in Chemical Biology* **2003,** *7* (5), 626-634.

9. Adams, K. E.; Ke, S.; Kwon, S.; Liang, F.; Fan, Z.; Lu, Y.; Hirshi, K.; Mawad, M. E.; Barry, M. A.; Sevick-Muraca, E. M., Comparison of visible and near-infrared wavelength-excitable fluorescent dyes for molecular imaging of cancer. *Journal of Biomedical Optics* **2007,** *12* (2), 1-9, 9.

10. Gioux, S.; Choi, H. S.; Frangioni, J. V., Image-guided surgery using invisible near-infrared light: fundamentals of clinical translation. *Mol Imaging* **2010,** *9* (5), 237-255.

11. Cheng, K.; Chen, H.; Jenkins, C. H.; Zhang, G.; Zhao, W.; Zhang, Z.; Han, F.; Fung, J.; Yang, M.; Jiang, Y.; Xing, L.; Cheng, Z., Synthesis, Characterization, and Biomedical Applications of a Targeted Dual-Modal Near-Infrared-II Fluorescence and Photoacoustic Imaging Nanoprobe. *ACS Nano* **2017,** *11* (12), 12276-12291.

12. Piruska, A.; Nikcevic, I.; Lee, S. H.; Ahn, C.; Heineman, W. R.; Limbach, P. A.; Seliskar, C. J., The autofluorescence of plastic materials and chips measured under laser irradiation. *Lab on a Chip* **2005,** *5* (12), 1348-1354.

13. Cheong, W. F.; Prahl, S. A.; Welch, A. J., A review of the optical properties of biological tissues. *IEEE Journal of Quantum Electronics* **1990,** *26* (12), 2166-2185.

14. Pal, A.; Glekas, A.; Doubrovin, M.; Balatoni, J.; Beresten, T.; Maxwell, D.; Soghomonyan, S.; Shavrin, A.; Ageyeva, L.; Finn, R.; Larson, S. M.; Bornmann, W.; Gelovani, J. G., Molecular Imaging of EGFR Kinase Activity in Tumors with 124I-Labeled Small Molecular Tracer and Positron Emission Tomography. *Molecular Imaging and Biology* **2006,** *8* (5), 262-277.

15. Shaul, M.; Abourbeh, G.; Jacobson, O.; Rozen, Y.; Laky, D.; Levitzki, A.; Mishani, E., Novel iodine-124 labeled EGFR inhibitors as potential PET agents for molecular imaging in cancer. *Bioorganic & Medicinal Chemistry* **2004,** *12* (13), 3421-3429.

16. Aldrich, S., Protein Tyrosine Kinase Assay Kit, Non-Radioactive Cataloge Number PTK101. In *Sigma Aldrich*, 1996; pp 1-8.

17. Good, N. E.; Winget, G. D.; Winter, W.; Connolly, T. N.; Izawa, S.; Singh, R. M. M., Hydrogen Ion Buffers for Biological Research. *Biochemistry* **1966,** *5* (2), 467-477.

18. Wampler, D. E.; Takahashi, M.; Westhead, E. W., Active subunits of the aspartokinase-homoserine dehydrogenase I complex from Escherichia coli. *Biochemistry* **1970,** *9* (21), 4210-4216.

19. Franz, A.; Burgstaller, W.; Müller, B.; Schinner, F., Influence of medium components and metabolic inhibitors on citric acid production by Penicillium simplicissimum. *Microbiology* **1993,** *139* (9), 2101-2107.

20. Tárrega, C.; Pulido, R., A one-step method to identify MAP kinase residues involved in inactivation by tyrosine- and dual-specificity protein phosphatases. *Analytical Biochemistry* **2009,** *394* (1), 81-86.

21. Koland, J. G.; Cerione, R. A., Activation of the EGF receptor tyrosine kinase by divalent metal ions: Comparison of holoreceptor and isolated kinase domain properties. *Biochimica et Biophysica Acta (BBA) - Molecular Cell Research* **1990,** *1052* (3), 489-498.

22. Zhang, X.; Gureasko, J.; Shen, K.; Cole, P. A.; Kuriyan, J., An Allosteric Mechanism for Activation of the Kinase Domain of Epidermal Growth Factor Receptor. *Cell* **2006,** *125* (6), 1137-1149.

23. Wieczorek, A.; Werther, P.; Euchner, J.; Wombacher, R., Green- to far-red-emitting fluorogenic tetrazine probes – synthetic access and no-wash protein imaging inside living cells. *Chemical Science* **2017,** *8* (2), 1506-1510.

24. Meimetis, L. G.; Carlson, J. C. T.; Giedt, R. J.; Kohler, R. H.; Weissleder, R., Ultrafluorogenic Coumarin–Tetrazine Probes for Real-Time Biological Imaging. *Angewandte Chemie International Edition* **2014,** *53* (29), 7531-7534.

25. Carlson, J. C. T.; Meimetis, L. G.; Hilderbrand, S. A.; Weissleder, R., BODIPY–Tetrazine Derivatives as Superbright Bioorthogonal Turn-on Probes. *Angewandte Chemie International Edition* **2013,** *52* (27), 6917-6920.

26. Li, L.; Zhang, C.-W.; Ge, J.; Qian, L.; Chai, B.-H.; Zhu, Q.; Lee, J.-S.; Lim, K.-L.; Yao, S. Q., A Small-Molecule Probe for Selective Profiling and Imaging of Monoamine Oxidase B Activities in Models of Parkinson's Disease. *Angewandte Chemie International Edition* **2015,** *54* (37), 10821-10825.

27. Gao, M.; Su, H.; Lin, G.; Li, S.; Yu, X.; Qin, A.; Zhao, Z.; Zhang, Z.; Tang, B. Z., Targeted imaging of EGFR overexpressed cancer cells by brightly fluorescent nanoparticles conjugated with cetuximab. *Nanoscale* **2016,** *8* (32), 15027-15032.

28. Lanning, B. R.; Whitby, L. R.; Dix, M. M.; Douhan, J.; Gilbert, A. M.; Hett, E. C.; Johnson, T. O.; Joslyn, C.; Kath, J. C.; Niessen, S.; Roberts, L. R.; Schnute, M. E.; Wang, C.; Hulce, J. J.; Wei, B.; Whiteley, L. O.; Hayward, M. M.; Cravatt, B. F., A road map to evaluate the proteome-wide selectivity of covalent kinase inhibitors. *Nature Chemical Biology* **2014,** *10*, 760.

29. Heath, C. H.; Deep, N. L.; Sweeny, L.; Zinn, K. R.; Rosenthal, E. L., Use of Panitumumab-IRDye800 to Image Microscopic Head and Neck Cancer in an Orthotopic Surgical Model. *Annals of Surgical Oncology* **2012,** *19* (12), 3879-3887.

30. Qian, L.; Pan, S.; Lee, J.-S.; Ge, J.; Li, L.; Yao, S. Q., Live-cell imaging and profiling of c-Jun N-terminal kinases using covalent inhibitor-derived probes. *Chemical Communications* **2019,** *55* (8), 1092-1095.

Chapter 5. Experimental Details

5.1. General Experimental Considerations

All reactions were performed under an atmosphere of dry nitrogen (unless mentioned otherwise). Column chromatography was performed on silica gel (Sorbent Technologies, 60 Å, 40-63 μm) slurry packed into glass columns. Dichloromethane was dried by passing through activated alumina, and N,N-dimethylformamide (DMF) was dried by passing through 3 Å molecular sieves, using a GS-SPS-7 Solvent Purification System from Pure Process Technology. The water content of the solvents was periodically monitored by Karl Fischer titration (using a DL32 coulometric titrator from Mettler Toledo). N,N-Diisopropylethylamine (DIPEA) was purchased from Aldrich, distilled over CaH_2 and stored over KOH. Fmoc-Rink amide resin was purchased from P3 Biosystems. All other reagents and solvents were purchased from Aldrich, Matrix, Oakwood Chemical, Alfa Aesar, Acros, VWR, or TCI and used without further purification.

Melting points were determined in open capillaries and were not corrected. UV/vis absorption spectra were recorded on either an Agilent Cary 4000 UV/vis spectrometer or Agilent Cary 5000 UV/vis spectrometer. Fluorescence studies were carried out using a PTI QuantaMaster4/2006SE spectrofluorimeter. Absolute quantum yields were determined using an integrating sphere interfaced with the spectrofluorimeter. The emission spectra were corrected for buffer blanks. Agitation of the resin beads was performed by passing N_2 through a column with a fritted disk which held the resin and reaction solution. Shaking of the resin was performed on a J-Kem Max 2000 shaker at 150 RPM. ^1H NMR spectra were recorded at 400 MHz and are

reported in ppm downfield from tetramethylsilane. High-resolution mass spectra (HRMS) were obtained at the Louisiana State University Mass Spectrometry Facility using an Agilent 6210 instrument with electrospray ionization.

5.2. Synthetic Procedures

5.2.1. 4-(4-Hydroxycarbonylphenoxy)-1,2-dicyanobenzene (7):[1]

4-Hydroxybenzoic acid (2.0 g, 14.48 mmol, 1.0 eq) and solid potassium carbonate (4.34 g, 31.43 mmol) were added to a solution of 4-nitrophthalonitrile **5** (2.5 g, 14.48 mmol) in dry DMF (30 mL) under dry nitrogen atmosphere. The mixture was stirred at room temperature for 16 h, poured onto water (50 mL) and acidified with 1M HCl until acidic to pH paper. Compound **7** was obtained as a colorless precipitate that was, collected by filtration, and dried *in vacuo* to yield 2.34 g (61%) of compound **7** as a colorless solid, m.p. 206-207 °C (Lit.[1] 199 °C). ^{1}H NMR ((CD_2Cl_2, 400 MHz) δ 8.20 (d, J = 8.8 Hz, 2H), 7.81 (d, J = 8.7 Hz, 1H), 7.40 (d, J = 2.5 Hz, 1H), 7.34 (dd, J_1 = 8.7 Hz, J_2 = 2.5 Hz, 1H), 7.18 (d, J = 8.8 Hz, 2H).

5.2.2. 4-(2-(2-(2-Methoxyethoxy)ethoxy)ethoxy)phthalonitrile (6):[2]

A solution of 4-nitrophthalonitrile **5** (2.0 g, 11.6 mmol) in dry DMF (10 mL) was added to an oven-dried, two-neck round-bottomed flask containing a solution of triethylene glycol monomethyl ether (3.90 mL, 23.10 mmol) and potassium carbonate (638 g, 46.2 mmol). Upon addition of the phthalonitrile solution, the reaction mixture changed color from yellow to brown. The mixture was stirred at room temperature for 24 h, poured into ice water (50 mL) and left standing overnight. The green precipitate was collected by vacuum filtration. The filtrate extracted using ethyl acetate until washes were colorless

(3 x 20 mL). The organic layers were combined, dried over Na_2SO_4, filtered and solvent removed *in vacuo* to afford **6** as a green-yellow solid which was combined with the initial solid collected by filtration (2.74 g, 81%), m.p. 63-64 °C (Lit[2] 63 °C). ^{1}H NMR ($CDCl_3$, 400 MHz) δ 7.70 (d, J = 8.8 Hz, 1H), 7.31 (d, J = 2.5 Hz, 1H), 7.22 (dd, J_1 = 8.8 Hz, J_2 = 2.5 Hz, 1H), 4.23 (t, J = 4.6 Hz, 2H), 3.88 (t, J = 4.6 Hz, 2H), 3.73–3.71 (m, 2H), 3.67–3.63 , (m, 4H), 3.56–3.53 (m, 2H), 3.38 (s, 3H).

5.2.3. Resin-Bound 4-(4-Hydroxycarbonylphenoxy)-1,2-dicyanobenzene (16a):[3]

(i) Fmoc-protected Rink amide resin (1.917 g, 1.17 mmol, 0.61 mmol/g loading) was swelled in DMF (20 mL; 3 x resin volume) for 30 min, then washed in 1:4 (v/v) 4-methylpiperidine/DMF solution (3 x resin volume) for 5–7 min (repeating 3 times). The resin was washed thoroughly with DMF, rinses checked for 4-methylpiperidine with Bromothymol Blue in ethanol. Presence of free amine was verified by the Kaiser ninhydrin test[3] (2 drops of each of the following added to small portion of resin and heated to 120 °C for 4 – 6 min: 5% ninhydrin in EtOH (w/v); 80% phenol in EtOH (w/v); 2 mL 0.001 M KCN solution in 98 mL pyridine).

(ii) A solution of Fmoc-Lys(Boc)-OH (1.096 g, 2.34 mmol, 2 eq), HOBt (0.316 g, 2.34 mmol, 2 eq), HBTU (0.870 g, 2.29 mmol, 1.96 eq), and DIPEA (0.45 mL, 0.61 g, 4.7 mmol, 4 eq) in dry DMF (15 mL) was sonicated for 3 min, then added to the resin. The mixture was aggitated for 1 h at room temperature. Completion of the coupling was verified by the Kaiser test, monitoring the disappearance of blue color of the beads, as free amine functionality was used up.

(iii) Deprotection of α-amine on Lys (Fmoc protecting group removal) on bead-imobilized lysine (ii) was performed as described in section (i) above. A solution of phthalonitrile

7 (1.02 g, 3.86 mmol, 3.3 eq), HOBt (0.316 g, 2.34 mmol, 2 eq), HBTU (0.870 g, 2.29 mmol, 1.96 eq), and DIPEA (0.82 mL, 0.61 g, 4.7 mmol, 4 eq) in dry DMF (15 mL), was sonicated for 3 min then added to the resin. The resin mixture was agitated, via N_2 bubbling, at room temperature for 1 h and the reaction monitored for completion using the Kaiser ninhydrin test. Upon completion, resin was washed with fresh DMF, CH_2Cl_2, then DMF again. Each wash was performed 3 times, 5 – 7 min per wash, with 3 resin volumes of solvent each time. The resin was finally washed with MeOH (3 × resin volume) for 30 min, filtration, dried under N_2, and stored in the refrigerator.

5.2.4. *tetrakis*-(4-(2-(2-(2-Methoxyethoxy)ethoxy)ethoxy))phthalocyanino zinc (II) (13):

A solution of anhydrous zinc(II) acetate (0.1580 g, 0.861 mmol, 1 eq), phthalonitrile **6** (1.00 g, 3.444 mmol, 4 eq), and 1,8-diazobicyclo[5.4.0]undec-7-ene (DBU, 0.4 mL, 0.4 g, 2.6 mmol, 3 eq; added once solution reached above 90 °C) in dry DMF (35 mL) and *n*-BuOH (2 mL) was reacted for 27 h at 106 °C, monitoring periodically via TLC (first eluted with 100% ethyl ether to remove DMF, then again in 10% MeOH in CH_2Cl_2, product **13** R_f 0.30). The room temperature reaction solution had 3 ×volume of water added and frozen. Following lyophilization, compound **13** was obtained as a green oil, (0.623 g, 59%).^{1}H NMR ($CDCl_3$, 400 MHz) δ ppm: 9.05 (br s, 1H), 7.62 (d, J = 8.3 Hz, 1H), 7.20 (s, 1H), 7.10 (dd, J_1 = 6.2 Hz, J_2 = 2.1 Hz, 1H), 4.17 (t, J = 4.5 Hz, 2H), 3.84 (t, J = 4.4 Hz, 2H), 3.69–3.68 (m, 2H), 3.64–3.59 (m, 6H), 3.50–3.48 (m, 2H), 3.3 (s, 3H).

5.2.5. Zinc Phthalocyanine (4):

The previously reported synthesis[5] was modified as described below. Phthalonitrile-functionalized Rink amide resin **16a** (0.20 g, 0.122 mmol, 1 eq) was swollen in dry DMF

(1 mL) for a minimum of 30 min in a two-neck round-bottom flask at room temperature. In a separate flask phthalonitrile **6** (0.5312 g, 1.83 mmol, 15 eq), and anhydrous zinc acetate (44.8 mg, 0.244 mmol, 2 eq) were dissolved in DMF (1 mL) and sonicated for 3 min before adding the solution in a single portion to the swollen resin. *n*-Butanol (0.5 mL) was added to the suspension and the solution was heated to 106 °C. DBU (0.13 mL, 0.13 g, 0.854 mmol, 7 eq) was added once the solution was at or above 90°C, and the reaction was kept at 106 °C for 24 h. The resin was collected by filtration and washed with hot DMF, hot DCM and hot MeOH until all solvents gave colorless filtrates (3 x 5 min x 15 mL [enough to cover resin] washes).

The resin-bound Zn phthalocyanine **22** was cleaved from the resin by treatment with a cleavage cocktail (TFA/DCM/triisopropylsilane; 20%/78%/2%; 5 – 10 mL [to cover resin]) and was shaken under N_2 atmosphere for 3 – 5 h at room temperature. After cleavage, the solution was filtered and the resin washed with hot CH_2Cl_2 then hot MeOH (5 min washes) until colorless. The combined organic fractions were concentrated *in vacuo* and the green solid was precipitated with ethyl ether and collected via centrifugation to yield 64 mg (39%) of Zn phthalocyanine **4** as a green-blue solid. ^{1}H NMR (DMF-d_7, 400 MHz) δ 9.48 (br. s, 1H), 9.35-9.17 (m, 2H), 9.15-8.93 (m, 3H), 8.48-8.10 (m, 4H), 7.81-7.58 (m, 3H), 7.50-7.47 (m, 3H), 7.09-6.90 (m, 1H), 4.74-4.67 (m, 6H), 4.13 (br. s, 6H), 3.84-3.60 (m, 17 H), 3.32-3.29 (m, 11H), 2.05-1.40 (m, 6H) [the total number of protons reported herein does not match the actual number of protons based on molecular formula of **4** due to some signals from **4** overlapping with signals from residual protons in DMF-d_7 (8.03, 2.92, and 2.75 ppm) as well as from water (3.5

ppm)]. HRMS (ESI-TOF) m/z 663.7437 $[M+2H]^{2+}$ (calcd. for $C_{66}H_{75}N_{11}O_{15}Zn$ 663.7437). UV-Vis: MeOH, 63 µM, Abs: 676 nm (log ε: 3.248). Emission: 689 nm.

5.2.6. 6-Nitro-4(*3H*)-quinazolinone (23):[4]

5-Nitroanthranilic acid (5.00 g, 27.5 mmol) and formamide (40 mL, 78.4 mmol) were placed in a 100 mL round bottomed flask. The mixture was stirred vigorously and heated to 160 °C for 4-6 h in air until completion of the reaction, as monitored by TLC (eluent 10% MeOH in ethyl acetate). Upon cooling, the solution was poured into ice water (100 mL). The yellow solid was collected by filtration, and dried *in vacuo*. More product was extracted with ethyl acetate (3 x 25 mL) from the filtrate. The organic layers were combined, dried over Na_2SO_4, filtered, and concentrated *in vacuo* to yield 4.29 g (82%) of compound **23** as a yellow solid, m.p. 279°C (decomp.) (Lit.[5] 276-277 °C). ^{1}H NMR (DMSO-d_6, 400 MHz) δ 12.75 (s, 1H), 8.81 (d, J = 2.7 Hz, 1H), 8.55 (dd, J_1 = 9.0 Hz, J_2 = 2.7 Hz, 1H), 8.32 (s, 1H), 7.87 (d, J = 9.0 Hz, 1H).

5.2.7. 4-Chloro-6-nitroquinazoline (24):[6]

Compound **23** (1.50 g, 7.845 mmol) was placed in a 100 mL round-bottomed flask under N_2. Thionyl chloride (20 mL) and DMF (1-2 drops from Pasteur pipet) were added and the solution was heated to reflux for 3 h. The excess thionyl chloride was removed *in vacuo* to afford compound **24** as a yellow-brown residue that was used immediately in the next reaction. ^{1}H NMR (DMSO-d_6, 400 MHz) δ 8.81 (d, J = 2.7 Hz, 1H), 8.56 (dd, J_1 = 9.0 Hz, J_2 = 2.7 Hz, 1H), 8.37 (s, 1H), 7.88 (d, J = 9.0 Hz, 1H).

5.2.8. 6-Nitro-4-(3-iodophenylamino)quinazoline (25):[6]

Compound **24** (1.64 g, 7.85 mmol) and 3-iodoaniline (1.719 g, 7.85 mmol, 1 eq) were dissolved in isopropyl alcohol (20 mL) and DIPEA (5.47 mL, 4.06 g, 31.34 mmol, 4 eq).

The mixture was stirred at 25 °C for 10 min wherein a yellow precipitate formed. The mixture was then heated to reflux for 3 h. Upon cooling, the solid was collected by filtration and washed with *i*-PrOH (12 mL) and dried *in vacuo* to yield 2.297g (75%) of compound **25** as a yellow solid, m.p. 236-237 °C. ^{1}H NMR (DMSO-d_6, 400 MHz) δ 10.44 (s, 1H), 9.67 (d, J = 2.4 Hz, 1H), 8.78 (s, 1H), 8.58 (dd, J_1 = 9.2 Hz, J_2 = 2.4 Hz, 1H), 8.30 (s, 1H), 7.97 – 7.96 (m, 2H), 7.55 (d, J = 7.9 Hz, 1H), 7.24 (t, J = 7.9 Hz, 1H).

5.2.9. 6-Amino-4-(3-iodophenylamino)quinazoline (26):[7]

Compound **25** (2.00 g, 5.100 mmol, 1 eq) was dissolved in EtOH (30 mL, 0.13 M) with conc. HCl (10 mL). Tin (II) chloride dihydrate (5.754 g, 25.5 mmol, 5 eq) was then added, giving rise to a yellow solution. The resulting solution was heated to reflux for 1-2 h, monitoring with TLC (1:1 EtOAc/Hexanes, R_f 0.083). Upon cooling, the reaction mixture was concentrated *in vacuo* to give a residue that was basified with sat. aq. $NaHCO_3$ until the solution was basic to pH paper. The $Sn(OH)_2$ was removed by filtration. The product was extracted from the filtrate with ethyl acetate (4 x 25 mL), washed with water (3 x 20 mL) and brine (3 x 20 mL), dried with Na_2SO_4, and concentrated *in vacuo*. The resulting oil slowly crystallized at room temperature to give 1.3429g (73%) of **26** as a yellow-brown solid, m.p. 190°C (decomp.) ^{1}H NMR (DMSO-d_6, 400 MHz) δ 9.36 (s, 1H), 8.36 (d, J = 1.8 Hz, 1H), 7.93 (dd, J_1 = 8.0 Hz, J_2 = 1.0 Hz, 2H), 7.54 (d, J = 8.8 Hz, 1H), 7.40 (dd, J_1 = 8.0 Hz, J_2 = 1.0 Hz, 1H), 7.33 (d, J = 2.3 Hz, 1H), 7.25 (dd, J_1 = 8.8 Hz, J_2 = 2.3 Hz, 1H), 7.15 (t, J = 8.0 Hz, 1H), 5.59 (br s, 2H).

5.2.10. Ethyl 4-[[4-[(3-iodophenyl)amino]-6-quinazolinyl]amino]-4-oxo-2(*E*)-butenoate (52):

Hydroxybenzotriazole (HOBt, 1.112 g,8.284 mmol, 2.0 eq), HBTU (3.079 g, 8.118 mmol, 1.96 eq), and diisopropylethylamine (DIPEA, 1.52 mL, 1.13 g, 8.698 mmol, 2.1

eq) were added to a solution of monoethyl fumarate (1.194 g, 8.284 mmol, 2.0 eq) in DMF (10 mL) and sonicated for 15 minutes. The reaction was monitored by TLC for disappearance of monoethyl fumarate. The resulting solution was added dropwise to a solution of compound **26** (1.500 g, 4.142 mmol, 1 eq) in DMF (2 mL) and cooled to 0 °C and left to stir and warm to room temperature overnight. The resulting yellow solution was concentrated *in vacuo*. Saturated aq. $NaHCO_3$ solution (50 mL) was added to the residual oil and the mixture then extracted with ethyl acetate (4 x 20 mL). The organic fractions were combined and dried over Na_2SO_4 and concentrated *in vacuo* to afford a yellow solid that was purified by column chromatography on silica gel (eluting with 3:2 ethyl acetate/hexanes) to give 0.816 g (40%) of compound **52** as a yellow solid, R_f 0.29, m.p. >250°C. ^{1}H NMR (400 MHz, Acetone-d_6) δ 10.02 (br s, 1H), 9.39 (br s, 1H), 8.88 (br s, 1H), 8.63 (br s, 1H), 8.47 (s, 1H), 7.99 (d, J = 8.0 Hz, 1H), 7.89 (dd, J_1 = 9.0 Hz, J_2 = 2.0 Hz, 1H), 7.83 (d, J = 9.0 Hz, 1H), 7.50 (d, J = 8.0 Hz, 1H), 7.28 (dd, J_1 = 15.4 Hz, J_2 = 4.3 Hz, 1H), 7.19 (t, J = 8.0 Hz, 1H), 6.88 (dd, J_1 = 15.4 Hz, J_2 = 4.3 Hz, 1H), 4.26 (q, J = 7.1 Hz, 2H), 1.31 (t, J = 7.1 Hz, 3H).

5.2.11. 4-[4-[(3-iodophenyl)amino]-6-quinazolinyl]amino-4-oxo-(2*E*)-2-butenoic acid (53):[7]

A mixture of compound **52** (500.0 mg, 1.0240 mmol, 1 eq) and LiOH (122.6 mg, 5.120 mmol, 5 eq) in 1:1 MeOH/H_2O (30 mL) was stirred at room temperature for 12 h. The reaction was monitored by TLC (1:1 ethyl acetate/hexanes). Upon completion of the reaction, the reaction was acidified with HCl (0.1 M) until the solution was around pH 1 by pH paper. Compound **53** was obtained as a yellow solid precipitated and was filtered off, rinsed with cold water and dried *in vacuo* yielding 430.1 mg (91%), m.p. 280 °C decomp. ^{1}H NMR (DMSO-d_6, 400 MHz) δ 11.14 (br s, 1H), 10.94 (br s, 1H), 9.02 (d, J =

1.6, 1H), 8.78 (br s, 1H), 8.17 (t, J = 1.6 Hz, 1H), 8.03 (dd, J_1 = 9.0 Hz, J_2 = 1.6 Hz, 1H), 7.90 (d, J = 9.0 Hz 1H), 7.79 (dd, J_1 = 8.2 Hz, J_2 = 1.6 Hz, 1H), 7.61 (d, J = 8.2 Hz, 1H); 7.27 – 7.24 (m, 2H), 6.76 (d, J = 15.4 Hz, 1H).

5.2.12. Zinc Phthalocyanine (2*E*)-but-2-en-4-quinazolinyl Adduct (54):

A mixture of compound **53** (86.7 mg, 0.188 mmol, 5 eq), HOBt (25.5 mg, 0.188 mmol, 5 eq), HBTU (71.5 mg, 0.188 mmol, 5 eq), and DIPEA (0.07 mL, 0.377 mmol, 10 eq) in 10 mL of dry DMF was placed in an oven-dried vial, that was covered by a septum, and sonicated until the appearance of an amber-red color (10 – 30 min). Use of TLC monitoring for activated ester formation was also performed as described below. The resulting solution was added dropwise to a solution of ZnPc **4** (50 mg, 0.0377 mmol, 1 eq) in 10 mL of dry DMF in an oven-dried 2 neck 50 mL round-bottomed flask, and the reaction mixture was stirred at room temperature. The reaction was monitored by TLC (first eluted with 100% ethyl ether to remove DMF, then again in 10% MeOH in CH_2Cl_2, product **54** R_f 0.37). Upon completion (24 – 26 h), the reaction mixture was concentrated *in vacuo* to remove most of the DMF, a small volume of MeOH (5 - 10 mL) was added, and the mixture was poured into large volume (50 – 100 mL) of ice-cold ethyl ether. The precipitate was collected by centrifugation, washed with ethyl ether, and dried*in vacuo*. The resulting solid product was additionally purified by filtration through a short silica plug (eluent 10% MeOH in CH_2Cl_2 with 2% (v/v) triethylamine) to yield 32.0 mg (48%) of product **54** as a green solid, ^{1}H NMR (DMF-d_7, 400 MHz) δ 10.10 (br. s, 1H), 9.52-9.25 (m, 1H), 9.15-8.85 (m, 2H), 8.78-8.45 (m, 5H), 8.30-8.10 (m, 4H), 7.84-7.75 (m, 5H), 7.52-7.47 (m, 3H), 7.38-7.20 (m, 7H), 7.20-6.95 (m, 3H), 4.85-4.50 (m, 6H), 4.50-4.05 (m, 6H), 3.86-3.54 (m, 14H), 3.33-3.23 (m, 9H), 3.10-3.01 (m, 2H), 2.05-

1.40 (m, 6H) [the total number of protons reported herein does not match the actual number of protons based on molecular formula of **54** due to some signals from **54** overlapping with signals from residual protons in DMF-d_7 (8.03, 2.92, and 2.75 ppm) as well as from water (3.5 ppm)]. HRMS (ESI-TOF) m/z 884.7416 $[M+2H]^{2+}$ (calcd. for $C_{84}H_{86}N_{15}O_{17}IZn$ 884.7404). UV-Vis: MeOH 63 µM, Abs: 676 nm (log ε: 3.483 M^{-1} cm^{-1}). Emission: 688 nm.

5.2.13. 4-[4-[(3-iodophenyl)amino]-6-quinazolinyl]amido-butanoic acid (59):

A solution of compound 6-aminoquinazoline (**26**) (50 mg, 0.138 mmol, 1 eq) was made in a mixture of CH_2Cl_2 (5 mL) and DMF (1 mL) and cooled to 0 °C. A solution of HOBt (93.3 mg, 0.690 mmol, 5.0 eq), HBTU (259.7 mg, 0.684 mmol, 4.9 eq), monomethyl succinic acid (91.2 mg, 0.690 mmol, 5.0 eq), and DIPEA (0.17 mL, 126.1 mg, 0.966 mmol, 7.0 eq) in CH_2Cl_2 (5 mL) and DMF (1 mL) in an oven-dried 20 mL vial covered with a septum was sonicated for 5 – 10 min until colorless solution became yellow. The HOBt solution was then added dropwise to the quinazoline solution. The mixture was allowed to stir for 24 h and slowly warm to RT. Upon reaction completion, the solution was concentrated *in vacuo* leaving a yellow oil. The oil was dissolved into ethyl acetate (15 mL) and washed with $NaHCO_3$ (3 x 25 mL), Brine (2 x 15 mL), and the organic layer dried over Na_2SO_4. The solvent was concentrated *in vacuo* to yield a yellow solid. The solid was then purified by silica gel flash column, eluting with 3:1 ethyl acetate/hexanes to yield 0.054g (82%) of compound **60** as a yellow solid, m.p. 193 – 195 °C decomp. ^{1}H NMR (DMSO-d_6, 400 MHz) δ 10.36 (br s, 1 H), 9.85 (br s, 1 H), 8.71 (br d, J = 1.7 Hz, 1 H), 8.54 (s, 1 H), 8.26 (t, J = 1.8 Hz, 1 H), 7.89 (br dd, J_1 = 7.0 Hz, J_2 = 1.2 Hz,1 H), 7.82, (dd, J_1 = 6.9 Hz, J_2 = 2.1 Hz, 1 H), 7.77 (d, J = 8.9 Hz, 1 H), 7.45 (br d, J = 8.3 Hz,

1 H), 7.18 (t, *J* = 8.0 Hz, 1 H), 3.61 (s, 3 H), 2.70 (br d, *J* = 6.1 Hz, 2 H), 2.66 (br d, *J* = 5.7 Hz, 2 H).

The methyl succinate ester **60** (46.9 mg, 0.098 mmol, 1 eq) and lithium hydroxide (11.8 mg, 0.492 mmol, 5 eq) were dissolved in a 1:1 mixture of MeOH and H_2O (8.4 mL). The mixture was stirred at RT under N_2 atmosphere for 16 h. Upon monitoring the reaction by TLC (10% MeOH in DCM, R_f 0.2 compound **60**) showed the consumption of the ester, the reaction was stopped and conc HCl was added dropwise (from Pasteur pipet) until acidic by pH paper (~ pH 1). The resultant yellow solid was isolated by filtration, washing with water, and dried under vacuum to yield compound **59** as a yellow solid (45 mg, quant.), m.p. >270 °C. ^{1}H NMR (DMSO-D_6, 400 MHz) δ 12.21 (br s, 1 H), 11.32 (br s, 1 H), 10.63 (br s, 1 H), 9.00 (s, 1 H), 8.86 (s, 1 H), 8.10 (s, 1 H), 7.97 (dd, J_1 = 7.1 Hz, J_2 = 2.0 Hz, 1 H), 7.89 (d, *J* = 9.0 Hz, 1 H), 7.72 (d, *J* = 8.0 Hz, 1 H), 7.66 (d, *J* = 7.9 Hz, 1 H), 7.28 (t, *J* = 8.0 Hz, 1 H), 2.69 (dd, J_1 = 6.6 Hz, J_2 = 5.9 Hz, 2 H), 2.58 (dd, J_1 = 6.5 Hz, J_2 = 6.5 Hz, 1 H).

5.2.14. *N*-(3-Chloro-4-fluorophenyl)-6-nitro-4-quinazolinamine (61):

A solution of compound **24** (as made in **5.2.7.**, *vide supra*, 2.193 g, 10.463 mmol, 1 eq), 3-chloro-4-fluoroaniline (1.523 g, 10.463 mmol, 1 eq) and DIPEA (18.0 mL, 13.36 g, 104.63 mmol, 10 eq) was made in isopropyl alcohol (20 mL) and stirred at room temperature for 10 minutes before heating the solution reflux for 3 h. Upon cooling to room temperature, a yellow brown precipitate formed and was collected by filtration, washed with fresh *i*-PrOH and dried *in vacuo* to yield 2.6404 g (79%) of compound **61** as a yellow brown solid (R_f 0.59, 3:1 ethyl acetate/hexanes), m.p. 239 °C (Lit.[8] 239°C). ^{1}H NMR (DMSO-d_6, 400 MHz) δ 10.54 (br s, 1H), 9.63 (br s, 1H), 8.76 (br s, 1H), 8.37

(d, *J* = 9.0 Hz, 1H), 8.15 (br s, 1H), 7.96 (d, *J* = 9.0 Hz, 1H), 7.82 (br s, 1H), 7.49 (t, *J* = 9.0 Hz, 1H).

5.2.15. *N*-(3-Chloro-4-fluorophenyl)-4,6-quinazolindiamine (62):

Compound **61** (1.00 g, 3.138 mmol, 1 eq) was reduced, by analogy to the reduction compound **25** (§ **5.2.9**) using tin (II) chloride dihydrate (3.54 g, 15.689 mmol, 5 eq) in EtOH (15 mL) with conc HCl (1-2 drops from Pasteur pipet). The reaction mixture was refluxed for 1 h (monitored by TLC, eluted with 3:1 ethyl acetate/hexanes, R_f 0.278 product **62**). The solid was dried *in vacuo* to yield 0.783 g (86%) of compound **62** as a yellow solid, m.p. 243.5 °C – 244.7 °C (Lit.[8] 244 °C). ^{1}H NMR (DMSO-d_6, 400 MHz) δ 9.48 (br s, 1H), 8.36 (s, 1H), 8.21 (dd, J_1 = 6.9 Hz, J_2 = 2.5 Hz, 1H), 7.84 – 7.81 (m, 1H), 7.54 (d, *J* = 8.8 Hz, 1H), 7.41 (t, *J* = 9.1 Hz), 7.31 (br s, 1H), 7.26 (dd, J_1 = 8.84 Hz, J_2 = 2.5 Hz, 1H), 5.64 (s, 2H).

5.2.16. Ethyl 4-[[4-[(3-chloro-4-fluorophenyl)amino]-6-quinazolinyl]amino]-4-oxo-2(*E*)-butenoate (63):

A solution of monoethyl fumarate (49.9 mg, 0.346 mmol, 2.0 eq), HBTU (128.7 mg, 0.339 mmol, 1.96 eq), HOBt (46.8 mg, 0.346 mmol, 2.0 eq), and DIPEA (0.12 mL, 89.8 mg, 0.693 mmol, 4.0 eq) in dry CH_2Cl_2 (10 mL) in an oven dried vial capped with a septum was sonicated for 30 minutes and the colorless solution formed a yellow color. In an oven-dried two-neck round-bottomed flask a solution of compound **62** (50.0 mg, 0.174 mmol, 1.0 eq) in dry CH_2Cl_2 (18 mL). The solution of monoethyl fumarate was added in a single portion to the solution of compound **62** and stirred at room temperature for 24 h. The reaction mixture was concentrated *in vacuo* to leave a reddish oil which was dissolved in ethyl acetate (25 mL). The organic layer was washed

with sat'd. aq. $NaHCO_3$ (20 mL), dried over Na_2SO_4, and solution concentrated *in vacuo* gave a yellow solid that was purified via silica gel column (eluted ethyl acetate/ hexanes 3:2, R_f 0.35). After purification, the compound was concentrated *in vacuo* to yield 39.0 mg (54%) of compound **63** as a yellow solid, m.p. >270 °C. ^{1}H NMR (Acetone-d_6, 400 MHz) δ 10.09 (br s, 1H), 9.51 (br s, 1H), 8.91 (s, 1H), 8.61 (s, 1H), 8.28 (dd, J_1 = 6.8 Hz, J_2 = 2.6 Hz, 1H), 7.90 – 7.82 (m, 3H), 7.35 – 7.26 (m, 2H), 6.87 (d, J = 15.4 Hz, 1H), 4.26 (q, J = 7.1 Hz, 2H), 1.31 (t, 3H).

5.2.17. Ethyl 4-[[4-[(3-chloro-4-fluorophenyl)amino]-6-quinazolinyl]amino]-4-oxo-2(*E*)-butenoic acid (64):

A solution of compound **63** (39.0 mg, 0.094 mmol, 1 eq) and lithium hydroxide (11.3 mg, 0.470 mmol, 5 eq) was dissolved in a 1:1 mixture of MeOH/water (3 mL) and stirred at room temperature for 18 h. Hydrochloric acid (2 M) was added to the reaction mixture until it was acidic to pH paper (~ pH 1). A yellow precipitate formed and was collected by filtration. The reaction gave 33.7 mg (93%) of compound **64** as a yellow solid, m.p. 276 – 278 °C (decomp). ^{1}H NMR (DMSO-d_6, 400 MHz) δ 13.12 (br s, 1H), 10.99 (s, 1H), 10.54 (br s, 1H), 8.96 (s, 1H), 8.70 (s, 1H), 8.08 (d, J = 6.6 Hz, 1H), 7.94 (d, J = 9.0 Hz, 1H), 7.86 (d, J = 9.0 Hz, 1H), 7.74 (br s, 1H), 7.49 (t, J = 9.0 Hz, 1H), 7.24 (d, J = 15.4 Hz, 1H), 6.75 (d, J = 15.4 Hz, 1H).

5.2.18. Sensor compound (65):

A solution of dihalogenated compound **64** (15.0 mg, 0.0388 mmol, 5 eq), HBTU (14.7 mg, 0.0388 mmol, 5 eq), HOBt (0.5 mg, 0.0388 mmol, 5 eq), and DIPEA (0.014 mL, 10.4 mg, 0.078 mmol, 10 eq) was dissolved in dry DMF (4.1 mL) in an oven-dried 20 mL vial capped with a rubber septum and stirred at room temperature. The solution

changed from yellow to ruby red over 15 min, indicating formation of the OBt ester. The ZnPc-NH_2 **4** (10.3 mg, 0.0078 mmol, 1 eq) was added to the solution as a solid, in a single portion, under a steady stream of N_2. The solution turned green and the mixture was stirred at room temperature for 28 h. Upon completion of the reaction (TLC monitoring eluted with ethyl ether then 10% MeOH in CH_2Cl_2 R_f 0.35 product **65**), the reaction mixture was poured into ice-cold ethyl ether (50 mL) and allowed to precipitate overnight. The green solid was collected by centrifugation to yield 6.8 mg (78%) of crude compound **65** as a green solid. Currently, the solid is undergoing further purification (via GPC) and characterication before use in kinase studies.

5.3. Kinase Experiments

Lyophilized EGFR kinase (500 units, 15,000 units/mg) was purchased from Sigma-Aldrich (P/N E2645). The powder was reconstituted with 100 µL of 10% aqueous glycerol, and eight (8) µL aliquots of reconstituted EGFR were sampled into PCR vials. The aliquots were stored at –80 °C until ready to use. The buffer for EGFR kinase/Pc **54** binding studies consisting of 50 mM HEPES, 20 mM $MgCl_2$, 100 µM $MnCl_2$, and 200 µM Na_3VO_4 at pH 7.4 was prepared in house. Pc **54** stock solutions were prepared in DMSO. For binding studies, 8 µL aliquots of EGFR kinase were reconstituted with 96 µL of kinase binding buffer. The reconstituted solutions were kept on ice until used. The samples for binding studies were prepared directly in a 100 µL quartz cuvette used for fluorescence or UV/vis measurements. Briefly, appropriate quantities of binding buffer and DMSO were pipetted into the cuvette, followed by addition of Pc **54** stock solution

and kinase. The measurements were started right after sample preparation. Amounts of buffer and DMSO were set to yield 10% of DMSO in the final preparation.

5.4. ^{1}H NMR of Pertinent Compounds

^{1}H NMR of Compound **7** in CD_2Cl_2 at 400 MHz

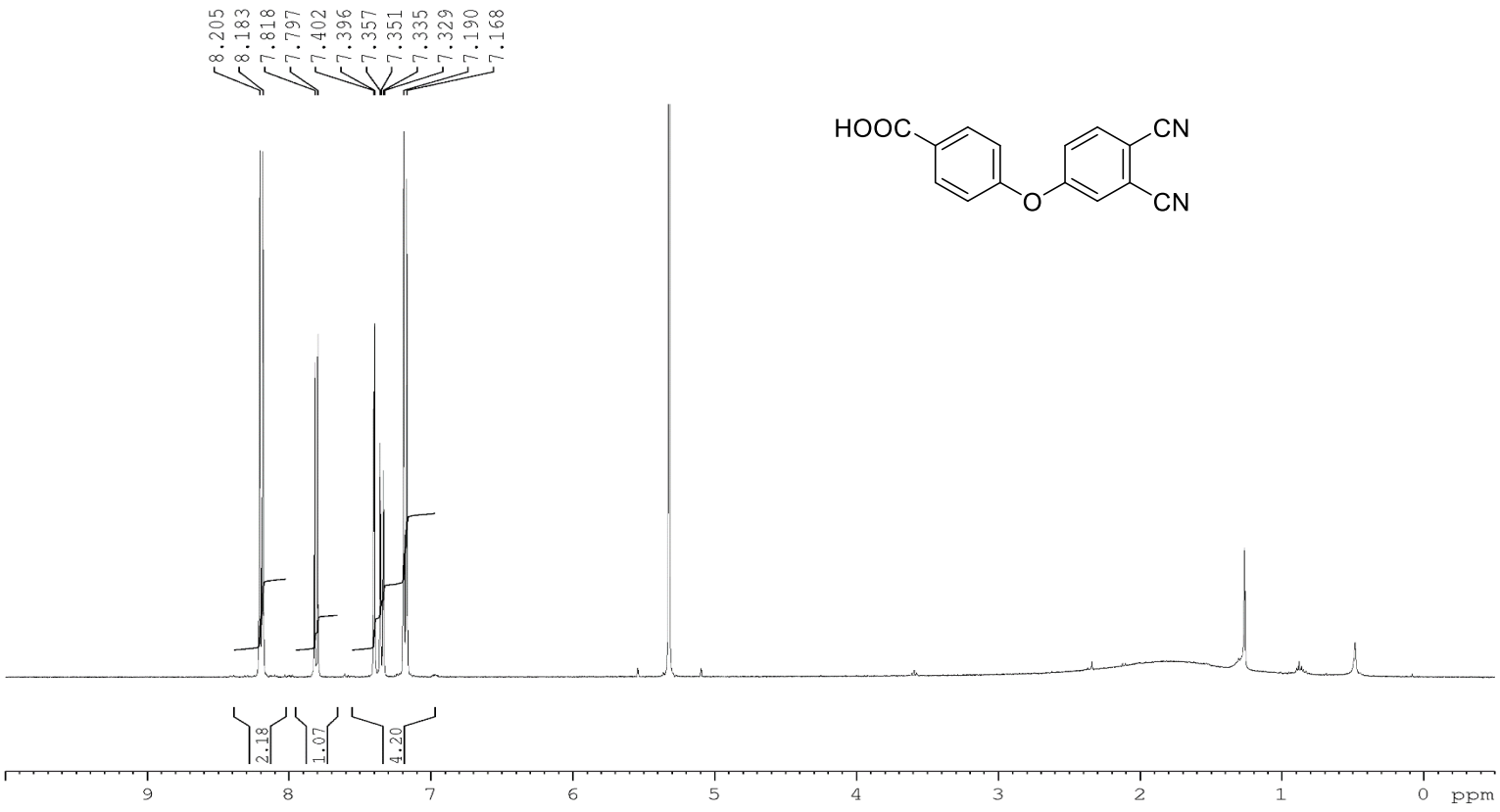

^{1}H NMR of Compound **6** in $CDCl_3$ at 400 MHz

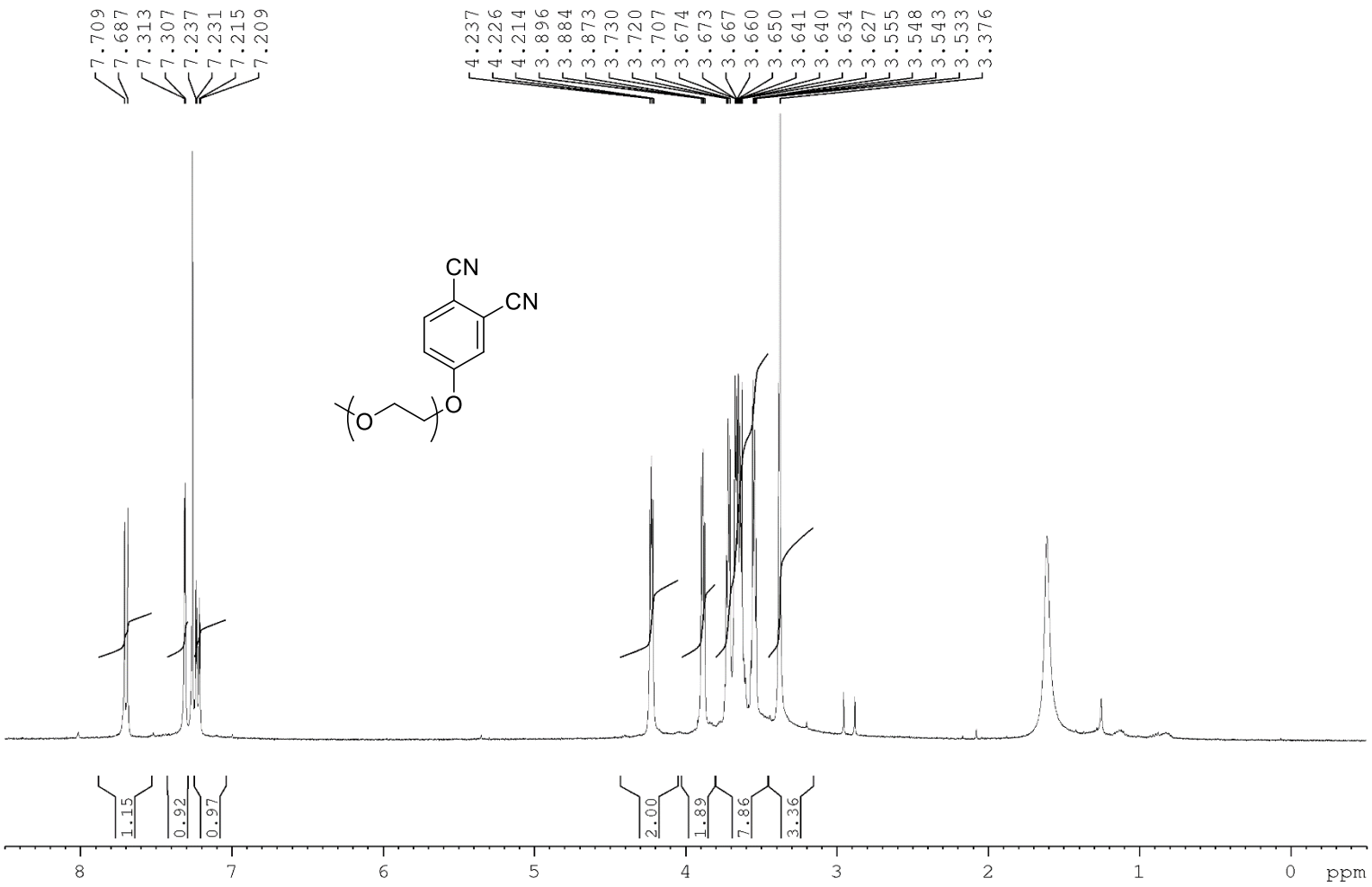

^{1}H NMR of Compound **13** in $CDCl_3$ at 400 MHz

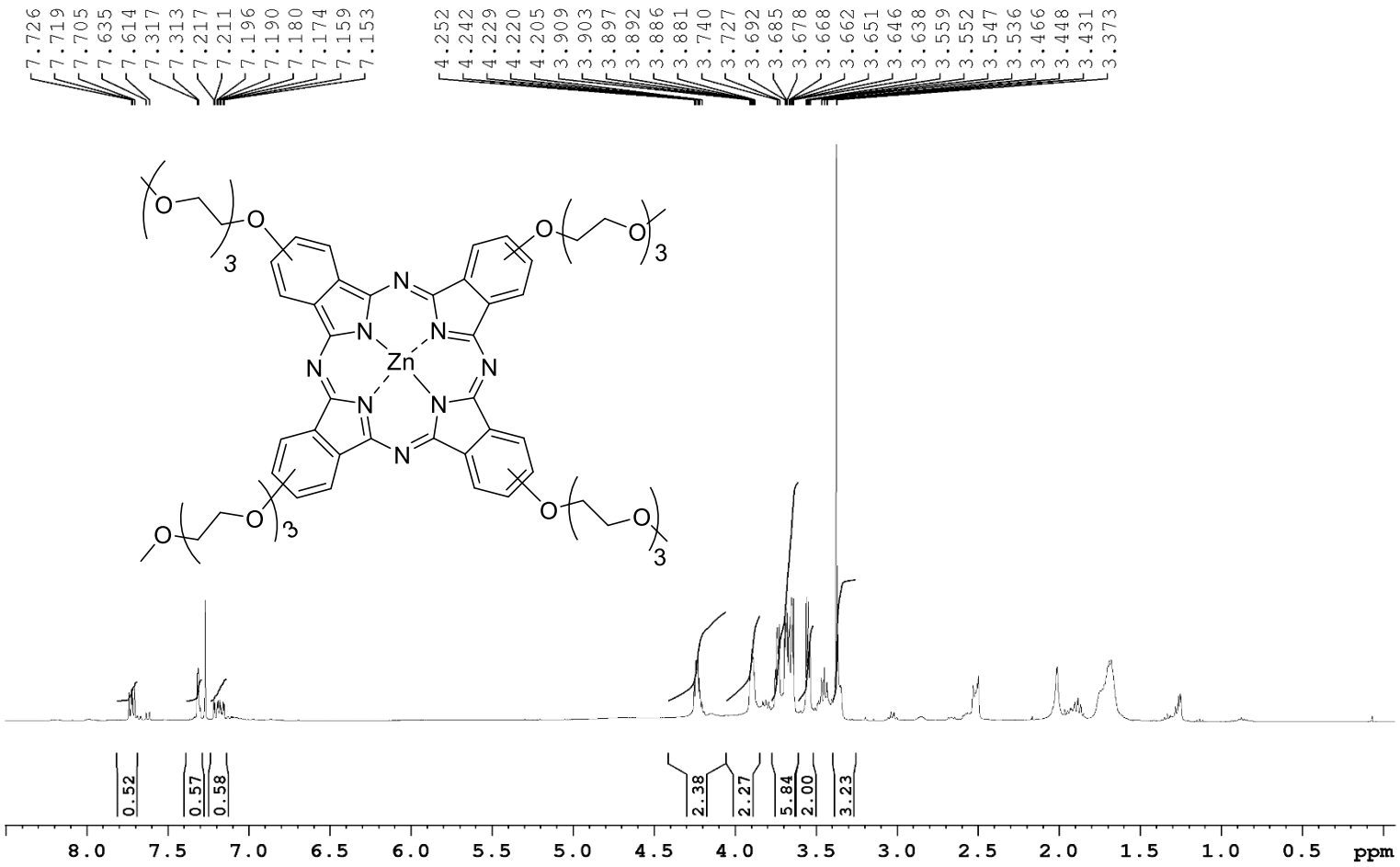

^{1}H NMR of Compound **4** in DMF-d_7 at 400 MHz

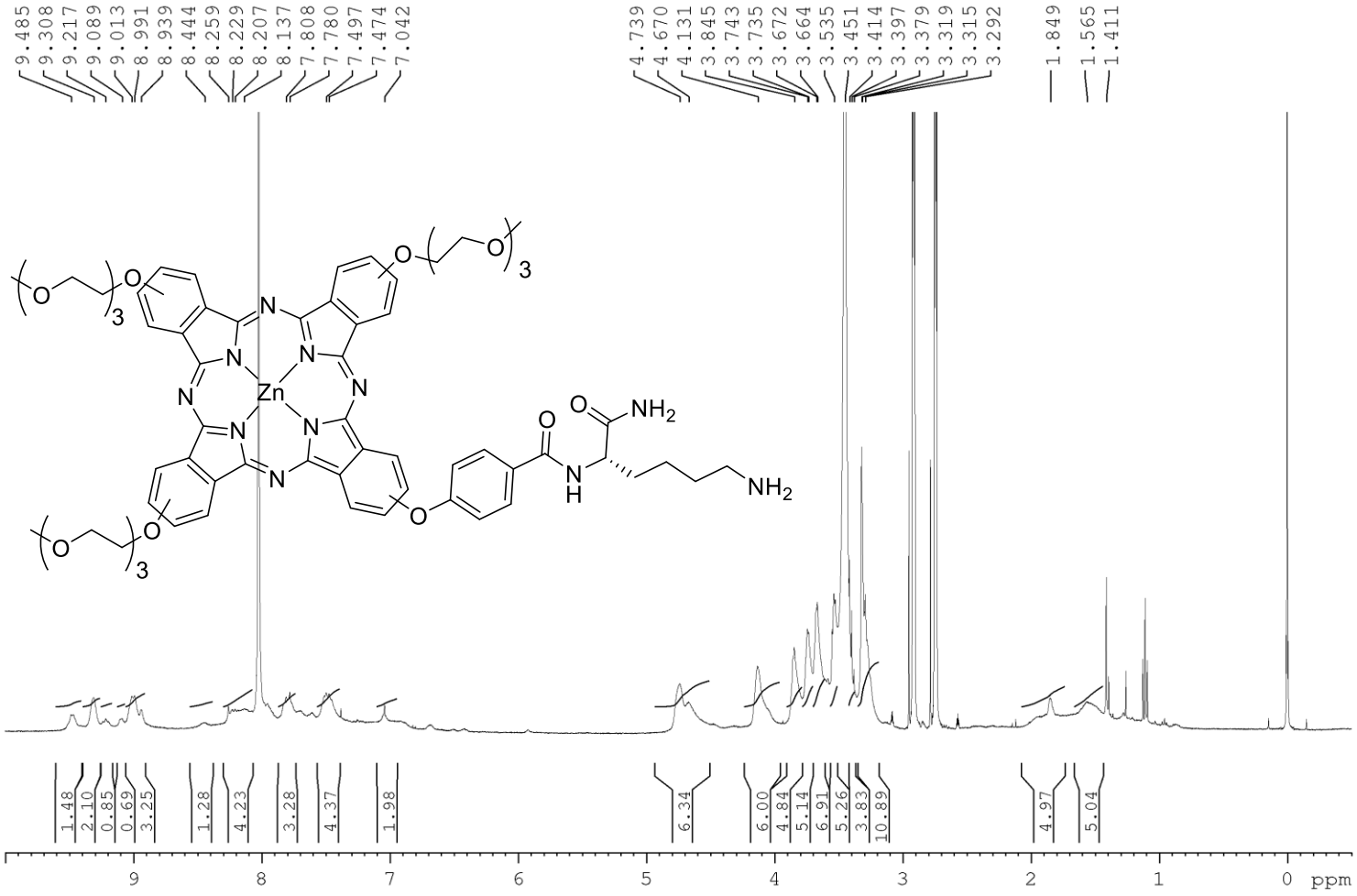

^{1}H NMR of Compound **23** in DMSO-d_6 at 400 MHz

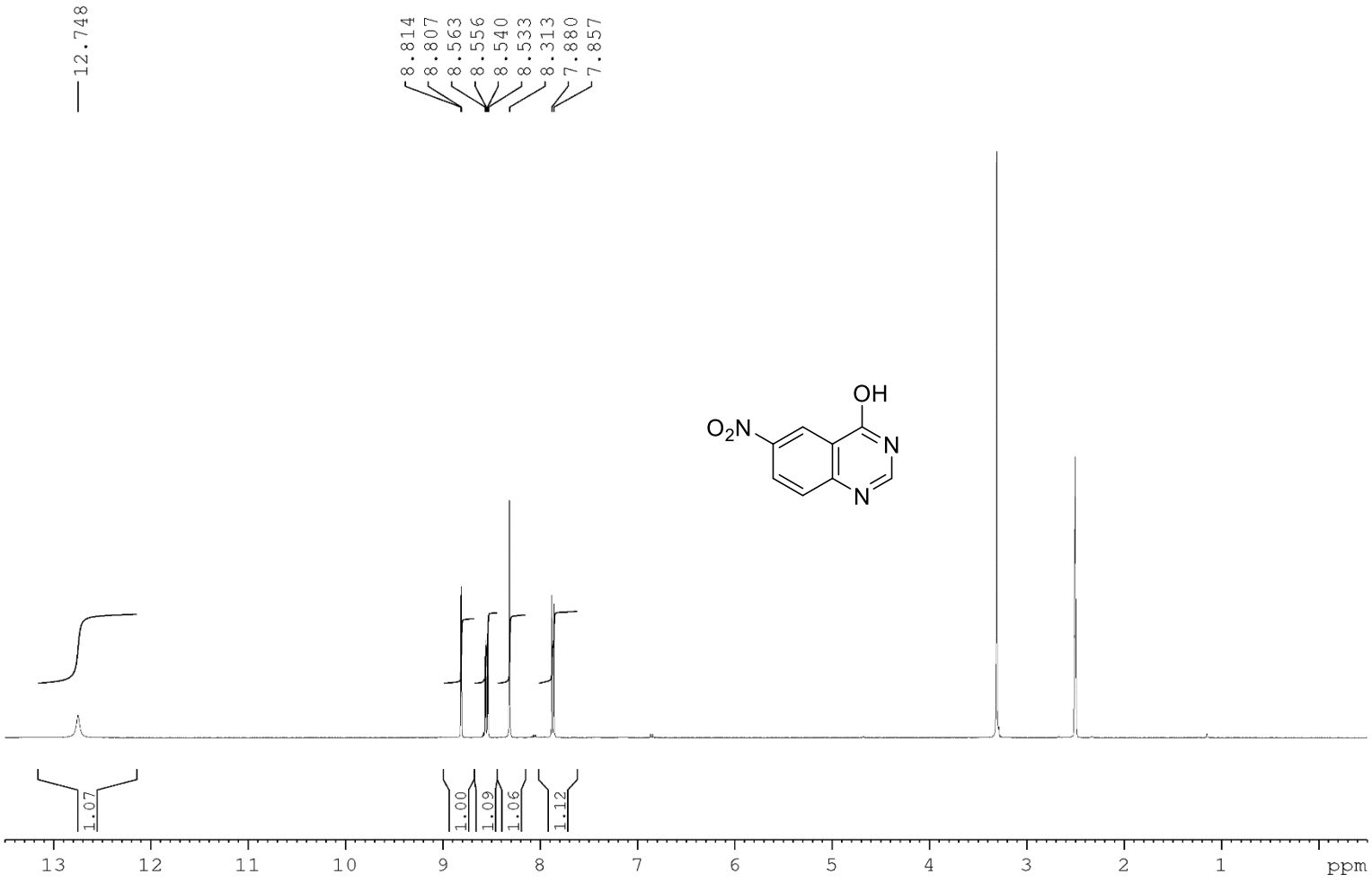

^{1}H NMR of Compound **24** in DMSO-d_6 at 400 MHz

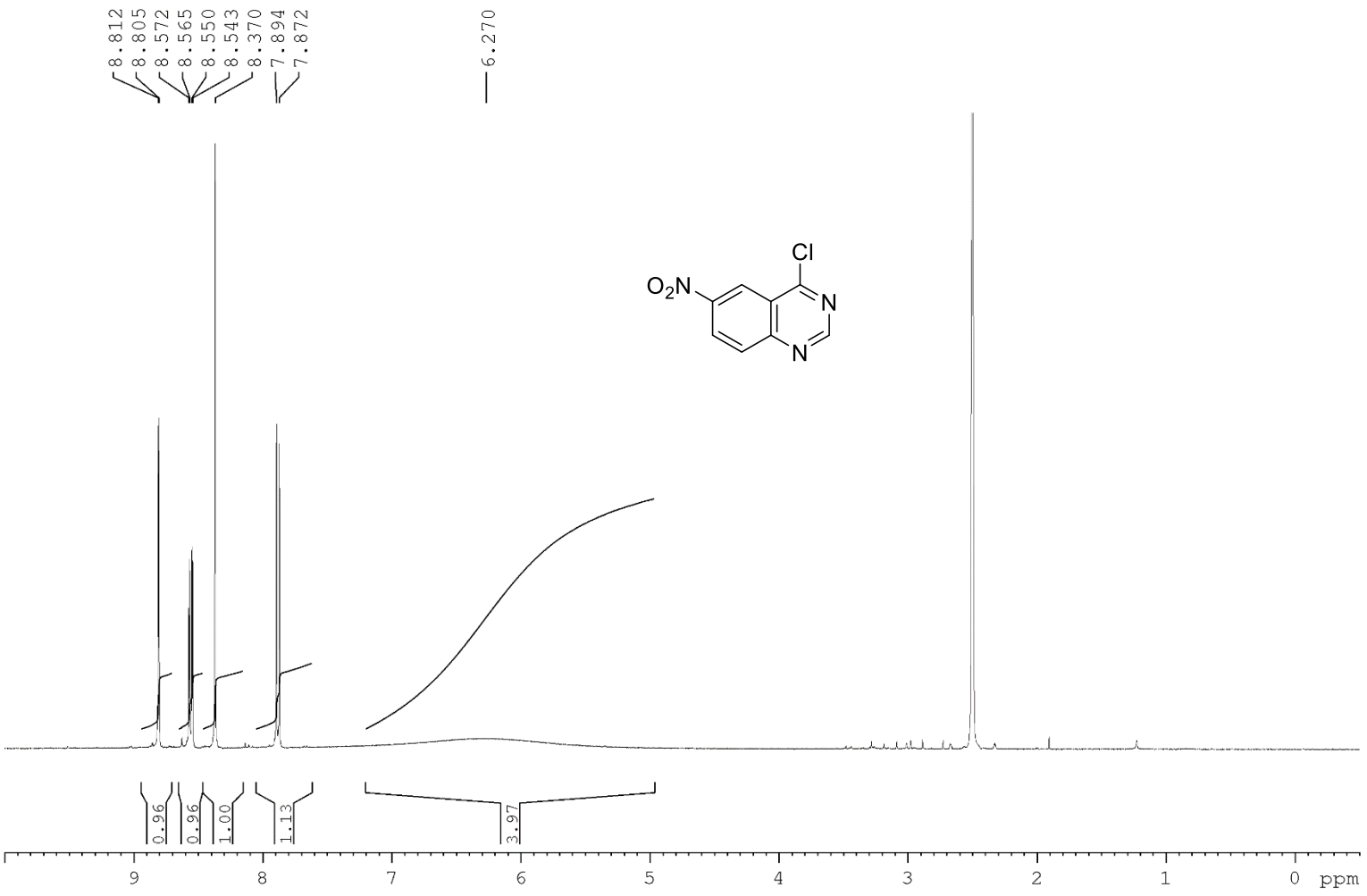

^{1}H NMR of Compound **25** in DMSO-d_6 at 400 MHz

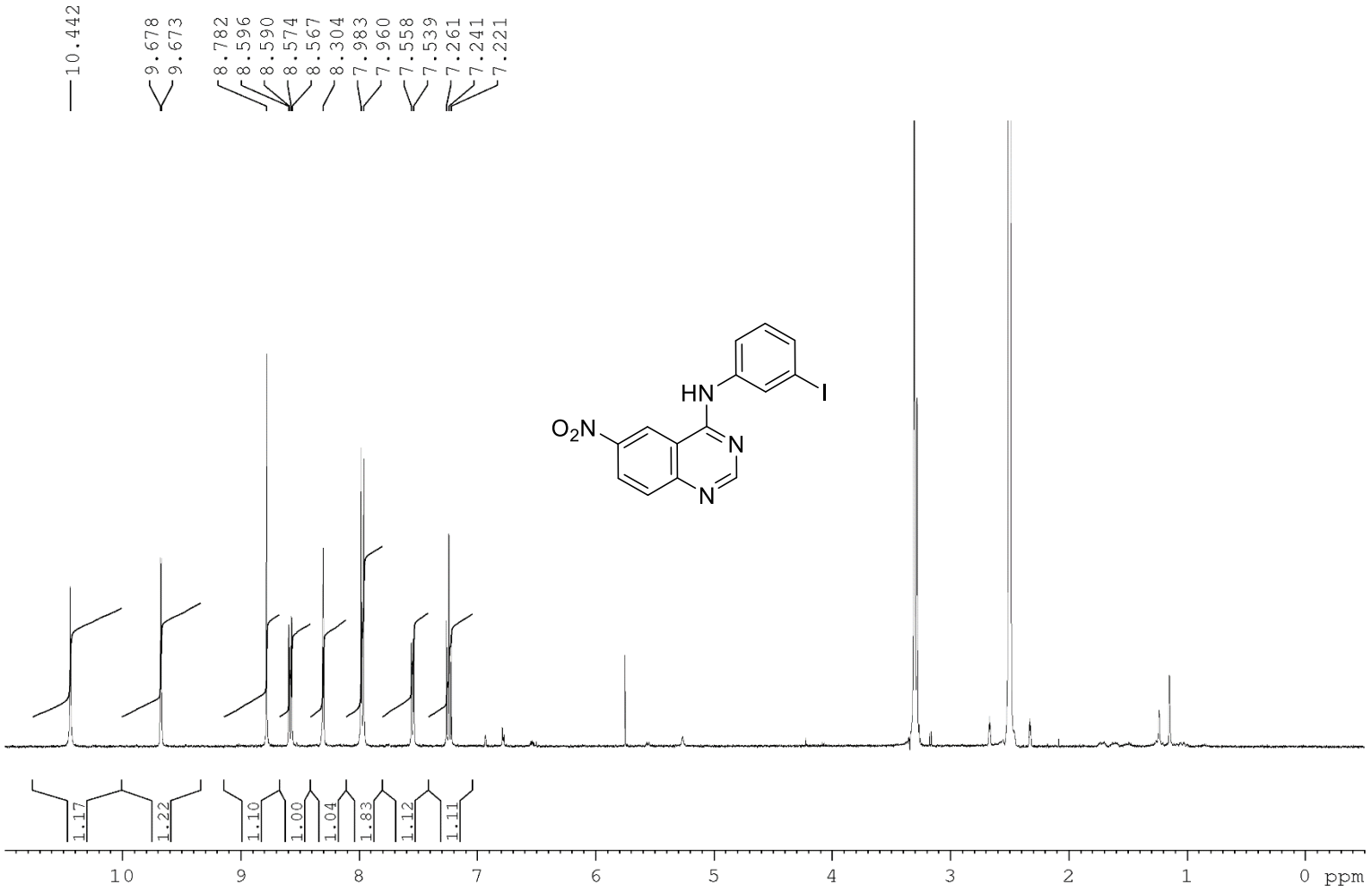

^{1}H NMR of Compound **26** in DMSO-d_6 at 400 MHz

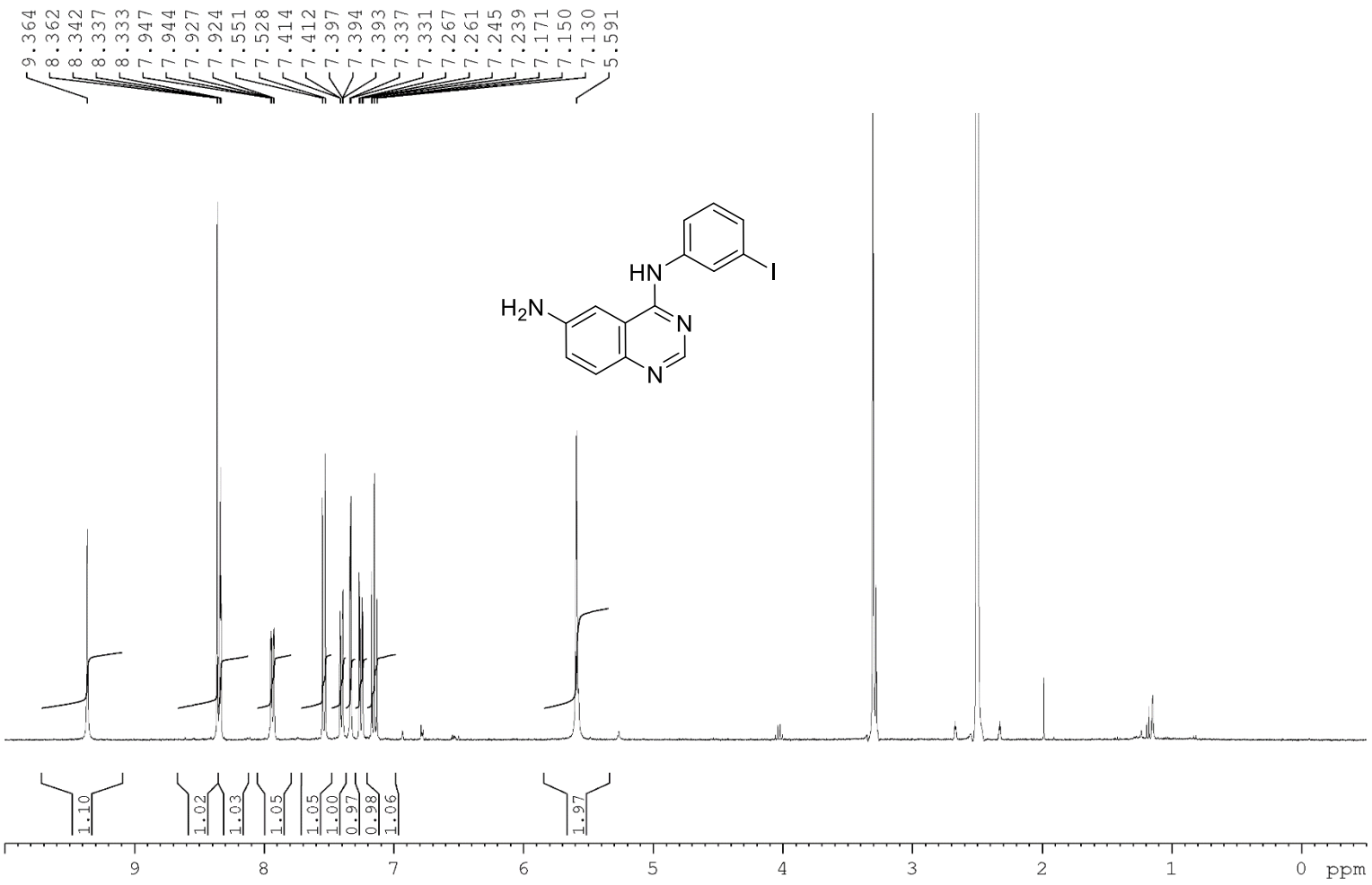

^{1}H NMR of Compound **51** in DMSO-d_6 at 400 MHz

^{1}H NMR of Compound **52** in Acetone-d_6 at 400 MHz

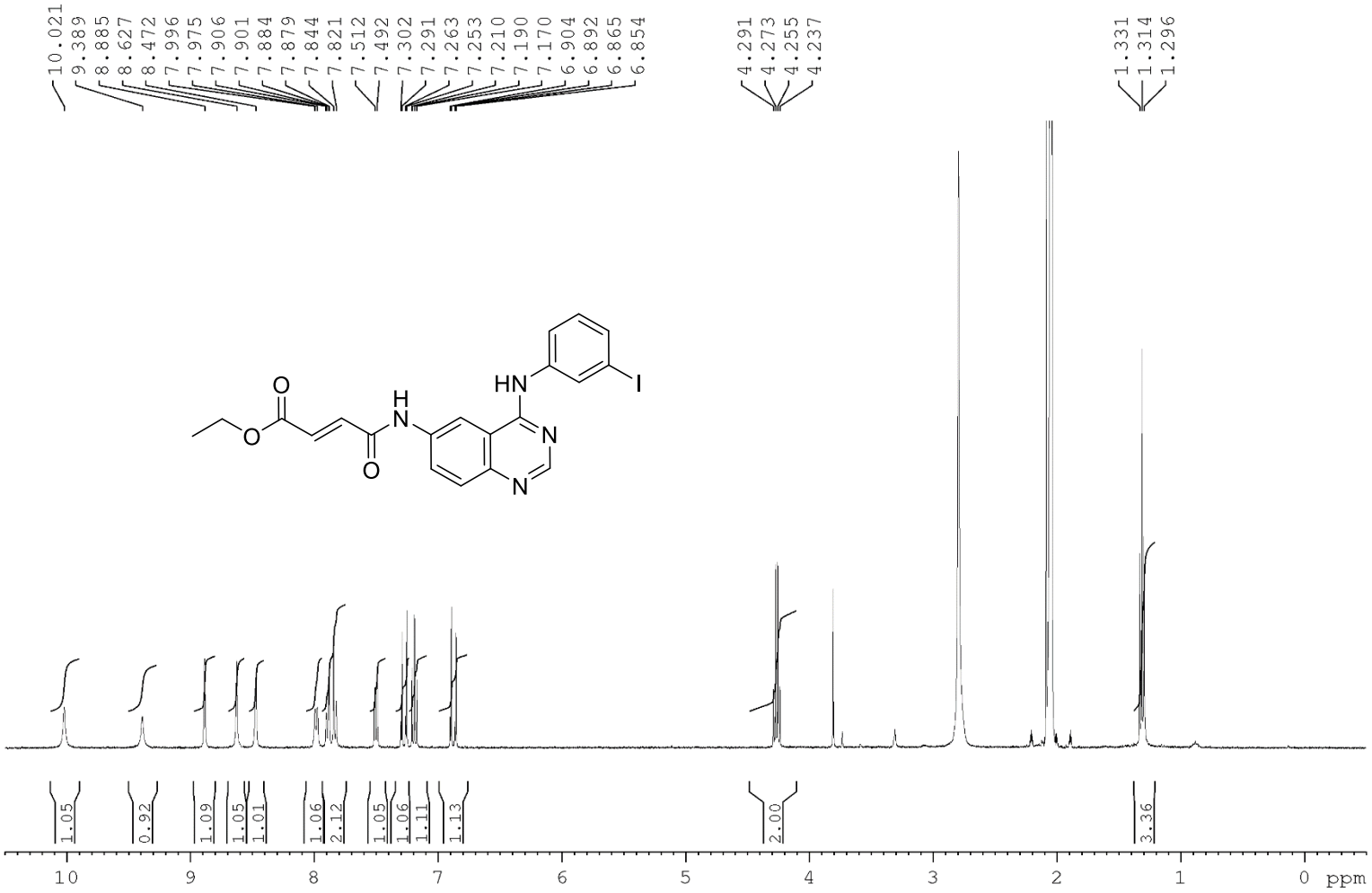

^{1}H NMR of Compound **53** in DMSO-d_6 at 400 MHz

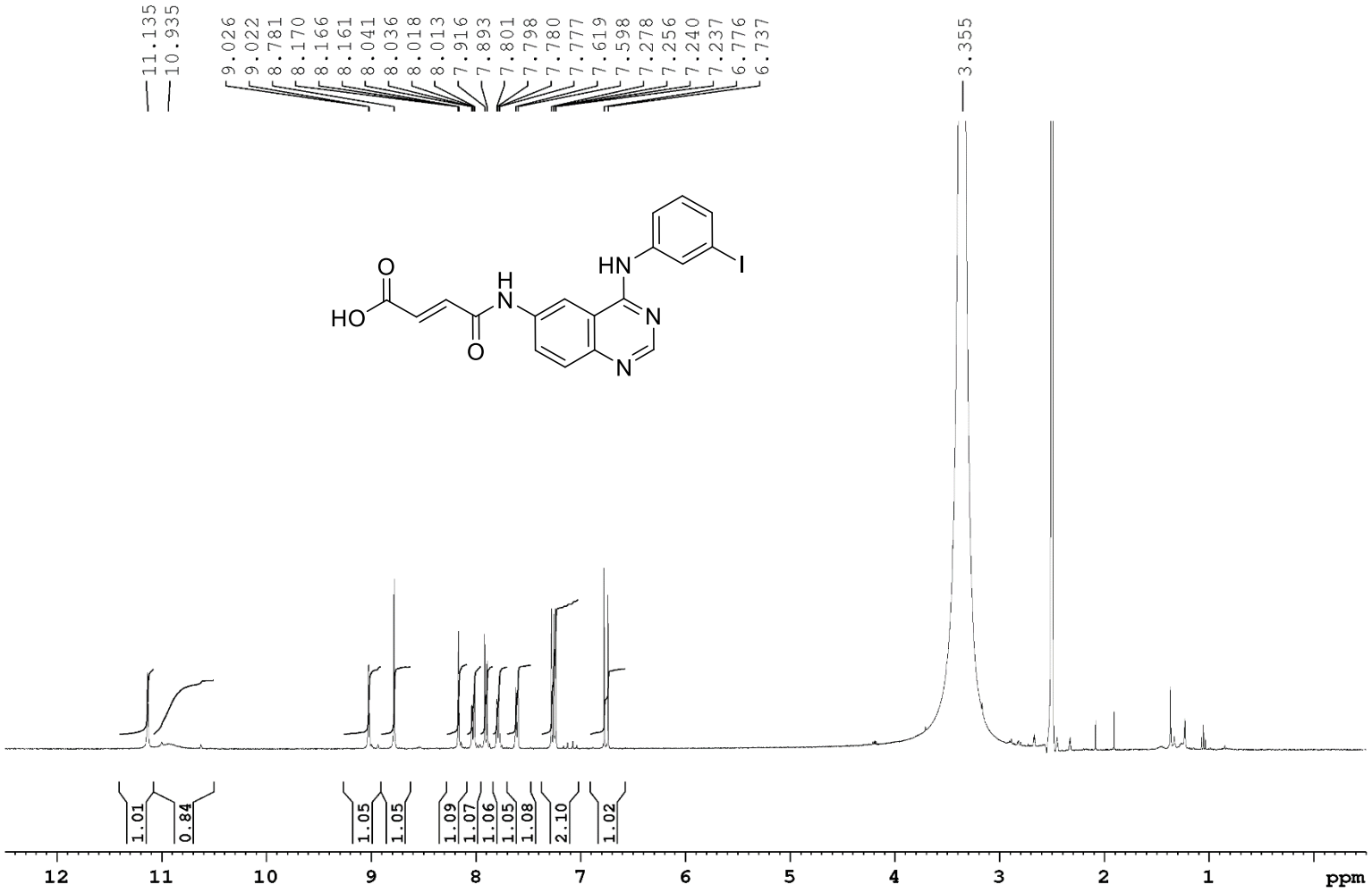

^{1}H NMR of Compound **54** in DMF-d_7 at 400 MHz

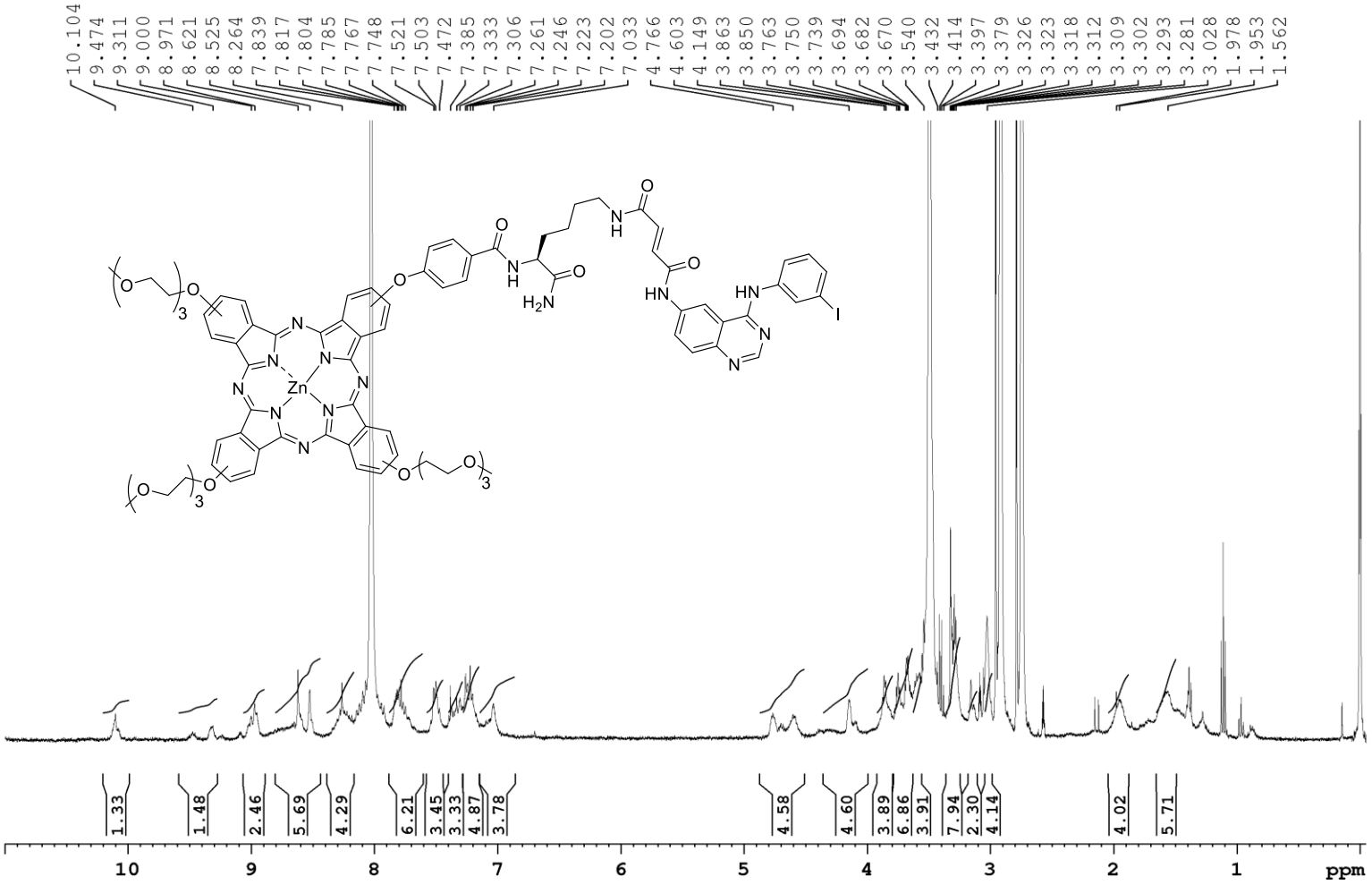

^{1}H NMR of Compound **61** in DMSO-d_6 at 400 MHz

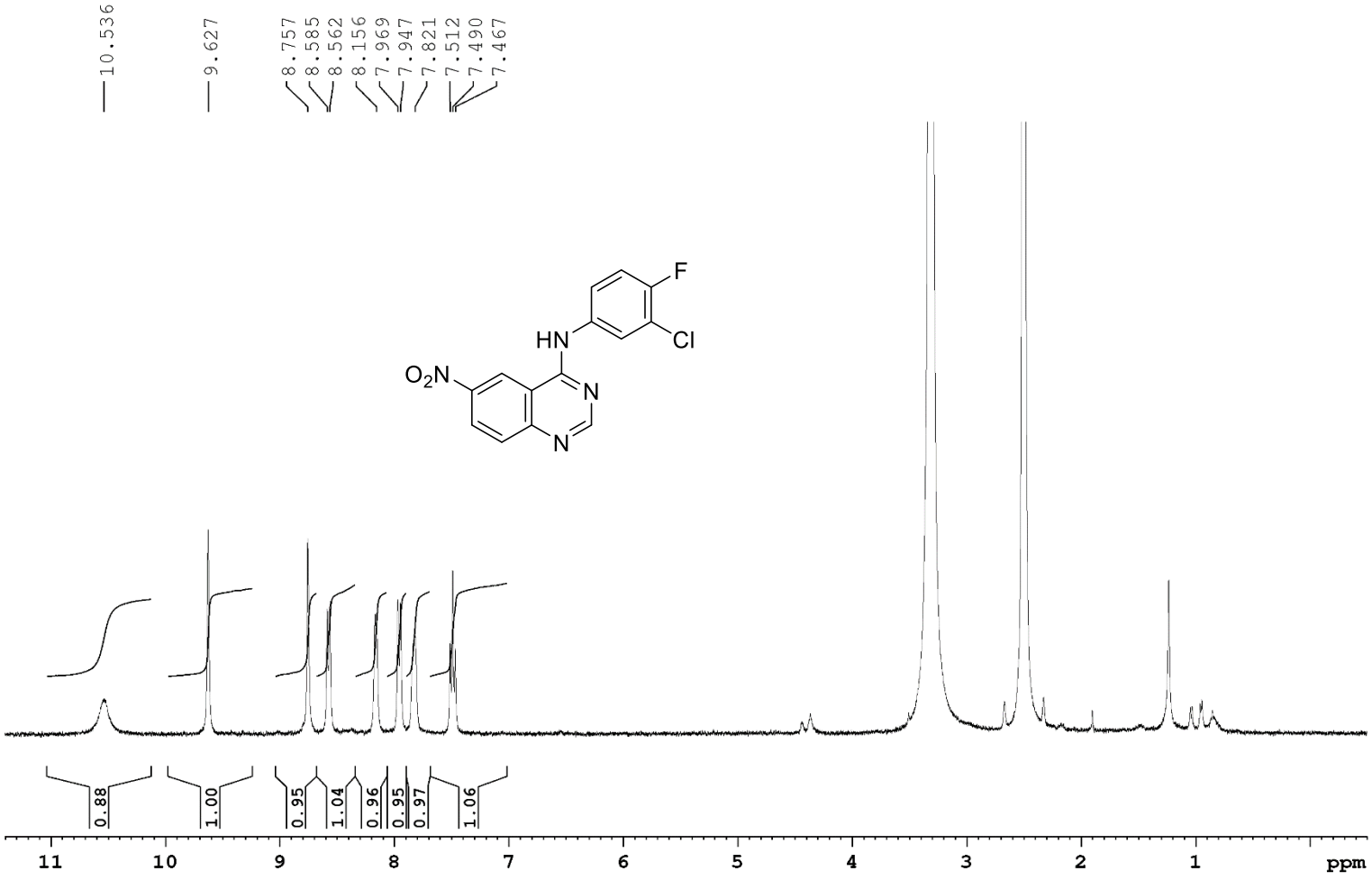

^{1}H NMR of Compound **62** in DMSO-d_6 at 400 MHz

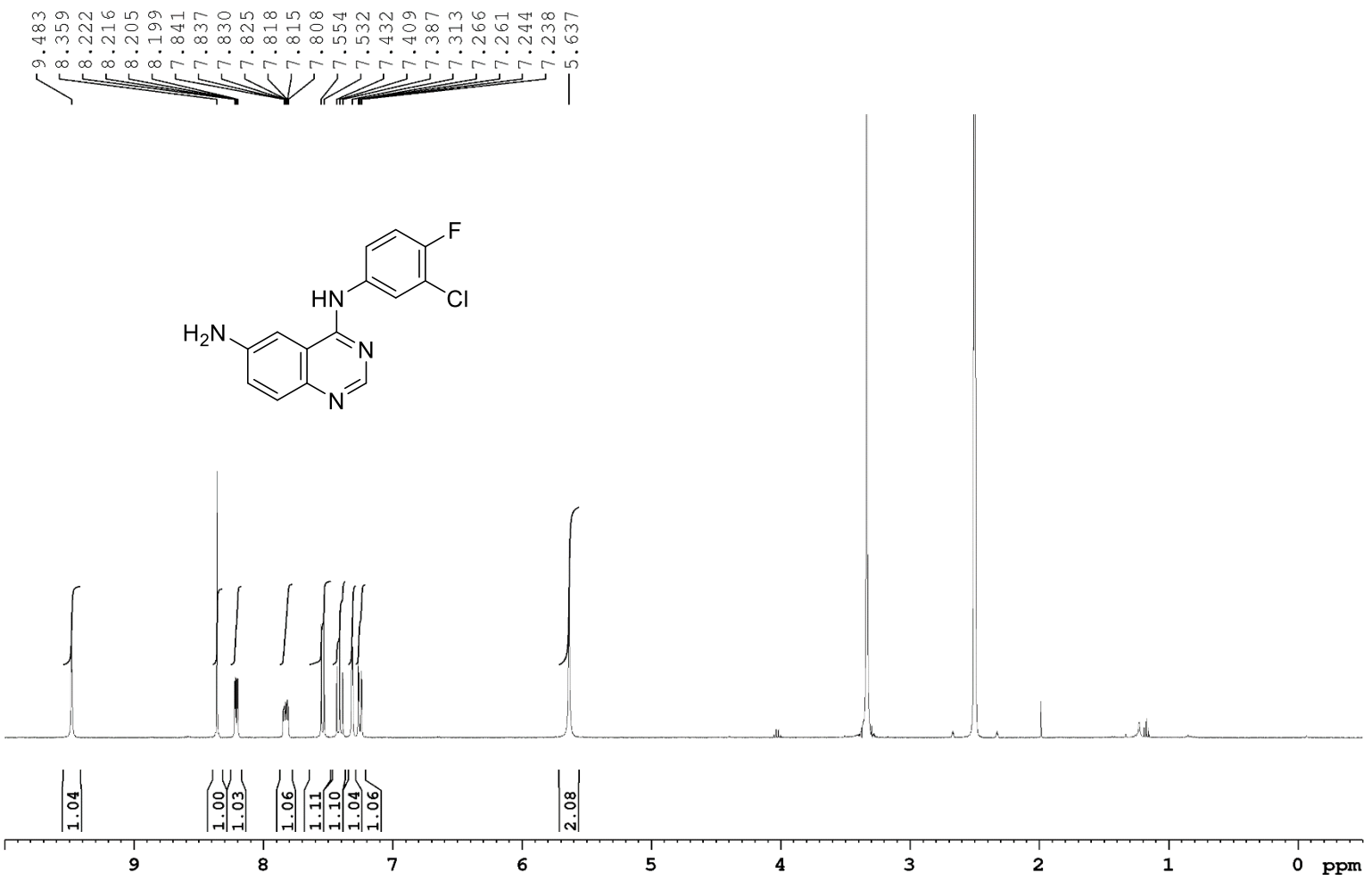

^{1}H NMR of Compound **63** in Acetone-d_6 at 400 MHz

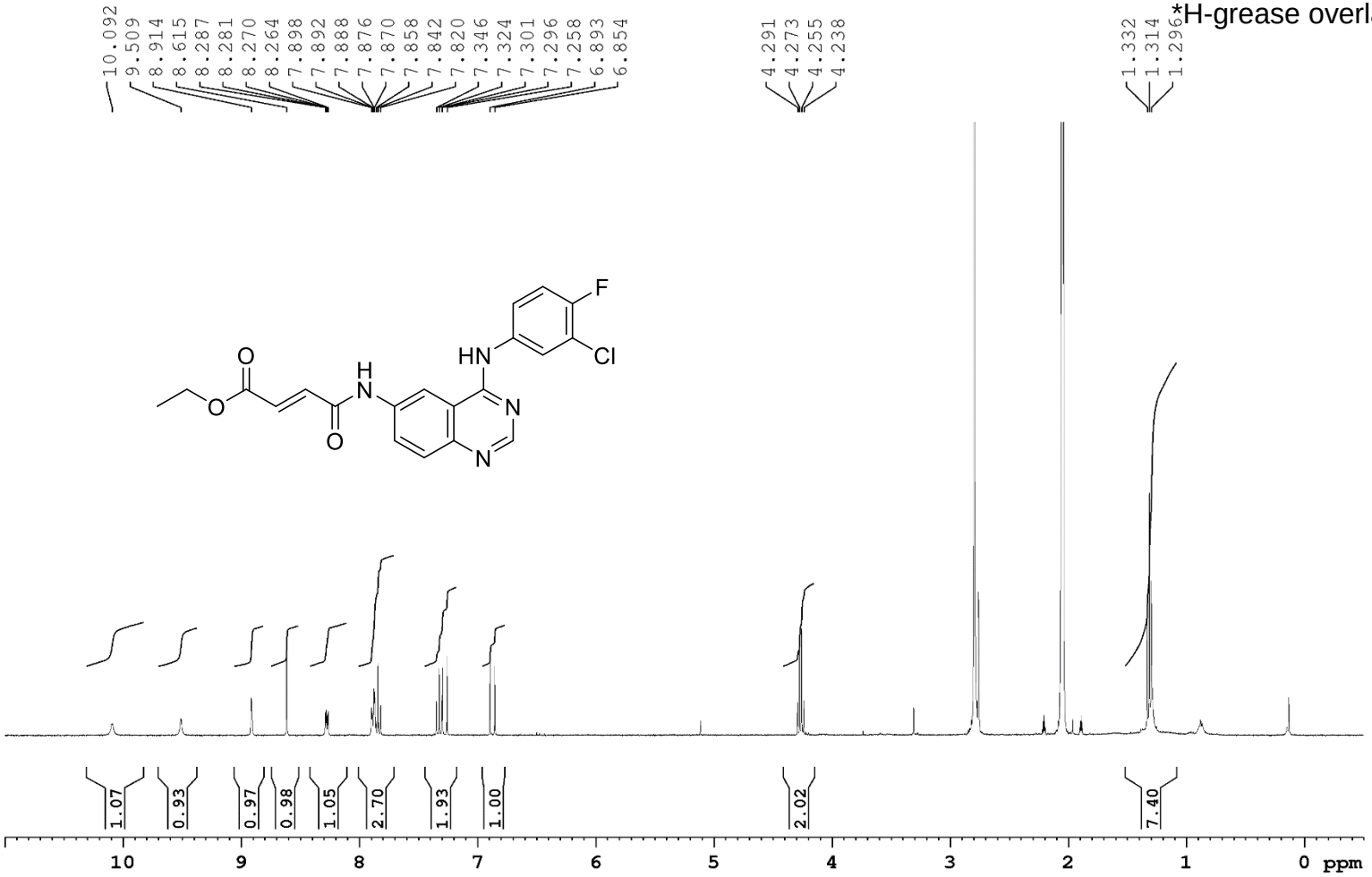

^{1}H NMR of Compound **64** in DMSO-d_6 at 400 MHz

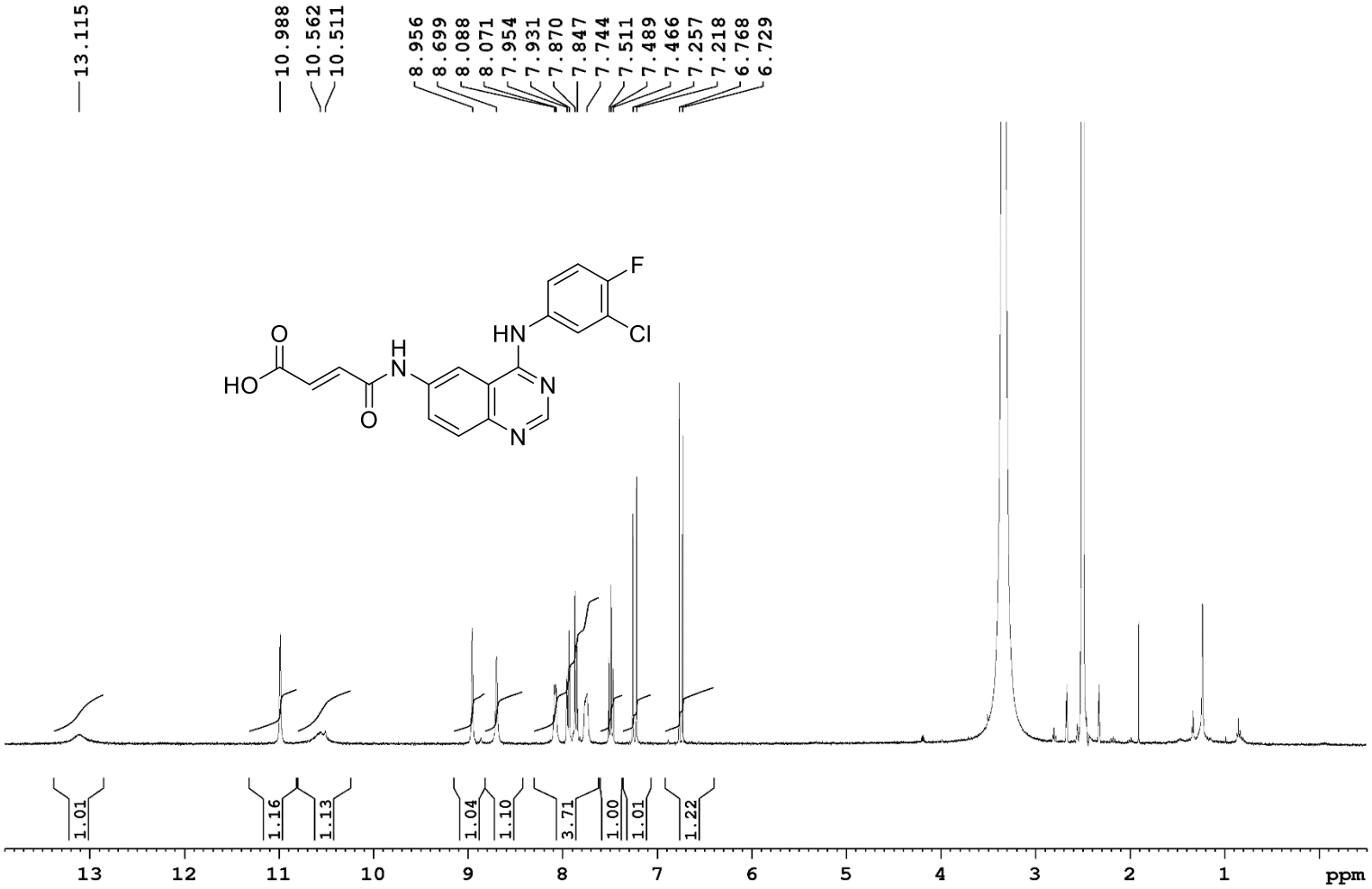

^{1}H NMR of Compound **60** in DMSO-d_6 at 400 MHz

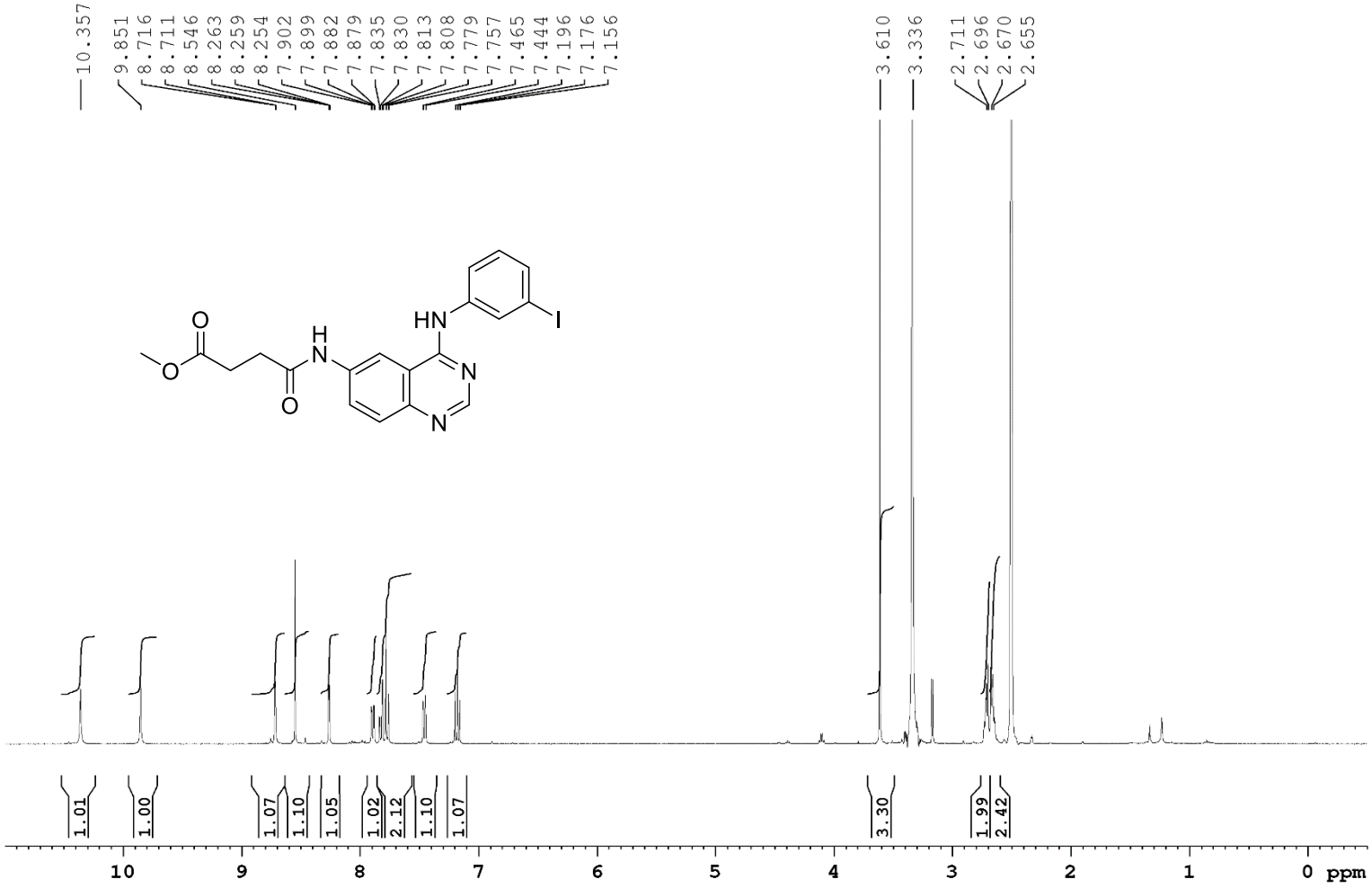

^{1}H NMR of Compound **59** in DMSO-d_6 at 400 MHz

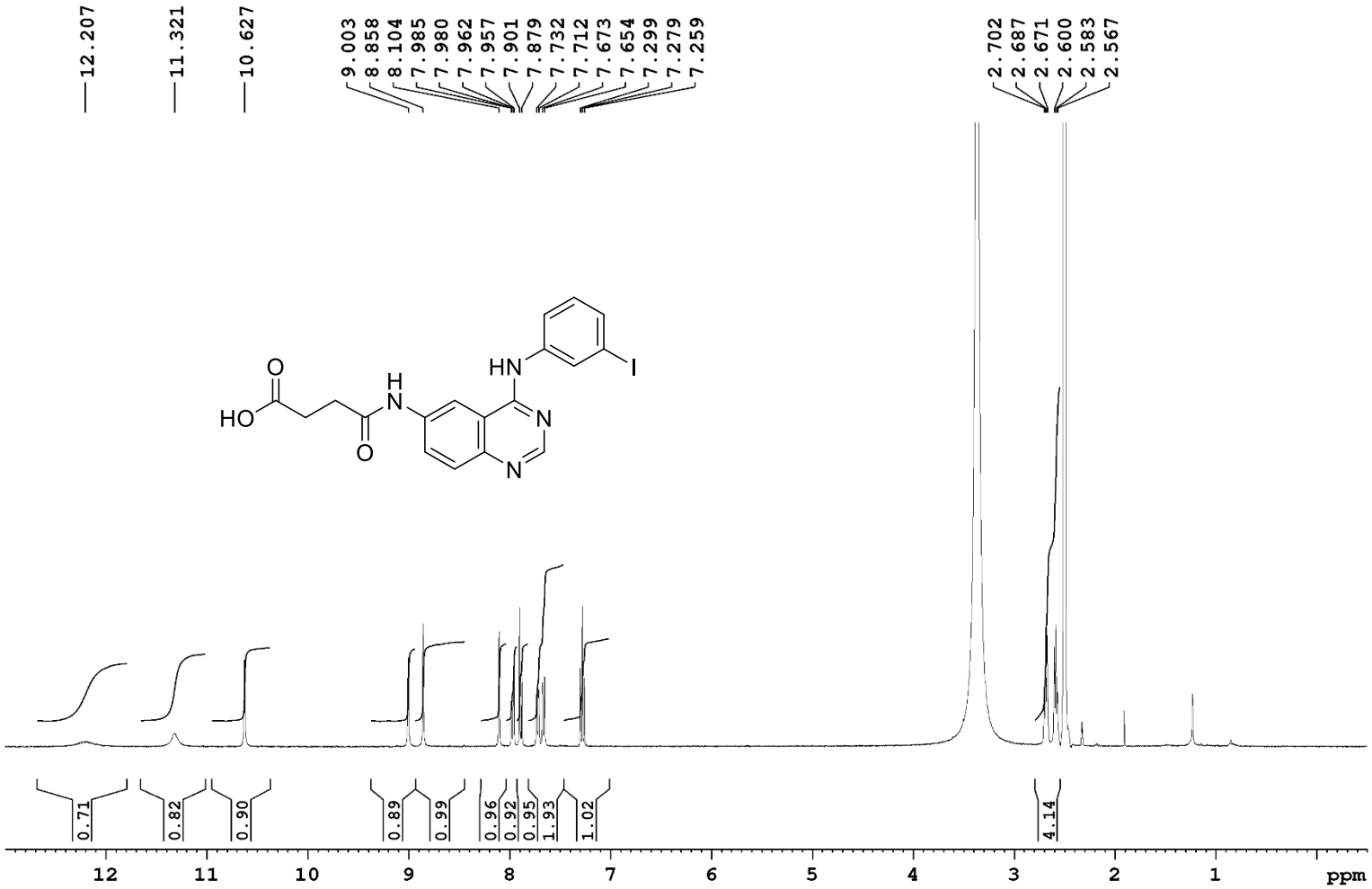

5.5. Notes

1. Wang, A.; Li, Y.; Zhou, L.; Yuan, L.; Lu, S.; Lin, Y.; Zhou, J.; Wei, S., Charge dependent photodynamic activity of alanine based zinc phthalocyanines. *Journal of Photochemistry and Photobiology B: Biology* **2014,** *141*, 10-19.

2. Erdem, S. S.; Nesterova, I. V.; Soper, S. A.; Hammer, R. P., Mono-amine Functionalized Phthalocyanines: Microwave-Assisted Solid-Phase Synthesis and Bioconjugation Strategies. *Journal of Organic Chemistry* **2009,** *74* (24), 9280-9286.

3. Chan, W. C.; White, P. D., *Fmoc Solid Phase Peptide Synthesis A Practical Approach*. Oxford University Press: New York, 2000.

4. Hou, X.; Zhang, J.; Zhao, X.; Chang, L.; Hu, P.; Liu, H., Design, Synthesis and Bioactivities Evaluation of Novel Quinazoline Analogs Containing Oxazole Units. *Chinese Journal of Chemistry* **2014,** *32* (6), 538-544.

5. Fernandes, C.; Oliveira, C.; Gano, L.; Bourkoula, A.; Pirmettis, I.; Santos, I., Radioiodination of new EGFR inhibitors as potential SPECT agents for molecular imaging of breast cancer. *Bioorganic & Medicinal Chemistry* **2007,** *15* (12), 3974-3980.

6. Shaul, M.; Abourbeh, G.; Jacobson, O.; Rozen, Y.; Laky, D.; Levitzki, A.; Mishani, E., Novel iodine-124 labeled EGFR inhibitors as potential PET agents for molecular imaging in cancer. *Bioorganic & Medicinal Chemistry* **2004,** *12* (13), 3421-3429.

7. Van Dort, M. E.; Robins, D. M.; Wayburn, B., Design, synthesis, and pharmacological characterization of a 4-[4,4-Dimethyl-3-(4-hydroxybutl)-5-oxo-2-thioxo-1-imidazolidinyl]-2-iodobenzonitrile as a high-affinity nonsteroidal androgen receptor ligand. *Journal of Medicinal Chemistry* **2000,** *43* (17), 3344 - 3347.

8. Albuschat, R.; Löwe, W.; Weber, M.; Luger, P.; Jendrossek, V., 4-Anilinoquinazolines with Lavendustin A subunit as inhibitors of epidermal growth factor receptor tyrosine kinase: syntheses, chemical and pharmacological properties. *European Journal of Medicinal Chemistry* **2004,** *39* (12), 1001-1011.

List of References

1. Adams, K. E.; Ke, S.; Kwon, S.; Liang, F.; Fan, Z.; Lu, Y.; Hirshi, K.; Mawad, M. E.; Barry, M. A.; Sevick-Muraca, E. M., Comparison of visible and near-infrared wavelength-excitable fluorescent dyes for molecular imaging of cancer. *Journal of Biomedical Optics* **2007,** *12* (2), 1-9, 9.

2. Adams, V. R.; Harvey, R. D., Histological and genetic markers for non-small-cell lung cancer: Customizing treatment based on individual tumor biology. *American Journal of Health-System Pharmacy* **2010,** *67* (1_Supplement_1), S3-S9.

3. Albuschat, R.; Löwe, W.; Weber, M.; Luger, P.; Jendrossek, V., 4-Anilinoquinazolines with Lavendustin A subunit as inhibitors of epidermal growth factor receptor tyrosine kinase: syntheses, chemical and pharmacological properties. *European Journal of Medicinal Chemistry* **2004,** *39* (12), 1001-1011.

4. Aldrich, S., Protein Tyrosine Kinase Assay Kit, Non-Radioactive Cataloge Number PTK101. In *Sigma Aldrich*, 1996; pp 1-8.

5. Allen, C. M.; Langlois, R.; Sharman, W. M.; La Madeleine, C.; van Lier, J. E., Photodynamic Properties of Amphiphilic Derivatives of Aluminum Tetrasulfophthalocyanine. *Photochemistry and Photobiology* **2002,** *76* (2), 208-216.

6. Ashokkumar, R.; Kathiravan, A.; Ramamurthy, P., Aggregation behaviour and electron injection/recombination dynamics of symmetrical and unsymmetrical Zn-phthalocyanines on TiO2 film. *Physical Chemistry Chemical Physics* **2014,** *16* (3), 1015-1021.

7. Bai, M.; Lo, P.-C.; Ye, J.; Wu, C.; Fong, W.-P.; Ng, D. K. P., Facile synthesis of pegylated zinc(II) phthalocyanines via transesterification and their in vitro photodynamic activities. *Organic & Biomolecular Chemistry* **2011,** *9* (20), 7028-7032.

8. Barrett, P. A.; Linstead, R. P.; Tuey, G. A. P.; Robertson, J. M., 371. Phthalocyanines and related compounds. Part XV. Tetrabenztriazaporphin : its preparation from phthalonitrile and a proof of its structure. With a note on a preliminary X-ray investigation. *Journal of the Chemical Society (Resumed)* **1939,** (0), 1809-1820.

9. Bezerin, B. D., *Coordination Compounds of Porphyrins and Phthalocyanines*. 1 ed.; Wiley, J. & Sons: New York, NY, 1981; p 300.

10. Blair, J. A.; Rauh, D.; Kung, C.; Yun, C.-H.; Fan, Q.-W.; Rode, H.; Zhang, C.; Eck, M. J.; Weiss, W. A.; Shokat, K. M., Structure-guided development of affinity probes for tyrosine kinases using chemical genetics. *Nature Chemical Biology* **2007,** *3*, 229-238.

11. Braun, A. a. T., J., Über die Produkte der Einwirkung von Acetanhydrid auf

Phthalamid. *Berichte der Deutschen Chemischen Gesellschaft* **1907,** *40*, 2709 - 2714.

12. Braun, S.; Raymond, W. E.; Racker, E., Synthetic tyrosine polymers as substrates and inhibitors of tyrosine-specific protein kinases. *Journal of Biological Chemistry* **1984,** *259* (4), 2051-4.

13. Brimioulle, R.; Bach, T., Enantioselective Lewis Acid Catalysis of Intramolecular Enone [2+2] Photocycloaddition Reactions. *Science* **2013,** *342* (6160), 840-843.

14. Byrne, G. T.; Linstead, R. P.; Lowe, A. R., 213. Phthalocyanines. Part II. The preparation of phthalocyanine and some metallic derivatives from o-cyanobenzamide and phthalimide. *Journal of the Chemical Society (Resumed)* **1934,** (0), 1017-1022.

15. Cao, L.; Jiang, R.; Zhu, Y.; Wang, X.; Li, Y.; Li, Y., Synthesis of 1,2,3-Triazole-4-carboxamide-Containing Foldamers for Sulfate Recognition. *European Journal of Organic Chemistry* **2014,** *2014* (13), 2687-2693.

16. Carey, F. A.; Sundberg, R. A., *Advanced Organic Chemistry Part B: Reaactions and Synthesis*. Springer Science+Business Media, LLC: 2007; Vol. 5th, p 1321.

17. Carlson, J. C. T.; Meimetis, L. G.; Hilderbrand, S. A.; Weissleder, R., BODIPY–Tetrazine Derivatives as Superbright Bioorthogonal Turn-on Probes. *Angewandte Chemie International Edition* **2013,** *52* (27), 6917-6920.

18. Castelli, R.; Nicole, B.; Cavazzoni, A.; Bonelli, M.; Vacondio, F.; Ferlenghi, F.; Callegari, D.; Silva, C.; Rivara, S.; Lodola, A.; Digiacomo, G.; Fumarola, C.; Alfieri, R.; Petronini, P. G.; Mor, M., Balancing reactivity and antitumor activity: heteroarylthioacetamide derivateds as poten and time-dependent inhibitors of EGFR. *European Journal of Medicinal Chemistry* **2019,** *162*, 507-524.

19. Chan, W. C.; White, P. D., *Fmoc Solid Phase Peptide Synthesis A Practical Approach*. Oxford University Press: New York, 2000.

20. Cheng, K.; Chen, H.; Jenkins, C. H.; Zhang, G.; Zhao, W.; Zhang, Z.; Han, F.; Fung, J.; Yang, M.; Jiang, Y.; Xing, L.; Cheng, Z., Synthesis, Characterization, and Biomedical Applications of a Targeted Dual-Modal Near-Infrared-II Fluorescence and Photoacoustic Imaging Nanoprobe. *ACS Nano* **2017,** *11* (12), 12276-12291.

21. Cheong, W. F.; Prahl, S. A.; Welch, A. J., A review of the optical properties of biological tissues. *IEEE Journal of Quantum Electronics* **1990,** *26* (12), 2166-2185.

22. Christie, R. M.; Deans, D. D., An investigation into the mechanism of the phthalonitrile route to copper phthalocyanines using differential scanning calorimetry. *Journal of the Chemical Society, Perkin Transactions 2* **1989,** (2), 193-198.

23. de Diesbach, H.; von der Weid, E., Quelques sels complexes des o-dinitriles avec le cuivre et la pyridine. *Helvetica Chimica Acta* **1927,** *10* (1), 886-888.

24. de Figueiredo, R. M.; Suppo, J.-S.; Campagne, J.-M., Nonclassical Routes for Amide Bond Formation. *Chemical Reviews* **2016,** *116* (19), 12029-12122.

25. Duan, W.; Smith, K.; Savoie, H.; Greenman, J.; Boyle, R. W., Near IR emitting isothiocyanato-substituted fluorophores: their synthesis and bioconjugation to monoclonal antibodies. *Organic & Biomolecular Chemistry* **2005,** *3* (13), 2384-2386.

26. Dumoulin, F.; Durmuş, M.; Ahsen, V.; Nyokong, T., Synthetic pathways to water-soluble phthalocyanines and close analogs. *Coordination Chemistry Reviews* **2010,** *254* (23), 2792-2847.

27. Dunlap, F. L., The Production of Acylamines by the Interaction of Sodium Salts of Monobasic Acids and Amine Hydrochlorides. *Journal of the American Chemical Society* **1902,** *24* (8), 758-763.

28. Ekblad, T.; Lindgren, A. E. G.; Andersson, C. D.; Caraballo, R.; Thorsell, A.-G.; Karlberg, T.; Spjut, S.; Linusson, A.; Schüler, H.; Elofsson, M., Towards small molecule inhibitors of mono-ADP-ribosyltransferases. *European Journal of Medicinal Chemistry* **2015,** *95*, 546-551.

29. Elderfield, R. C.; Williamson, T. A.; Gensler, W. J.; Kremer, C. B., Synthesis of Bz-Substituted Quinazoline and Antimalarials from them. A Contribution to the Chemistry of Quinazoline. *The Journal of Organic Chemistry* **1947,** *12* (3), 405-421.

30. Erdem, S. S.; Nesterova, I. V.; Soper, S. A.; Hammer, R. P., Solid-Phase Synthesis of Asymmetrically Substituted “AB3-Type” Phthalocyanines. *Journal of Organic Chemistry* **2008,** *73* (13), 5003-5007.

31. Erdem, S. S.; Nesterova, I. V.; Soper, S. A.; Hammer, R. P., Mono-amine Functionalized Phthalocyanines: Microwave-Assisted Solid-Phase Synthesis and Bioconjugation Strategies. *Journal of Organic Chemistry* **2009,** *74* (24), 9280-9286.

32. Fernandes, C.; Oliveira, C.; Gano, L.; Bourkoula, A.; Pirmettis, I.; Santos, I., Radioiodination of new EGFR inhibitors as potential SPECT agents for molecular imaging of breast cancer. *Bioorganic & Medicinal Chemistry* **2007,** *15* (12), 3974-3980.

33. Frangioni, J. V., In vivo near-infrared fluorescence imaging. *Current Opinion in Chemical Biology* **2003,** *7* (5), 626-634.

34. Franz, A.; Burgstaller, W.; Müller, B.; Schinner, F., Influence of medium components and metabolic inhibitors on citric acid production by Penicillium simplicissimum. *Microbiology* **1993,** *139* (9), 2101-2107.

35. Fry, D. W.; Kraker, A. J.; McMichael, A.; Ambroso, L. A.; Nelson, J. M.; R., L. W.; Conners, R. W.; Bridges, A. J., A Specific Inhibitor of the Epidermal Growth Factor Receptor Tyrosine Kinase. *Science* **1994,** *265* (5175), 1093-1095.

36. Fukuda, T.; Kobayashi, N., UV-Visible Absorption Spectroscopic Properties of

Phthalocyanines and Related Macrocycles. In *Handbook of Porphyrin Science*, Kadish, K. M.; Smith, K. M.; Guilard, R., Eds. World Scientific: Singapore, 2010; Vol. 9, pp 1-644.

37. Furst, A.; Berlo, R. C.; Hooton, S., Hydrazine as a Reducing Agent for Organic Compounds (Catalytic Hydrazine Reductions). *Chemical Reviews* **1965,** *65* (1), 51-68.

38. Gao, M.; Su, H.; Lin, G.; Li, S.; Yu, X.; Qin, A.; Zhao, Z.; Zhang, Z.; Tang, B. Z., Targeted imaging of EGFR overexpressed cancer cells by brightly fluorescent nanoparticles conjugated with cetuximab. *Nanoscale* **2016,** *8* (32), 15027-15032.

39. Gioux, S.; Choi, H. S.; Frangioni, J. V., Image-guided surgery using invisible near-infrared light: fundamentals of clinical translation. *Mol Imaging* **2010,** *9* (5), 237-255.

40. Göksel, M.; Durmuş, M.; Atilla, D., A comparative study on photophysical and photochemical properties of zinc phthalocyanines with different molecular symmetries. *Journal of Porphyrins and Phthalocyanines* **2012,** *16*, 895-906.

41. Göksel, M.; Durmuş, M.; Atilla, D., Amino-functionalized water-soluble zinc phthalocyanines: Synthesis, photophysical, photochemical and protein binding properties. *Journal of Photochemistry and Photobiology A: Chemistry* **2013,** *266*, 37-46.

42. Good, N. E.; Winget, G. D.; Winter, W.; Connolly, T. N.; Izawa, S.; Singh, R. M. M., Hydrogen Ion Buffers for Biological Research. *Biochemistry* **1966,** *5* (2), 467-477.

43. Götz, M. G.; James, K. E.; Hansell, E.; Dvořák, J.; Seshaadri, A.; Sojka, D.; Kopáček, P.; McKerrow, J. H.; Caffrey, C. R.; Powers, J. C., Aza-peptidyl Michael Acceptors. A New Class of Potent and Selective Inhibitors of Asparaginyl Endopeptidases (Legumains) from Evolutionarily Diverse Pathogens. *Journal of Medicinal Chemistry* **2008,** *51* (9), 2816-2832.

44. Güzel, E.; Günsel, A.; Bilgiçli, A. T.; Atmaca, G. Y.; Erdoğmuş, A.; Yarasir, M. N., Synthesis and photophysicochemical properties of novel thiadiazole-substituted zinc (II), gallium (III) and silicon (IV) phthalocyanines for photodynamic therapy. *Inorganica Chimica Acta* **2017,** *467*, 169-176.

45. Hammer, R. P.; Owens, C. V.; Hwang, S.-H.; Sayes, C. M.; Soper, S. A., Asymmetrical, Water-Soluble Phthalocyanine Dyes for Covalent Labeling of Oligonucleotides. *Bioconjugate Chemistry* **2002,** *13* (6), 1244-1252.

46. Han, W.; Du, Y., Recent Development of the Second and Third Generation Irreversible Epidermal Growth Factor Receptor Inhibitors. *Chemistry & Biodiversity* **2017,** *14* (7), e1600372.

47. Hanack, M.; Schmid, G.; Sommerauer, M., Chromatographic Separation of the Four Possible Structural Isomers of a Tetrasubstituted Phthalocyanine: Tetrakis(2-ethylhexyloxy)phthalocyaninatonickel(II). *Angewandte Chemie International Edition in*

English **1993,** *32* (10), 1422-1424.

48. Hari, Sanjay B.; Merritt, Ethan A.; Maly, Dustin J., Sequence Determinants of a Specific Inactive Protein Kinase Conformation. *Chemistry & Biology* **2013,** *20* (6), 806-815.

49. Haruhiko, T.; Shojiro, S.; Shinsaku, S., Synthesis of Metallophthalocyanines From Phthalonitrile With Strong Organic Bases. *Chemistry Letters* **1983,** *12* (3), 313-316.

50. Haruhiko, T.; Shojiro, S.; Shojiro, O.; Shinsaku, S., Synthesis of Phthalocyanines From Phthalonitrile With Organic Strong Bases. *Chemistry Letters* **1980,** *9* (10), 1277-1280.

51. Heath, C. H.; Deep, N. L.; Sweeny, L.; Zinn, K. R.; Rosenthal, E. L., Use of Panitumumab-IRDye800 to Image Microscopic Head and Neck Cancer in an Orthotopic Surgical Model. *Annals of Surgical Oncology* **2012,** *19* (12), 3879-3887.

52. Heravi, M. M.; Ghavidel, M.; Mohammadkhani, L., Beyond a solvent: triple roles of dimethylformamide in organic chemistry. *RSC Advances* **2018,** *8* (49), 27832-27862.

53. Higuchi, T.; Miki, T., Reversible Formation of Amides From Free Carboxylic Acid And Amine in Aqueous Solution. A Case of Neighboring Group Facilitation. *Journal of the American Chemical Society* **1961,** *83* (18), 3899-3901.

54. Hou, X.; Zhang, J.; Zhao, X.; Chang, L.; Hu, P.; Liu, H., Design, Synthesis and Bioactivities Evaluation of Novel Quinazoline Analogs Containing Oxazole Units. *Chinese Journal of Chemistry* **2014,** *32* (6), 538-544.

55. Hu, M.; Brasseur, N.; Yildiz, S. Z.; van Lier, J. E.; Leznoff, C. C., Hydroxyphthalocyanines as Potential Photodynamic Agents for Cancer Therapy. *Journal of Medicinal Chemistry* **1998,** *41* (11), 1789-1802.

56. Institute, T. N. A. a. t. K., The Nobel Prize in Physiology or Medicine 1986. MediaAB, N., Ed. Switzerland, 1986.

57. Jad, Y. E.; Acosta, G. A.; Khattab, S. N.; de la Torre, B. G.; Govender, T.; Kruger, H. G.; El-Faham, A.; Albericio, F., Peptide synthesis beyond DMF: THF and ACN as excellent and friendlier alternatives. *Organic & Biomolecular Chemistry* **2015,** *13* (8), 2393-2398.

58. Jha, A.; Dimmock, J. R., Syntheses of 4-(3,5-Bisphenylmethylene-4-oxo-piperidin-1-yl)-4-oxo-but-2 Z -enoic Acid Arylamides as Candidate Cytotoxic Agents. *Synthetic Communications* **2003,** *33* (7), 1211-1223.

59. Jha, A.; Mukherjee, C.; Prasad, A. K.; Parmar, V. S.; Clercq, E. D.; Balzarini, J.; Stables, J. P.; Manavathu, E. K.; Shrivastav, A.; Sharma, R. K.; Nienaber, K. H.; Zello, G. A.; Dimmock, J. R., E,E,E-1-(4-Arylamino-4-oxo-2-butenoyl)-3,5-bis(arylidene)-

4-piperidones: A topographical study of some novel potent cytotoxins. *Bioorganic & Medicinal Chemistry* **2007,** *15* (17), 5854-5865.

60. Jia, Y.; Yun, C.-H.; Park, E.; Ercan, D.; Manuia, M.; Juarez, J.; Xu, C.; Rhee, K.; Chen, T.; Zhang, H.; Palakurthi, S.; Jang, J.; Lelais, G.; DiDonato, M.; Bursulaya, B.; Michellys, P.-Y.; Epple, R.; Marsilje, T. H.; McNeill, M.; Lu, W.; Harris, J.; Bender, S.; Wong, K.-K.; Jänne, P. A.; Eck, M. J., Overcoming EGFR(T790M) and EGFR(C797S) resistance with mutant-selective allosteric inhibitors. *Nature* **2016,** *534*, 129 - 143.

61. Jones, R. A.; Rustidge, D. C.; Sarin, R., Pyrrole Studies. Part. 44.1 Synthesis of Potentially Biologically Active Pyrroloylanilines. *Synthetic Communications* **1993,** *23* (6), 771-777.

62. Kazuhiro, M.; Kazutoshi, T.; Yoshinori, Y., Highly efficient valence isomerization between norbornadiene and quadricyclane derivatives under sunlight. *Chemistry Letters* **1981,** *10* (7), 839-842.

63. Kobayashi, S.; Boggon, T. J.; Dayaram, T.; Jänne, P. A.; Kocher, O.; Meyerson, M.; Johnson, B. E.; Eck, M. J.; Tenen, D. G.; Halmos, B., EGFR Mutation and Resistance of Non–Small-Cell Lung Cancer to Gefitinib. *New England Journal of Medicine* **2005,** *352* (8), 786-792.

64. Koland, J. G.; Cerione, R. A., Activation of the EGF receptor tyrosine kinase by divalent metal ions: Comparison of holoreceptor and isolated kinase domain properties. *Biochimica et Biophysica Acta (BBA) - Molecular Cell Research* **1990,** *1052* (3), 489-498.

65. Lanning, B. R.; Whitby, L. R.; Dix, M. M.; Douhan, J.; Gilbert, A. M.; Hett, E. C.; Johnson, T. O.; Joslyn, C.; Kath, J. C.; Niessen, S.; Roberts, L. R.; Schnute, M. E.; Wang, C.; Hulce, J. J.; Wei, B.; Whiteley, L. O.; Hayward, M. M.; Cravatt, B. F., A road map to evaluate the proteome-wide selectivity of covalent kinase inhibitors. *Nature Chemical Biology* **2014,** *10*, 760.

66. Lebedeva, N. S., Aggregation properties of water-soluble metal p hthalocyanines: effect of ionic strength of solution. *Russian Chemical Bulletin* **2004,** *53* (12), 2674-2683.

67. Levitzki, A.; Gazit, A., Tyrosine kinase inhibition: an approach to drug development. *Science* **1995,** *267* (5205), 1782-1788.

68. Leznoff, C. C.; Hall, T. W., The synthesis of a soluble, unsymmetrical phthalocyanine on a polymer support. *Tetrahedron Letters* **1982,** *23* (30), 3023-3026.

69. Leznoff, C. C.; Hu, M.; McArthur, C. R.; Qin, Y.; van Lier, J. E., The syntheses of 2,9,16,23- and 1,8,15,22-tetrahydroxyphthalocyanines. *Canadian Journal of Chemistry* **1994,** *72* (9), 1990-1998.

70. Li, L.; Zhang, C.-W.; Ge, J.; Qian, L.; Chai, B.-H.; Zhu, Q.; Lee, J.-S.; Lim,

K.-L.; Yao, S. Q., A Small-Molecule Probe for Selective Profiling and Imaging of Monoamine Oxidase B Activities in Models of Parkinson's Disease. *Angewandte Chemie International Edition* **2015,** *54* (37), 10821-10825.

71. Liu, J.-Y.; Jiang, X.-J.; Fong, W.-P.; Ng, D. K. P., Highly photocytotoxic 1,4-dipegylated zinc(II) phthalocyanines. Effects of the chain length on the in vitro photodynamic activities. *Organic & Biomolecular Chemistry* **2008,** *6* (24), 4560-4566.

72. Liu, W.; Jensen, T. J.; Fronczek, F. R.; Hammer, R. P.; Smith, K. M.; Vicente, M. G. H., Synthesis and Cellular Studies of Nonaggregated Water-Soluble Phthalocyanines. *Journal of Medicinal Chemistry* **2005,** *48* (4), 1033-1041.

73. Ma, Y.-L.; Zhou, R.-J.; Zeng, X.-Y.; An, Y.-X.; Qiu, S.-S.; Nie, L.-J., Synthesis, DFT and antimicrobial activity assays in vitro for novel cis/trans-but-2-enedioic acid esters. *Journal of Molecular Structure* **2014,** *1063*, 226-234.

74. Mali, S. M.; Ganesh Kumar, M.; Katariya, M. M.; Gopi, H. N., HBTU mediated 1-hydroxybenzotriazole (HOBt) conjugate addition: synthesis and stereochemical analysis of β-benzotriazole N-oxide substituted γ-amino acids and hybrid peptides. *Organic & Biomolecular Chemistry* **2014,** *12* (42), 8462-8472.

75. Manna, D.; Ghosh, R., Effect of radiofrequency radiation in cultured mammalian cells: A review. *Electromagnetic Biology and Medicine* **2016,** *35* (3), 265-301.

76. Marvania, B.; Lee, P.-C.; Chaniyara, R.; Dong, H.; Suman, S.; Kakadiya, R.; Chou, T.-C.; Lee, T.-C.; Shah, A.; Su, T.-L., Design, synthesis and antitumor evaluation of phenyl N-mustard-quinazoline conjugates. *Bioorganic & Medicinal Chemistry* **2011,** *19* (6), 1987-1998.

77. McInnes, C.; Sykes, B. D., Growth factor receptors: Structure, mechanism, and drug discovery. *Peptide Science* **1997,** *43* (5), 339-366.

78. McKeown, N. B., 98 - The Synthesis of Symmetrical Phthalocyanines. In *The Porphyrin Handbook*, Kadish, K. M.; Smith, K. M.; Guilard, R., Eds. Academic Press: Amsterdam, 2003; pp 61-124.

79. Meimetis, L. G.; Carlson, J. C. T.; Giedt, R. J.; Kohler, R. H.; Weissleder, R., Ultrafluorogenic Coumarin–Tetrazine Probes for Real-Time Biological Imaging. *Angewandte Chemie International Edition* **2014,** *53* (29), 7531-7534.

80. Mendelsohn, J., Targeting the epidermal growth factor receptor for cancer therapy. *Journal of Clinical Oncology* **2000,** *20*, 1S-13S.

81. Mendelsohn, J.; Baselga, J., The EGF receptor family as targets for cancer therapy. *Oncogene* **2000,** *19* (56), 6550-6565.

82. Mendelsohn, J.; Baselga, J., Status of Epidermal Growth Factor Receptor Antagonists in the Biology and Treatment of Cancer. *Journal of Clinical Oncology* **2003,**

21 (14), 2787-2799.

83. Milik, S. N.; Lasheen, D. S.; Serya, R. A. T.; Abouzid, K., A. M., How to train your inhibitor: Design strategies to overcome resistance to Epidermal Growth Factor Receptor inhibitors. *European Journal of Medicinal Chemistry* **2017,** *142*, 131-151.

84. Miura, T.; Mikano, Y.; Murakami, M., Nickel-Catalyzed Synthesis of 1,3,5-Trisubstituted Hydantoins from Acrylates and Isocyanates. *Organic Letters* **2011,** *13* (14), 3560-3563.

85. Mohammadi, M.; Honegger, A.; Sorokin, A.; Ullrich, A.; Schlessinger, J.; Hurwitz, D. R., Aggregation-induced activation of the epidermal growth factor receptor protein tyrosine kinase. *Biochemistry* **1993,** *32* (34), 8742-8748.

86. Nesterova, I. V.; Bennett, C. A.; Erdem, S. S.; Hammer, R. P.; Deininger, P. L.; Soper, S. A., Near-IR single fluorophore quenching system based on phthalocyanine (Pc) aggregation and its application for monitoring inhibitor/activator action on a therapeutic target: L1-EN. *Analyst* **2011,** *136* (6), 1103-1105.

87. Nesterova, I. V.; Erdem, S. S.; Pakhomov, S.; Hammer, R. P.; Soper, S. A., Phthalocyanine Dimerization-Based Molecular Beacons Using Near-IR Fluorescence. *Journal of the American Chemical Society* **2009,** *131* (7), 2432-2433.

88. Nesterova, I. V.; Verdree, V. T.; Pakhomov, S.; Strickler, K. L.; Allen, M. W.; Hammer, R. P.; Soper, S. A., Metallo-Phthalocyanine Near-IR Fluorophores: Oligonucleotide Conjugates and Their Applications in PCR Assays. *Bioconjugate Chemistry* **2007,** *18* (6), 2159-2168.

89. Ojeda-Porras, A.; Gamba-Sánchez, D., Recent Developments in Amide Synthesis Using Nonactivated Starting Materials. *The Journal of Organic Chemistry* **2016,** *81* (23), 11548-11555.

90. Ongarora, B. G.; Hu, X.; Verbern-Sutton, S. D.; Garno, J. C.; Vicente, M. G. H., Synthesis and Photodynamic Activity of Pegylated Cationic Zn(II)-Phthalocyanines in HEp2 Cells. *Theranostics* **2012,** *2* (9), 850-870.

91. Ongarora, B. G.; Zhou, Z.; Okoth, E. A.; Kolesnichenko, I.; Smith, K. M.; Vicente, M. G. H., Synthesis, spectroscopic, and cellular properties of α-pegylated cis-A2B2- and A3B-types ZnPcs. *Journal of Porphyrins and Phthalocyanines* **2014,** *18* (10n11), 1021-1033.

92. Ortu, G.; Ben-David, I.; Rozen, Y.; Freedman, N. M. T.; Chisin, R.; Levitzki, A.; Mishani, E., Labeled EGFr-TK irreversible inhibitor (ML03): In vitro and in vivo properties, potential as PET biomarker for cancer and feasibility as anticancer drug. *International Journal of Cancer* **2002,** *101* (4), 360-370.

93. Paez, J. G.; Jänne, P. A.; Lee, J. C.; Tracy, S.; Greulich, H.; Gabriel, S.; Herman, P.; Kaye, F. J.; Lindeman, N.; Boggon, T. J.; Naoki, K.; Sasaki, H.; Fujii, Y.;

Eck, M. J.; Sellers, W. R.; Johnson, B. E.; Meyerson, M., EGFR Mutations in Lung Cancer: Correlation with Clinical Response to Gefitinib Therapy. *Science* **2004,** *304* (5676), 1497-1500.

94. Pal, A.; Glekas, A.; Doubrovin, M.; Balatoni, J.; Beresten, T.; Maxwell, D.; Soghomonyan, S.; Shavrin, A.; Ageyeva, L.; Finn, R.; Larson, S. M.; Bornmann, W.; Gelovani, J. G., Molecular Imaging of EGFR Kinase Activity in Tumors with 124I-Labeled Small Molecular Tracer and Positron Emission Tomography. *Molecular Imaging and Biology* **2006,** *8* (5), 262-277.

95. Pattabiraman, V. R.; Bode, J. W., Rethinking amide bond synthesis. *Nature* **2011,** *480*, 471.

96. Piruska, A.; Nikcevic, I.; Lee, S. H.; Ahn, C.; Heineman, W. R.; Limbach, P. A.; Seliskar, C. J., The autofluorescence of plastic materials and chips measured under laser irradiation. *Lab on a Chip* **2005,** *5* (12), 1348-1354.

97. Poeylaut-Palena, A. A.; Mata, E. G., Unravelling the olefin cross metathesis on solid support. Factors affecting the reaction outcome. *Organic & Biomolecular Chemistry* **2010,** *8* (17), 3947-3956.

98. Qian, L.; Pan, S.; Lee, J.-S.; Ge, J.; Li, L.; Yao, S. Q., Live-cell imaging and profiling of c-Jun N-terminal kinases using covalent inhibitor-derived probes. *Chemical Communications* **2019,** *55* (8), 1092-1095.

99. Quinn, S. D.; Srinivasan, S.; Gordon, J. B.; He, W.; Carraway, K. L.; Coleman, M. A.; Schlau-Cohen, G. S., Single-Molecule Fluorescence Detection of the Epidermal Growth Factor Receptor in Membrane Discs. *Biochemistry* **2019,** *58* (4), 286-294.

100. Rijksen, G.; Van Oirschot, B. A.; Staal, G. E. J., [6] Nonradioactive assays of protein-tyrosine kinase activity using anti-phosphotyrosine antibodies. In *Methods in Enzymology*, Academic Press: 1991; Vol. 200, pp 98-107.

101. Saka, E. T.; Durmuş, M.; Kantekin, H., Solvent and central metal effects on the photophysical and photochemical properties of 4-benzyloxybenzoxy substituted phthalocyanines. *Journal of Organometallic Chemistry* **2011,** *696* (4), 913-924.

102. Semelková, L.; Janošcová, P.; Fernandes, C.; Bouz, G.; Janďourek, O.; Konečná, K.; Paterová, P.; Navrátilová, L.; Kuneš, J.; Doležal, M.; Zitko, J., Design, Synthesis, Antimycobacterial Evaluation, and In Silico Studies of 3-(Phenylcarbamoyl)-pyrazine-2-carboxylic Acids. *Molecules* **2017,** *22* (9), 1491.

103. Shaul, M.; Abourbeh, G.; Jacobson, O.; Rozen, Y.; Laky, D.; Levitzki, A.; Mishani, E., Novel iodine-124 labeled EGFR inhibitors as potential PET agents for molecular imaging in cancer. *Bioorganic & Medicinal Chemistry* **2004,** *12* (13), 3421-3429.

104. Shepherd, F. A.; Tsao, M.-S., Unraveling the Mystery of Prognostic and

Predictive Factors in Epidermal Growth Factor Receptor Therapy. *Journal of Clinical Oncology* **2006,** *24* (7), 1219-1220.

105. Shi, R.; Wang, F.; Yan, B., Site–Site Isolation and Site–Site Interaction – Two Sides of the Same Coin. *International Journal of Peptide Research and Therapeutics* **2007,** *13* (1), 213-219.

106. Soper, S. A.; Mattingly, Q. L.; Vegunta, P., Photon burst detection of single near-infrared fluorescent molecules. *Analytical Chemistry* **1993,** *65* (6), 740-747.

107. Staderini, M.; Martin, M. A.; Bolognesi, M. L.; Menendez, J. C., Imaging of [small beta]-amyloid plaques by near infrared fluorescent tracers: a new frontier for chemical neuroscience. *Chemical Society Reviews* **2015,** *44* (7), 1807-1819.

108. Synak, A.; Gil, M.; Organero, J. A.; Sánchez, F.; Iglesias, M.; Douhal, A., Fast to Ultrafast Dynamics of Palladium Phthalocyanine Covalently Bonded to MCM-41 Mesoporous Material. *Journal of Physical Chemistry C* **2009,** *113* (44), 19199-19207.

109. Tárrega, C.; Pulido, R., A one-step method to identify MAP kinase residues involved in inactivation by tyrosine- and dual-specificity protein phosphatases. *Analytical Biochemistry* **2009,** *394* (1), 81-86.

110. Ullrich, A.; Coussens, L.; Hayflick, J. S.; Dull, T. J.; Gray, A.; Tam, A. W.; Lee, J.; Yarden, Y.; Libermann, T. A.; Schlessinger, J.; Downward, J.; Mayes, E. L. V.; Whittle, N.; Waterfield, M. D.; Seeburg, P. H., Human epidermal growth factor receptor cDNA sequence and aberrant expression of the amplified gene in A431 epidermoid carcinoma cells. *Nature* **1984,** *309* (5967), 418-425.

111. Valeur, E.; Bradley, M., Amide bond formation: beyond the myth of coupling reagents. *Chemical Society Reviews* **2009,** *38* (2), 606-631.

112. Van Dort, M. E.; Robins, D. M.; Wayburn, B., Design, synthesis, and pharmacological characterization of a 4-[4,4-Dimethyl-3-(4-hydroxybutl)-5-oxo-2-thioxo-1-imidazolidinyl]-2-iodobenzonitrile as a high-affinity nonsteroidal androgen receptor ligand. *Journal of Medicinal Chemistry* **2000,** *43* (17), 3344 - 3347.

113. Wampler, D. E.; Takahashi, M.; Westhead, E. W., Active subunits of the aspartokinase-homoserine dehydrogenase I complex from Escherichia coli. *Biochemistry* **1970,** *9* (21), 4210-4216.

114. Wang, A.; Li, Y.; Zhou, L.; Yuan, L.; Lu, S.; Lin, Y.; Zhou, J.; Wei, S., Charge dependent photodynamic activity of alanine based zinc phthalocyanines. *Journal of Photochemistry and Photobiology B: Biology* **2014,** *141*, 10-19.

115. Wang, S.; Song, Y.; Liu, D., EAI045: The fourth-generation EGFR inhibitor overcoming T790M and C797S resistance. *Cancer Letters* **2017,** *385*, 51-54.

116. Wedegaertner, P. B.; Gill, G. N., Activation of the purified protein tyrosine kinase

domain of the epidermal growth factor receptor. *Journal of Biological Chemistry* **1989,** *264* (19), 11346-11353.

117. Weijer, R.; Broekgaarden, M.; Kos, M.; van Vught, R.; Rauws, E. A. J.; Breukink, E.; van Gulik, T. M.; Storm, G.; Heger, M., Enhancing photodynamic therapy of refractory solid cancers: Combining second-generation photosensitizers with multi-targeted liposomal delivery. *Journal of Photochemistry and Photobiology C: Photochemistry Reviews* **2015,** *23*, 103-131.

118. Wheeler, B. L.; Nagasubramanian, G.; Bard, A. J.; Schechtman, L. A.; Kenney, M. E., A silicon phthalocyanine and a silicon naphthalocyanine: synthesis, electrochemistry, and electrogenerated chemiluminescence. *Journal of the American Chemical Society* **1984,** *106* (24), 7404-7410.

119. Wieczorek, A.; Werther, P.; Euchner, J.; Wombacher, R., Green- to far-red-emitting fluorogenic tetrazine probes – synthetic access and no-wash protein imaging inside living cells. *Chemical Science* **2017,** *8* (2), 1506-1510.

120. Williams, D. C.; Soper, S. A., Ultrasensitive Near-IR Fluorescence Detection for Capillary Gel Electrophoresis and DNA Sequencing Applications. *Analytical Chemistry* **1995,** *67* (19), 3427-3432.

121. Wissner, A.; Fraser, H. L.; Ingalls, C. L.; Dushin, R. G.; Floyd, M. B.; Cheung, K.; Nittoli, T.; Ravi, M. R.; Tan, X.; Loganzo, F., Dual irreversible kinase inhibitors: Quinazoline-based inhibitors incorporating two independent reactive centers with each targeting different cysteine residues in the kinase domains of EGFR and VEGFR-2. *Bioorganic & Medicinal Chemistry* **2007,** *15* (11), 3635-3648.

122. Wöhrle, D.; Eskes, M.; Shigehara, K.; Yamada, A., A Simple Synthesis of 4,5-Disubstituted 1,2-Dicyanobenzenes and 2,3,9,10,16,17,23,24-Octasubstituted Phthalocyanines. *Synthesis* **1993,** *1993* (02), 194-196.

123. Ximing, D.; Huijun, X., The synthesis and film-forming property of a new amphiphilic phthalocyanine. *Dyes and Pigments* **1998,** *39* (4), 223-229.

124. Yanagisawaa, S.; Okumaa, K.; Inaokaa, T.; Hamada, I., Recent progress in predicting structural and electronic properties of organic solids with the van der Waals density functional. *Journal of Electron Spectroscopy and Related Phenomena* **2015,** *204*, 159-167.

125. Yang, K. S.; Budin, G.; Reiner, T.; Vinegoni, C.; Weissleder, R., Bioorthogonal Imaging of Aurora Kinase A in Live Cells. *Angewandte Chemie International Edition* **2012,** *51* (27), 6598-6603.

126. Yarden, Y.; Ullrich, A., Growth Factor Receptor Tyrosine Kinases. *Annual Review of Biochemistry* **1988,** *57* (1), 443-478.

127. Yin, D. M.; Hammler, D.; Peter, M. F.; Marx, A.; Schmitz, A.; Hagelueken, G.,

Inhibitor-Directed Spin Labelling—A High Precision and Minimally Invasive Technique to Study the Conformation of Proteins in Solution. *Chemistry – A European Journal* **2018,** *24* (26), 6665-6671.

128. Yu, L.; Shi, W.; Lin, L.; Guo, Y.; Li, R.; Peng, T., Asymmetric zinc phthalocyanines with large steric hindrance as efficient red/near-IR responsive sensitizer for dye-sensitized solar cells. *Dyes and Pigments* **2015,** *114*, 231-238.

129. Yun, C.-H.; Boggon, T. J.; Li, Y.; Woo, M. S.; Greulich, H.; Meyerson, M.; Eck, M. J., Structures of Lung Cancer-Derived EGFR Mutants and Inhibitor Complexes: Mechanism of Activation and Insights into Differential Inhibitor Sensitivity. *Cancer Cell* **2007,** *11* (3), 217-227.

130. Zeng, F.; Harris, R. C., Epidermal Growth factor, from gene organization to bedside. *Seminars in Cell & Developmental Biology* **2014,** *28*, 2-11.

131. Zhang, X.; Gureasko, J.; Shen, K.; Cole, P. A.; Kuriyan, J., An Allosteric Mechanism for Activation of the Kinase Domain of Epidermal Growth Factor Receptor. *Cell* **2006,** *125* (6), 1137-1149.

132. Zorlu, Y.; Dumoulin, F.; Durmuş, M.; Ahsen, V., Comparative studies of photophysical and photochemical properties of solketal substituted platinum(II) and zinc(II) phthalocyanine sets. *Tetrahedron* **2010,** *66* (17), 3248-3258.

Appendix. Journal Permissions

RE: Obtain Right for Dissertation - Article not available through Copyright Clearance Center

Rights <rights@wspc.com>

Fri 6/7/2019 1:49 AM

To:Gerard T Ducharme <gducha2@lsu.edu>;

Dear Gerard Ducharme

Thanks for getting in touch.
We will be pleased to grant you the permission of reproducing Fig 2 from the below concerned article in your dissertation, provided that full credit been given to the original source in the following format:

Title of the Work, Author (s) and/or Editor(s) Name (s), Copyright @ year and name of the publisher

Kind regards,
Tu Ning

From: Gerard T Ducharme <gducha2@lsu.edu>
Sent: Thursday, 30 May, 2019 5:51 AM
To: Rights <rights@wspc.com>
Subject: Obtain Right for Dissertation - Article not available through Copyright Clearance Center

To Whom It May Concern,

I am attempting to request permission to use a figure from https://doi.org/10.1142/9789814307246_0014 (Fukuda T., Kobayashi N. UV-Visible Absorption Spectroscopic Properties of Phthalocyanines and Related Macrocycles. Handbook of Porphyrin Science, June 2010, 1-644.) Searching for this volume of Porphyrin Science has yielded no result using the doi above or the ISBN (978-981-4307-22-2) as given from the World Scientific webpage for the volume.

My dissertation will be completed by December 2019 and is entitled "Development and Characterization of Phthalocyanine-Quinazoline Conjugate as a NIR Fluorescent Probe for Kinase Activity." I will have to both print and upload an electronic version of the dissertation as a requirement for its completion. I will only use Figure 2 (article numbering) from this reference.

Gerard Ducharme

Ph. D. Candidate

ELSEVIER LICENSE
TERMS AND CONDITIONS

Jun 07, 2019

This Agreement between Gerard T Ducharme ("You") and Elsevier ("Elsevier") consists of your license details and the terms and conditions provided by Elsevier and Copyright Clearance Center.

License Number	4594880068921
License date	May 23, 2019
Licensed Content Publisher	Elsevier
Licensed Content Publication	Inorganica Chimica Acta
Licensed Content Title	Synthesis and photophysicochemical properties of novel thiadiazole-substituted zinc (II), gallium (III) and silicon (IV) phthalocyanines for photodynamic therapy
Licensed Content Author	Emre Güzel,Armağan Günsel,Ahmet T. Bilgiçli,Göknur Yaşa Atmaca,Ali Erdoğmuş,M. Nilüfer Yarasir
Licensed Content Date	Oct 1, 2017
Licensed Content Volume	467
Licensed Content Issue	n/a
Licensed Content Pages	8
Start Page	169
End Page	176
Type of Use	reuse in a thesis/dissertation
Portion	figures/tables/illustrations
Number of figures/tables/illustrations	1
Format	both print and electronic
Are you the author of this Elsevier article?	No
Will you be translating?	No
Order reference number	1.1
Original figure numbers	Figure 1
Title of your thesis/dissertation	Development and Characterization of Phthalocyanine-Quinazoline Conjugate as a NIR Fluorescent Probe for Kinase Activity
Expected completion date	Dec 2019
Estimated size (number of pages)	150
Requestor Location	Accounting Services c/o Department of Chemistry 204 Thomas Boyd Hall BATON ROUGE, LA 70802 United States Attn: Accounting Services c/o Department of Chemistry
Publisher Tax ID	98-0397604

ELSEVIER LICENSE TERMS AND CONDITIONS

Jul 01, 2019

This Agreement between Gerard T Ducharme ("You") and Elsevier ("Elsevier") consists of your license details and the terms and conditions provided by Elsevier and Copyright Clearance Center.

License Number	4620261152005
License date	Jul 01, 2019
Licensed Content Publisher	Elsevier
Licensed Content Publication	Journal of Photochemistry and Photobiology A: Chemistry
Licensed Content Title	Amino-functionalized water-soluble zinc phthalocyanines: Synthesis, photophysical, photochemical and protein binding properties
Licensed Content Author	Meltem Göksel,Mahmut Durmuş,Devrim Atilla
Licensed Content Date	Aug 15, 2013
Licensed Content Volume	266
Licensed Content Issue	n/a
Licensed Content Pages	10
Start Page	37
End Page	46
Type of Use	reuse in a thesis/dissertation
Portion	figures/tables/illustrations
Number of figures/tables/illustrations	1
Format	both print and electronic
Are you the author of this Elsevier article?	No
Will you be translating?	No
Original figure numbers	Figure 3 A
Title of your thesis/dissertation	Development and Characterization of Phthalocyanine-Quinazoline Conjugate as a NIR Fluorescent Probe for Kinase Activity
Publisher of new work	Louisiana State University
Expected completion date	Dec 2019
Requestor Location	Gerard T Ducharme 133 Choppin Hall Louisiana State University BATON ROUGE, LA 70802 United States Attn: Gerard Ducharme
Publisher Tax ID	98-0397604
Total	**0.00 USD**
Terms and Conditions	

INTRODUCTION

1. The publisher for this copyrighted material is Elsevier. By clicking "accept" in connection with completing this licensing transaction, you agree that the following terms and conditions apply to this transaction (along with the Billing and Payment terms and conditions established by Copyright Clearance Center, Inc. ("CCC"), at the time that you opened your Rightslink account and that are available at any time at http://myaccount.copyright.com).

GENERAL TERMS

RE: Permission Request - RightsLink Unavailable Title G. Ducharme

Wiley Global Permissions <permissions@wiley.com>

Tue 7/2/2019 5:17 AM

To:Gerard T Ducharme <gducha2@lsu.edu>;

Dear Gerard,

Thank you for your email.

Permission is granted for you to use the material requested for your thesis/dissertation subject to the usual acknowledgements (author, title of material, title of book/journal, ourselves as publisher) and on the understanding that you will reapply for permission if you wish to distribute or publish your thesis/dissertation commercially.

You should also duplicate the copyright notice that appears in the Wiley publication in your use of the Material. Permission is granted solely for use in conjunction with the thesis, and the material may not be posted online separately.

Any third-party material is expressly excluded from this permission. If any material appears within the article with credit to another source, authorisation from that source must be obtained.

Should you require any further information, please do not hesitate to contact me.

Kind regards,

Paisley Chesters
Permissions Co-Ordinator

Wiley
The Atrium
Southern Gate
Chichester
West Sussex
PO19 8SQ
www.wiley.com

WILEY

From: Gerard T Ducharme <gducha2@lsu.edu>
Sent: 01 July 2019 16:30
To: Wiley Global Permissions <permissions@wiley.com>
Subject: Permission Request - RightsLink Unavailable Title G. Ducharme

To Whom It May Concern,

I am contacting you to request reprint permission for use in my dissertation. The title of my dissertation is as follows:

Development and Characterization of Phthalocyanine-Quinazoline Conjugate as a NIR Fluorescent Probe for Kinase Activity.

My graduation date is in December 2019 and the document will be physically printed and electronically uploaded to the university database.

The article I wish to use is as follows:

Campbell McInnes and Brian D. Sykes. Growth factor receptors: Structure, mechanism, and drug discovery. *Peptide Science*. **1997**, *43 (5)*, 339-316.
I would only need to use Figure 1 from the document.

Gerard Ducharme

Ph. D. Candidate

Nesterov Research Group

CMB 366

gducha2@lsu.edu

Dept. of Chemistry

Louisiana State University

ELSEVIER LICENSE
TERMS AND CONDITIONS

Jul 01, 2019

This Agreement between Gerard T Ducharme ("You") and Elsevier ("Elsevier") consists of your license details and the terms and conditions provided by Elsevier and Copyright Clearance Center.

License Number	4620271105237
License date	Jul 01, 2019
Licensed Content Publisher	Elsevier
Licensed Content Publication	Cancer Cell
Licensed Content Title	Structures of Lung Cancer-Derived EGFR Mutants and Inhibitor Complexes: Mechanism of Activation and Insights into Differential Inhibitor Sensitivity
Licensed Content Author	Cai-Hong Yun,Titus J. Boggon,Yiqun Li,Michele S. Woo,Heidi Greulich,Matthew Meyerson,Michael J. Eck
Licensed Content Date	Mar 13, 2007
Licensed Content Volume	11
Licensed Content Issue	3
Licensed Content Pages	11
Start Page	217
End Page	227
Type of Use	reuse in a thesis/dissertation
Intended publisher of new work	other
Portion	figures/tables/illustrations
Number of figures/tables/illustrations	1
Format	both print and electronic
Are you the author of this Elsevier article?	No
Will you be translating?	No
Original figure numbers	Figure 1.B
Title of your thesis/dissertation	Development and Characterization of Phthalocyanine-Quinazoline Conjugate as a NIR Fluorescent Probe for Kinase Activity
Publisher of new work	Louisiana State University
Expected completion date	Dec 2019
Requestor Location	Gerard T Ducharme 133 Choppin Hall Louisiana State University BATON ROUGE, LA 70802 United States Attn: Gerard Ducharme
Publisher Tax ID	98-0397604

ELSEVIER LICENSE
TERMS AND CONDITIONS

Jul 01, 2019

This Agreement between Gerard T Ducharme ("You") and Elsevier ("Elsevier") consists of your license details and the terms and conditions provided by Elsevier and Copyright Clearance Center.

License Number	4620271379295
License date	Jul 01, 2019
Licensed Content Publisher	Elsevier
Licensed Content Publication	Bioorganic & Medicinal Chemistry
Licensed Content Title	Dual irreversible kinase inhibitors: Quinazoline-based inhibitors incorporating two independent reactive centers with each targeting different cysteine residues in the kinase domains of EGFR and VEGFR-2
Licensed Content Author	Allan Wissner,Heidi L. Fraser,Charles L. Ingalls,Russell G. Dushin,M. Brawner Floyd,Kinwang Cheung,Thomas Nittoli,Malini R. Ravi,Xingzhi Tan,Frank Loganzo
Licensed Content Date	Jun 1, 2007
Licensed Content Volume	15
Licensed Content Issue	11
Licensed Content Pages	14
Start Page	3635
End Page	3648
Type of Use	reuse in a thesis/dissertation
Intended publisher of new work	other
Portion	figures/tables/illustrations
Number of figures/tables/illustrations	1
Format	both print and electronic
Are you the author of this Elsevier article?	No
Will you be translating?	No
Original figure numbers	Figure 1
Title of your thesis/dissertation	Development and Characterization of Phthalocyanine-Quinazoline Conjugate as a NIR Fluorescent Probe for Kinase Activity
Publisher of new work	Louisiana State University
Expected completion date	Dec 2019
Requestor Location	Gerard T Ducharme 133 Choppin Hall Louisiana State University BATON ROUGE, LA 70802 United States Attn: Gerard Ducharme

Vita

Gerard Thomas Ducharme, born in Lafayette, Louisiana, was always fascinated by the world around him. After receiving his Bachelor of Science Degree, in Chemistry, from the University of Louisiana at Lafayette, where he fell in love with the puzzle that is organic chemistry, he decided to work toward his doctoral degree in the Department of Chemistry at Louisiana State University in the Nesterov research group. Upon completion of his doctoral degree, he will venture out to further study the world around him.